Universitat Internacional de Catalunya
Facultat d'Odontologia

Tesis doctoral

Estudio de las tensiones por fuerzas oclusales dinámicas en prótesis implantosoportadas según el material rehabilitador. Elementos finitos 3D dinámicos.

Raúl Medina Gálvez

Estudio de las tensiones por fuerzas oclusales dinámicas en prótesis implantosoportadas según el material rehabilitador. Elementos finitos 3D dinámicos.

Raúl Medina Gálvez

TESIS DOCTORAL

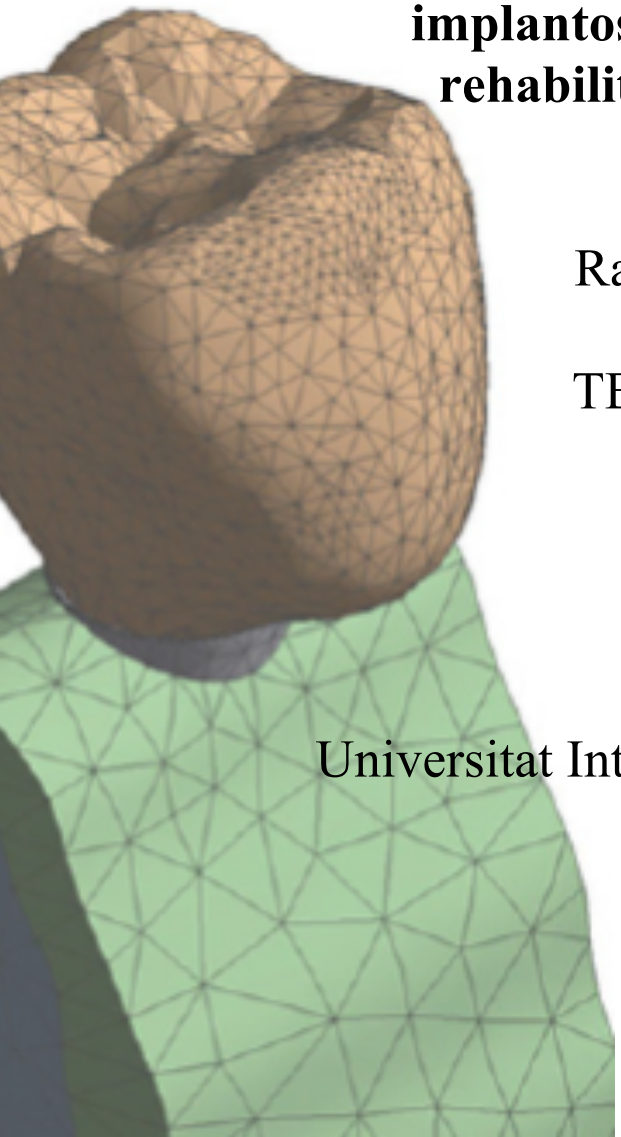

Universitat Internacional de Catalunya, 2022

Estudio de las tensiones por fuerzas oclusales dinámicas en prótesis implantosoportadas según el material rehabilitador. Elementos finitos 3D dinámicos.

Raúl Medina Gálvez

TESIS DOCTORAL

Universitat Internacional de Catalunya, 2022

Directores:

Josep Cabratosa Termés
Oriol Cantó Navés
Miquel Ferrer Ballester

Programa de Doctorado en Ciencias de la Salud

Línea de Investigación:
Tecnología digital en prótesis bucal y maxilofacial

Dedicatoria

A mi mujer por su amor incondicional, esfuerzo y cariño. Sin ella no podría ser quien soy.

Te quiero.

"Por muy alta que esté la cumbre
siempre está bajo el cielo
por eso todo aquel que se lo proponga
podrá alcanzarla.
Sin embargo, todo aquel que no lo intente
dirá que está demasiado alta"

Proverbio oriental

Agradecimientos

En primer lugar, deseo dar mi agradecimiento a mis directores de tesis: el Dr. Josep Cabratosa Termés, por guiarme en la tesis y en el mundo académico, por su apoyo y sugerencias; al Dr. Oriol Cantó Navés por enseñarme tanto, acompañarme y apoyarme, por ser mi amigo; al Dr. Miquel Ferrer Ballester por ayudarme en la parte técnica, por entender mi falta de conocimientos y ser capaz de hacerme entender conceptos de manera tan simple.

Así mismo, quiero agradecer a Xavier Marimón Serra por sus explicaciones y su ayuda en el desarrollo de las investigaciones, por todas esas partes técnicas tan complejas y por su tesón en las publicaciones; a Miguel Cerrolaza y al Dr. Òscar Figueras Álvarez sin los cuales no habría sido posible la publicación de los artículos incluidos en esta tesis. También agradecer a Jordi Martí Vigil por su tesón en la investigación y esa alegría que desprende.

Sin embargo, no podemos olvidar las personas que nos apoyan y nos empujan a ser mejores cada día. Gracias a mi madre por estar siempre ahí cuando la he necesitado, por escucharme y apoyarme siempre. Gracias a mis suegros, a los que considero como a mis padres, siempre me han querido como a un hijo. Gracias a mi padre, qué a su manera, me inculcó cualidades como la responsabilidad y el tesón.

Pero sobretodo gracias a mi mujer Olga y a mis hijos Héctor e Inés por su paciencia y compresión, por el tiempo que les he robado en mis proyectos y trabajo.

Muchas gracias a todos

Resumen

Título: Estudio de las tensiones por fuerzas oclusales dinámicas en prótesis implantosoportadas según el material rehabilitador. Elementos finitos 3D dinámicos.

Introducción: Reponer un diente ausente mediante un implante dental y una corona es un tratamiento habitual en la práctica clínica odontológica. La decisión del material rehabilitador a utilizar, muchas veces, se hace con el desconocimiento de las propiedades mecánicas, entre ellas las tensiones transferidas por las fuerzas oclusales a nivel de la prótesis implantosoportada y el hueso periimplantario. Un exceso de tensión a nivel del hueso periimplantario, junto con inflamación del tejido gingival puede ocasionar la pérdida de hueso periimplantario y condicionar la supervivencia del implante. La ausencia de hueso cortical, en situaciones como la periimplantitis, los implantes inmediatos post extracción, los implantes en hueso regenerado o posición subcortical, previsiblemente influirán en las tensiones generadas en el hueso trabecular periimplantario. Los estudios dinámicos de elementos finitos 3D son una herramienta muy útil para hacer estimaciones de las tensiones generadas en la corona y transferidas al pilar y al hueso por una fuerza de impacto en una restauración implantosoportada, lo cual sería complicado de determinar con otros métodos.

Hipótesis: Se planteó la hipótesis de que las tensiones transferidas a una prótesis implantosoportada y al hueso periimplantario cortical y trabecular por una fuerza oclusal dinámica varían según el material rehabilitador utilizado.

Objetivos: El objetivo general de esta tesis doctoral fué estudiar las tensiones transferidas por fuerzas oclusales dinámicas en prótesis implantosoportadas según el material rehabilitador.

Métodos: Se realizó un modelo de elementos finitos 3D de una sección mandibular (hueso cortical y hueso trabecular) con un implante y una corona estructurada en pilar, estructura interna y recubrimiento estético. La absorción de las fuerzas oclusales dinámicas de los distintos materiales, se valoró mediante un análisis dinámico de elementos finitos de las tensiones generadas en la corona y transferidas al pilar y al hueso periimplantario, por una fuerza de impacto provocada por una masa total de 8,62 gr a una velocidad de 1,25 m/s. Se analizaron seis tipos de rehabilitaciones: fibra de carbono - composite (FCOM), Cr-Co - cerámica (MCEM), Cr-Co - composite (METCOM), monolítica de Cr-Co (MET), fibra de carbono – cerámica (FCCER) y PEEK - composite (PKCOM). El tiempo de la simulación fue de 0,4 ms. Se valoraron las tensiones de von Mises en la corona, el pilar y el hueso cortical. Así mismo, se realizó un nuevo análisis dando el supuesto de la ausencia de la cortical ósea y se compararon las tensiones de von Mises en el hueso cortical y en el hueso trabecular.

Resultados: En la corona se observaron las máximas tensiones en MET y MCER seguido de FCCER. Los valores fueron menores en MCOM, FCOM y PKCOM, siendo el más bajo este último. Todos los modelos mostraron altas tensiones en el pilar excepto en FCOM. En el hueso cortical MCOM, FCOM y PKCOM mostraron menores tensiones que MCER, FCCER o MET. En la simulación sin hueso cortical las tensiones aumentaban en el hueso trabecular en todos los modelos, siendo FCCER el que mayor tensión transmitía y PKCOM el que menos.

Conclusiones: El uso de materiales menos rígidos reduce la tensión transmitida por una fuerza de impacto a la corona implantosoportada, al pilar y al hueso, tanto cortical como trabecular. La ausencia de cortical ósea hace que aumente considerablemente la tensión generada en el hueso trabecular.

Summary

Title: Analysis of tensions due dynamic occlusal forces in implant-supported prostheses according to the restorative material. Dynamic 3D finite elements.

Introduction: Replacing missing tooth by dental implant and crown is a common treatment in dental practice. The decision of rehabilitative material to use is doing without knowing the mechanical properties. Mechanical properties like tensions transferred by the occlusal forces at the level of the implant-supported prosthesis and the peri-implant bone. An excess of tension at level of the peri-implant bone with inflammation of the gingival tissue could cause the loss of peri-implant bone. The absence of cortical bone in situations such as, peri-implantitis, immediate post-extraction implants, implants on regenerated bone or subcortical position, must influence the stresses generated in the peri-implant trabecular bone. 3D dynamic finite element studies are useful tool to estimate the stresses generated at the crown and transferred to the abutment and bone by an impact force on implant-supported restoration. These would be difficult to determine with other methods.

Hypothesis: It was hypothesized that the stresses transferred to an implant-supported prosthesis and at cortical and trabecular peri-implant bone by dynamic occlusal force depends on the restorative material used.

Objectives: The general objective of this doctoral thesis was to study the tensions transferred by dynamic occlusal forces on implant-supported prostheses according to the restorative material.

Methods: A 3D finite element model of a mandibular section (cortical bone and trabecular bone) with an implant and an abutment, crown (internal structure and esthetic coating) was made. The absorption of the dynamic occlusal forces of the different materials was assessed by dynamic finite element analysis. An impact force caused by a mass of 8, 62 gr at 1.25 m/s. speed in the crown and transferred to the abutment and peri-implant bone, towards six types of restorations were analyzed: carbon fiber - composite (FCOM), CoCr - ceramic (MCEM), CoCr - composite (METCOM), monolithic CoCr (MET), carbon fiber - ceramic (FCCER) and PEEK-composite (PKCOM). The simulation time was 0.4 ms. Von Mises stresses in the crown, abutment, and cortical bone were assessed. Likewise, a new analysis was performed assuming the absence of cortical bone and the von Mises stresses in cortical and trabecular bone were compared.

Results: In the crown, the maximum tensions were observed in MET and MCER followed by FCCER. The values were lower on MCOM, FCOM and lowest in PKCOM. All the models showed high stresses except FCOM. Cortical bone MCOM, FCOM and PKCOM showed lower stresses than MCER, FCCER or MET. On the simulation without cortical bone, the tensions increased in the trabecular bone in all the models. FCCER transmitted the greatest tension and PKCOM the least.

Conclusions: The use of less rigid materials reduces the stress transmitted by an impact force to the implant-supported crown, abutment and bone (cortical and trabecular). The absence of cortical bone increases considerably the tension generated in the trabecular bone.

Índice de contenidos

I. ÍNDICE DE ABREVIATURAS

FCOM: Corona con estructura interna de fibra de carbono y recubrimiento estético de composite.

MCER: Corona con estructura interna de aleación de metal de Cromo-Cobalto y recubrimiento estético de cerámica.

MCOM: Corona con estructura interna de aleación de metal y recubrimiento estético de composite.

MET: Corona completamente de aleación metálica de Cromo-Cobalto.

FCCER: Corona con estructura interna de fibra de carbono y recubrimiento estético de cerámica.

PKCOM: Corona con estructura interna de polieteretercetona y recubrimiento estético de composite.

STL: *Standard Tessellation Language*, formato de archivo informático para diseño asistido por ordenador que define la geometría de objetos 3D.

CAD: *Computed Aided Design,* diseño asistido por ordenador.

CBCT: *Cone beam computed tomography*, es una técnica de imagen medica donde una tomografía de rayos X es divergente formando un cono.

IGS: *Graphics Exchange Specification,* formato de archivo informático neutral de datos que permite el intercambio digital de información entre sistemas de diseño asistido por ordenador.

CAM: *Computed aided manufacturing*, técnica de fabricación asistida por ordenador.

FDA: *Food and Drug Admninistration,* agencia del Gobierno de Estados Unidos responsable de la regulación de alimentos medicamentos, aparatos médicos.

II. INTRODUCCIÓN

Uno de los mayores retos a los que nos enfrentamos en odontología es devolver el estado de salud óptimo al sistema estomatognático cuando se ha perdido y, por ende, la salud integral de nuestros pacientes. Así mismo, no solo tenemos que recuperar esta salud integral a corto plazo, si no poder mantenerla a lo largo de los años.

Cuando nos enfrentamos a la situación de un paciente con ausencias dentales, lo que el paciente nos demanda es que le devolvamos, en la medida de lo posible, la situación previa en la que estaba antes de perder esos dientes. Eso conlleva ciertas cosas. Por un lado el paciente quiere volver a tener una función general óptima a nivel de masticación, fonación y estética. Por otro lado, que esta función se mantenga a lo largo de los años sin detrimento.

Podríamos decir que en la práctica odontológica actual la primera parte la tenemos bastante bien "resuelta" con los tratamientos implantológico-quirúrgicos, estéticos-periodontales y estético-rehabilitadores sobre implantes. Pero una vez hemos solucionado el problema surge un importante reto, el mantenimiento de la situación a lo largo de los años. No podemos dejar de tener en cuenta que un paciente que actualmente tiene una situación de salud óptima, no está libre de que en un futuro no pueda sufrir alteraciones en su salud oral, como podría ser una gingivitis, o a nivel sistémico una diabetes, por ejemplo (1,2).

Además, sabemos que los pacientes rehabilitados con implantes no están exentos de sufrir problemas biológicos como la periimplantitis (pérdida de hueso alrededor de los implantes) o mecánicos como fracturas de los materiales de rehabilitación (1,3) en un futuro.

Diversos estudios demuestran que un exceso de carga o fuerza sobre un implante en estado de salud gingival óptima, sin inflamación gingival, no afecta la integración ósea del implante(4–6). Por otro lado, hay investigaciones que demuestran que en una situación de inflamación gingival un exceso de carga sobre una rehabilitación implanto-protésica unitaria o múltiple puede ocasionar una pérdida ósea periimplantar y la posible pérdida del implante y de la rehabilitación (2,4–10). Por lo tanto, es importante conocer las fuerzas que intervienen en el sistema estomatognático y que inciden sobre las rehabilitaciones implantológicas y sus efectos.

2.1.-Tipos de fuerzas que intervienen en el sistema estomatognático

Según el glosario de la *Academy of Prosthodontics*, la oclusión (*occlusion*) es definida como el acto de cierre entre los arcos dentarios y también, como la relación estática entre las superficies de contacto de los dientes maxilares o mandibulares o análogos de dientes (11).

El proceso masticatorio oral (*masticatory cycle*) es definido, según el mismo glosario, como el movimiento mandibular tridimensional que relaciona ambos arcos dentales para triturar el alimento (11). Como movimiento, se genera el desplazamiento de una masa (mandíbula) a una determinada aceleración, generándose una fuerza dinámica controlada que permite triturar los alimentos. La fuerza masticatoria ejercida en cada momento depende de muchos factores como son: edad, sexo, la zona de contacto (molares, premolares o sector anterior), las propias características físicas del paciente y el alimento o material a masticar, entre otros (12–14).

Existen diversos estudios que valoran la fuerza máxima que se puede ejercer al ocluir estáticamente (15–19), pero dicho valor de fuerza tiene un interés clínico relativo, en tanto en cuanto, la carga masticatoria ejercida es estática, a diferencia de la producida durante el proceso de masticación, que es de naturaleza dinámica. En todo caso, dichos valores de fuerza servirían para valorar cuál es la carga estática que podrían llegar a realizar los pacientes en casos de bruxismo céntrico o "clenching" y cuáles serían los valores de fuerza que deberían soportar los materiales

rehabilitadores en estas situaciones (16,18–20). A su vez, debemos tener presente y conocer las fuerzas dinámicas, entre ellas las fuerzas de impacto y que los materiales de rehabilitación tienen distintas respuestas a las mismas dependiendo de sus propiedades mecánicas.

Es conveniente definir, según el glosario de *The Academy of Prosthodontics* (11), algunos términos:

- *Contacto oclusal (occlusal contact):* El contacto entre dientes opuestos al elevar la mandíbula.
- *Contacto oclusal inicial (initial occlusal contact):* durante el cierre de la mandíbula, el primer contacto entre dientes de arcos opuestos.
- *Masticación (mastication*): el proceso de triturar la comida para tragar y digerir.
- *Fuerza de masticación (masticatory force):* la fuerza aplicada por los músculos orofaciales durante el proceso de masticación.
- *Fuerza oclusal (occlusal force):* el resultado de la fuerza muscular aplicada a dientes opuestos, la fuerza ejercida entre dientes opuestos (acción-reacción) y generada por la acción dinámica mandibular durante el acto fisiológico de la masticación.
- *Apretar los dientes (clenching):* la fuerza estática de los maxilares y dientes, asociada, frecuentemente, con tensión nerviosa aguda o esfuerzo físico.

Por tanto, la rehabilitación implanto-protésica puede verse afectada por dos tipos de fuerzas: las estáticas, cuando apretamos los dientes (o *clenching)* y las dinámicas, por ejemplo, al masticar. Durante la masticación se dan unas fuerzas de impacto, cuya intensidad es de difícil determinación, puesto que está generada no solo por la acción muscular dependiente del alimento a masticar, sino también por la inercia de la masa mandibular en movimiento y las características de cada paciente.

2.2.-Fundamentos de física y mecánica de los materiales

La práctica odontológica está basada en el diagnóstico, el establecimiento de un plan de tratamiento, la ejecución del tratamiento y el mantenimiento. Para la ejecución del tratamiento, sea cual sea, estamos condicionados al uso de materiales los cuales tienen características propias y específicas que condicionan su utilidad.

Es necesario saber cuales son las propiedades de cada material en cualquier ámbito de la odontología para poder elegir el material idóneo en cada ocasión y, para ello, debemos tener unos conceptos básicos sobre física y mecánica de los materiales (21–23).

2.2.1.-Principio de acción-reacción. Postulado de Euler-Cauchy

El primer concepto que tenemos que tener presente sobretodo cuando hablamos de someter a los materiales restauradores a fuerzas, es el concepto físico de

"acción-reacción". Cuando se aplica una fuerza a un objeto se produce una reacción de la misma intensidad y en sentido opuesto. Esta reacción se identifica como una tensión interna que se puede cuantificar y que varía en el interior del objeto dependiendo de su forma, dimensiones y del material que lo forma. La tensión se define como fuerza por unidad de área (24).

2.2.2.-Tensión y principio de uniformidad

Dependiendo de las características de la fuerza aplicada pueden ocurrir distintos efectos en los materiales, como podrían ser cambios estructurales o dimensionales, entre otros. La variación de la dimensión original que resulta en una deformación ocasiona tensión. Si el objeto reacciona igual en todos sus puntos se dice que la deformación es homogénea o de uniformidad (25).

2.2.3.-Curva de tensión-deformación. Rigidez

La relación entre la tensión y la deformación en un material es relevante para determinar su comportamiento mecánico puesto que define la rigidez del material. Si la relación es proporcional, el cociente entre la tensión y la deformación recibe el nombre de Módulo de Young (26).

Cuando se ejerce una fuerza sobre un objeto de un material determinado, esta genera una tensión, como hemos comentado. Cuando el objeto puede deformarse, diremos que es un material flexible. Si al dejar de recibir la fuerza el objeto vuelve a la forma original, es decir, no ha tenido una deformación permanente, hablamos de deformación elástica del material (Fig.1).

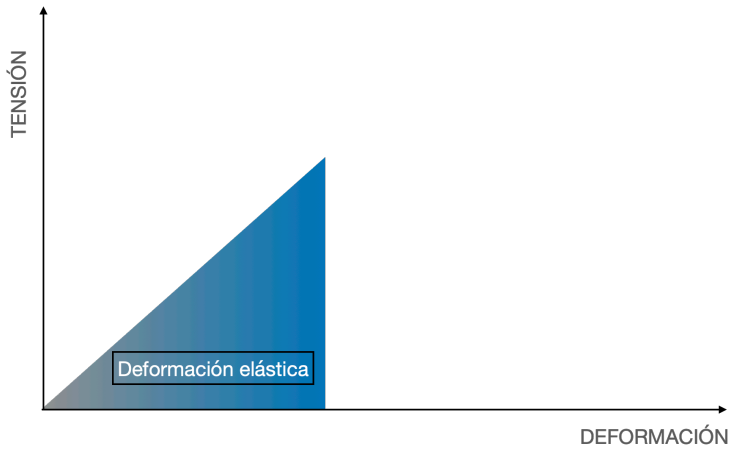

Fig.1. Curva de tensión-deformación. Fase de deformación elástica.

Si al mismo objeto le continuamos ejerciendo un aumento de fuerza, llega un punto en que se crea una deformación permanente o plástica, es decir, al retirar la fuerza externa la forma original del objeto no se recupera. La tensión y la deformación acostumbran a ser proporcionales hasta este punto llamado tensión de límite elástico. Este punto se determina a partir de la curva tensión-deformación.

El módulo elástico o módulo de Young en un diagrama tensión-deformación (Fig.2) viene representado por la tangente a la curva en cada punto dentro del límite elástico y mide la rigidez de un material.

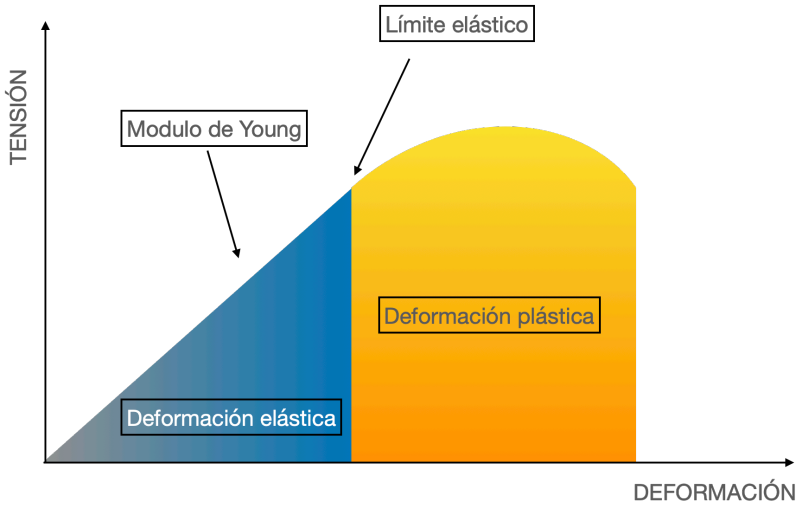

Fig. 2. Curva de tensión-deformación. Modulo de Young. Límite elástico. Área que representa la deformación plástica.

Todo material tiene una resistencia a la deformación. Superado el punto de deformación plástica, si continuamos ejerciendo fuerza, llegaremos al punto de rotura del material. El valor obtenido en este punto de fractura es lo que definimos como resistencia a la rotura del material.

El área de la curva que se encuentra debajo de la curva representa la energía de deformación y nos informa de la cantidad de energía que hay que aplicarle al material para deformarlo. (Fig.3).

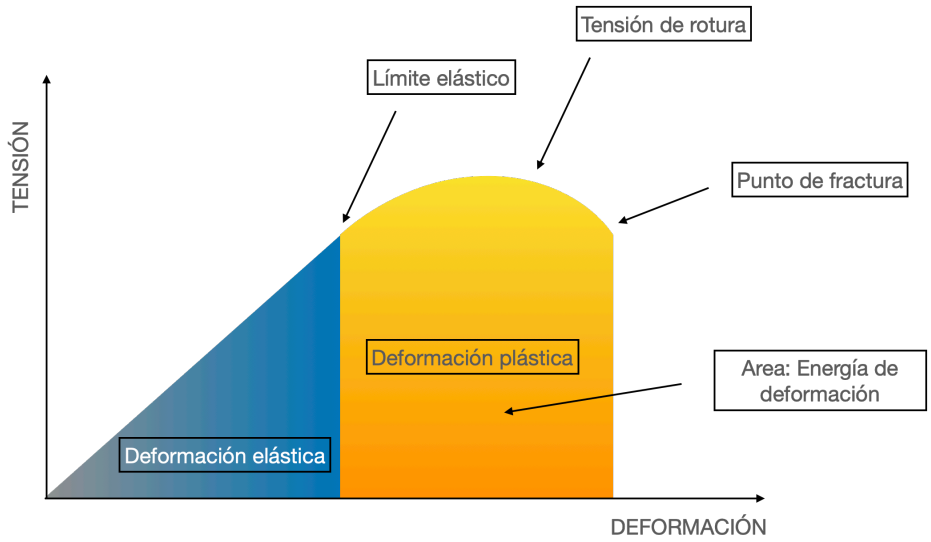

Fig. 3. Curva de tensión-deformación. Tensión de rotura. Punto de fractura. Energía de deformación.

Todos estos principios y parámetros son relevantes para caracterizar cualquier material rehabilitador en odontología y en ellos nos basamos en nuestros estudios.

2.2.4.-Ensayos Mecánicos

Existen diferentes ensayos para caracterizar los materiales y que son importantes de conocer. Dependiendo del tipo de material y de las fuerzas a las que estén sujetos, serán de elección unos ensayos u otros (27,28).

Ensayo de tracción

Consiste en aplicar a un cuerpo fuerzas axiales en direcciones opuestas. La resistencia del material a esta fuerza se llama resistencia a la tracción (Fig. 4). Este ensayo sirve para conocer el límite elástico, tensión de rotura y punto de fractura, así como la elongación, que es la deformación que sufre este cuerpo antes de la rotura. El valor de esta resistencia se mide por N/mm^2 . Los ensayos de tracción se utilizan para materiales como los metales o los polímeros pero no para materiales como las cerámicas. (28,29).

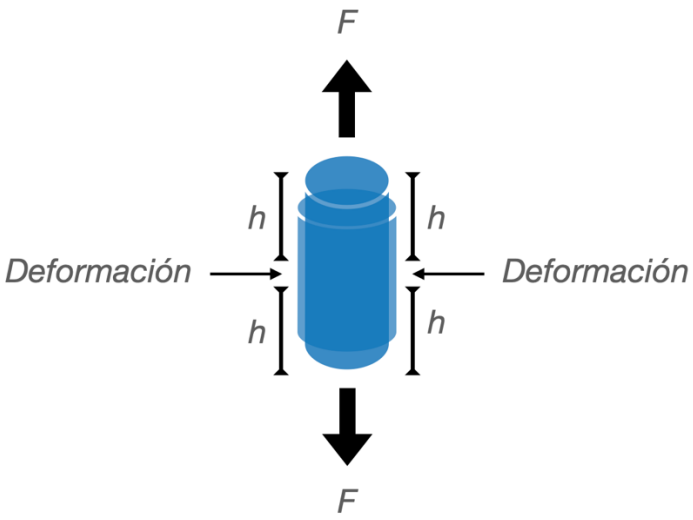

Fig. 4. Representación de ensayo a la tracción.

Ensayo de tracción mediante compresión diametral

Una alternativa al ensayo de tracción es el ensayo de compresión diametral. Se usa en materiales frágiles cuando resulta difícil la sujeción de la probeta por sus extremos en el ensayo de tracción pura. Consiste en aplicar una compresión diametral sobre una probeta cilíndrica que produce una tracción indirecta en el centro del cilindro, pudiéndose determinar así el punto de rotura por tracción (Fig.5) (29).

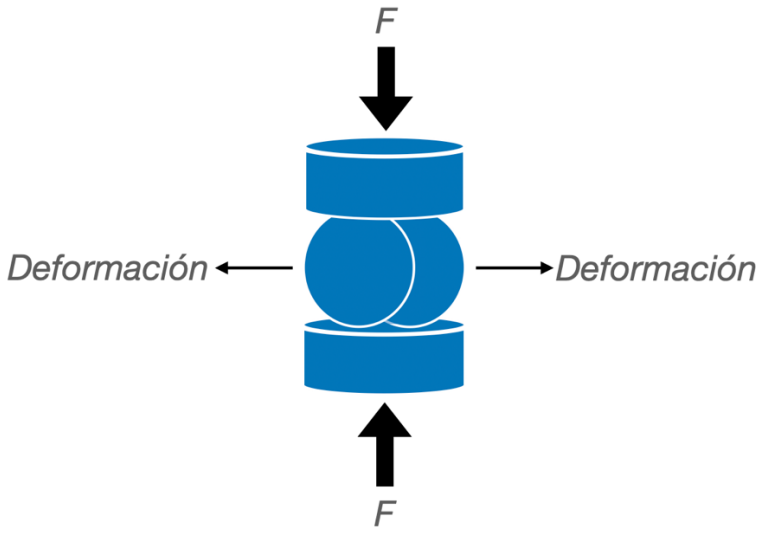

Fig.5. Representación de ensayo de tracción mediante compresión diametral (22).

Ensayo de compresión

Para materiales como las cerámicas es más propio el uso del ensayo de compresión para conocer sus propiedades mecánicas. El ensayo de compresión consiste en aplicar una compresión axial en los dos extremos de una probeta cilíndrica en dirección opuesta pudiéndose determinar así el límite elástico y la resistencia a la compresión (28,29).

Una de las fuerzas que nos podemos encontrar en el sistema estomatognático es la fuerza compresiva, por ejemplo, la ejercida al apretar los dientes y es importante investigar los materiales sujetos a esta condición. Los materiales acostumbran a ser más resistentes a la compresión que a la tracción, tal es el caso de las cerámicas (Fig.6).

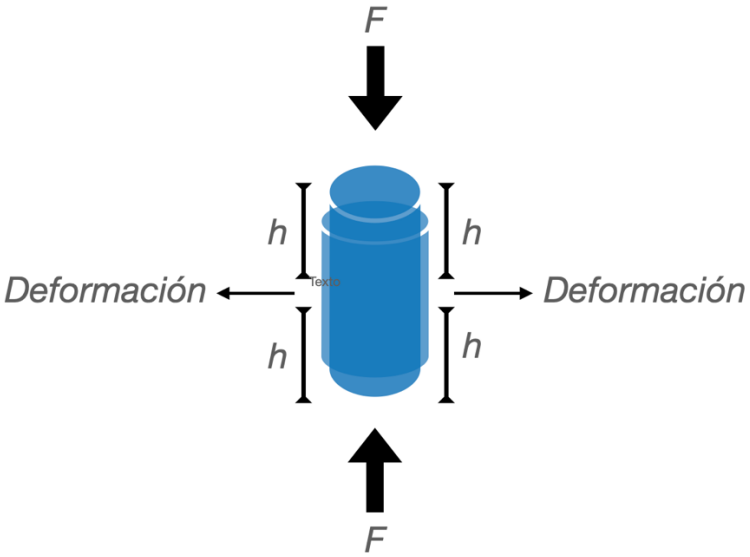

Fig.6. Representación de ensayo de compresión (21).

Ensayo de dureza

El ensayo de dureza consiste en evaluar la dureza de la superficie de un material al deterioro provocado por parte de un instrumento que ejerce una fuerza con la intención de crear una indentanción. Hay distintos métodos para evaluarlo como son Brinell, Rockwell, Vickers y Knoop. Estos distintos ensayos tienen gran importancia en odontología, ya que nos permite conocer la capacidad del material rehabilitador a no sufrir cambios permanentes en su superficie, por ejemplo, durante la masticación.(28,29)

2.2.5.-Parametros Mecánicos

Coeficiente de Poisson

Cuando un material se encuentra bajo una fuerza axial, tensional o compresiva hay una deformación en sentido axial, pero también en sentido lateral. Ante una fuerza tensional se da una elongación del material y una reducción de su sección transversal. Así mismo, si tenemos una fuerza compresiva habrá un incremento de la sección transversal y una reducción de la longitud original. Si esto ocurre dentro del límite elástico, la ratio entre la tensión lateral y la axial se denomina coeficiente de Poisson (25).

Resistencia a la deformación

La resistencia a la deformación de un material es su capacidad para doblarse antes de que se rompa o se deforme. Los materiales dentales deben soportar compresiones, flexiones y torsiones repetidas. Se desea que los materiales tengan una alta resistencia a la deformación, es decir, que los materiales tengan mucha capacidad de flexión antes de llegar al punto de deformación y de fractura (25).

Resistencia a la fatiga

En el entorno de la cavidad oral, los materiales de restauración están normalmente sujetos a fuerzas leves pero intermitentes, como serían las de masticación. Una de las características que debemos buscar en los materiales de rehabilitación es la resistencia a estas fuerzas, que llamamos resistencia a la fatiga. La fatiga permite medir el límite de fatiga sin fractura a un determinado número de ciclos de tensión. La presencia de defectos en la microestructura deriva en la fractura del material. El entorno clínico de la boca puede influir en la resistencia a la fatiga y el desarrollo de fractura del material (25).

2.3.-El método de los Elementos Finitos

En ingeniería de los materiales la investigación basada en estudios de elementos finitos está muy instaurada y validada desde hace muchos años. Estos estudios permiten conocer el comportamiento de los materiales sometidos a distintas situaciones de carga y condiciones de contorno gracias a los métodos numéricos computacionales (30) .

El método de los elementos finitos es un método numérico para analizar las tensiones y las deformaciones en una estructura con una geometría determinada. Esa estructura está formada por unos puntos, llamados nodos, unidos entre si forman elementos (finitos), que es una división en partes de una estructura mayor. El tipo, la cantidad y la disposición de los elementos afecta a la precisión de los resultados, cuanto

más pequeños y más cantidad de elementos mayor precisión. La secuencia para hacer un estudio de elementos finitos pasa por la creación de la estructura, la asignación de las propiedades mecánicas de los materiales implicados, la carga y las condiciones de contorno (31). Cuando hablamos de aplicar las propiedades mecánicas de los materiales, es importante conocer si el material en cuestión es isótropo o anisótropo. Los materiales isótropos presentan siempre el mismo comportamiento mecánico independientemente de la dirección de la carga, mientras que los anisótropos varían sus propiedades con la dirección de la carga.

Los datos de las propiedades mecánicas de los elementos a investigar se obtienen a partir de los ensayos anteriormente citados en el apartado de fundamentos de física de los materiales.

El análisis de elementos finitos presenta algunas ventajas, por ejemplo, mientras en un estudio *in vitro* es necesario un gran número de muestras sometidas al estudio para que el resultado del mismo sea estadísticamente significativo, en el caso de los estudios con elementos finitos, la variabilidad que nos pueda dar entre las distintas muestras no existe, así pues, no necesitamos distintas muestras del mismo objeto a investigar. Tampoco requieren consideraciones éticas, son repetibles y los diseños del estudio pueden ser modificados (32,33).

Los estudios de elementos finitos son una simulación, y como tal, son una aproximación. Nunca reproduciremos exactamente la realidad y el contorno tampoco

será exactamente el mismo al real, como podría ser el caso del entorno oral (32,34). A pesar de ello, se ha demostrado la fiabilidad de los elementos finitos como metodología de estudio (35) y además, nos permite valorar parámetros que sería imposible o muy difícil de valorar en estudios *in vivo* o *in vitro* de laboratorio.

En nuestra investigación queríamos evaluar la tensión generada, a nivel de la corona, el pilar y del hueso periimplantario, por las fuerzas oclusales según el material rehabilitador utilizado en la prótesis unitaria. Después de valorar posibles metodologías, llegamos a la conclusión que la mejor opción era un análisis dinámico de elementos finitos en el que se aplicara una fuerza de impacto. Los parámetros utilizados respecto a los materiales fueron la densidad, el coeficiente de Poisson y el módulo elástico o Módulo de Young.

Como se ha comentado la secuencia para realizar un análisis de elementos finitos sería: realizar el diseño del modelo, establecer las condiciones del contorno y realizar el análisis.

El diseño del modelo de estudio puede obtenerse mediante diseño digital o a partir de un escaneado, se obtiene un archivo STL que posteriormente es procesado mediante un programa como Solid Works (Dassault Systèmes, SolidWorks Corp., Waltham, MA, USA) que permite obtener la estructura formada por puntos unidos entre sí, los nodos. Respecto a las condiciones del contorno debemos tener en cuenta, en el caso de estudios de impactos, la distancia entre el modelo y la superficie de contacto, si

existe fricción o no en el momento del contacto, la masa del modelo y la velocidad del mismo. En el caso de estudios estáticos, la fuerza aplicada y por donde están sujetas o fijadas las superficies.

La gran mayoría de análisis de elementos finitos encontrados en la bibliografía son estudios estáticos, es decir, que al modelo de estudio se le aplica una fuerza constante en el tiempo (27–29, 31–34). A nivel del sistema estomatognático concurren dos situaciones en las que se pueden dar una fuerza que podría calificarse como estática. Una sería cuando un sujeto ocluye con fuerza sus dientes o sobre un objeto entre los dientes; otra, durante la parafunción de apretar los dientes (*clenching*). Estas dos situaciones no podemos contarlas como una acción fisiológica normal ya que de forma habitual una persona no tiene en contacto constante los dientes, si no que se mantienen a una distancia conocida como posición de reposo (11). Por otro lado, cuando una persona está efectuando el acto fisiológico de la masticación se crea un contacto entre el bolo alimenticio y los dientes y entre los dientes antagonistas. Este contacto es puntual en el tiempo y está producido por el movimiento mandibular, un movimiento definido por una masa (la mandíbula) y una velocidad imprimida por los músculos masticatorios. Es decir, un movimiento que produce una fuerza de impacto. Gracias a la ingeniería, hoy podemos realizar estudios de elementos finitos aplicando fuerzas de impacto, es decir, podemos aplicar a una masa una velocidad y analizar en el tiempo cuál es la reacción mecánica y física de los objetos de estudio. Esto es realmente novedoso y aún más en el ámbito de la investigación odontológica, permitiéndonos aproximarnos mucho más a la realidad del proceso masticatorio (38–41).

2.4.- Complementariedad entre los artículos publicados

Teniendo en cuenta lo mencionado anteriormente el objetivo de esta tesis es valorar la respuesta físico-mecánica de algunos de los materiales utilizados para rehabilitar ausencias dentales unitarias mediante implantes. Concretamente, conocer las tensiones generadas al complejo implante-hueso por las fuerzas oclusales, a fin de preservar la osteointegración del implante y el tratamiento protésico, manteniendo un adecuado estado de salud oral de nuestros pacientes a lo largo de los años.

Para dar respuesta a esta pregunta se han realizado dos estudios complementarios que se han publicado en sendos artículos.

El primer estudio publicado tenía por objetivo conocer las tensiones generadas en la corona, pilar protésico y hueso cortical periimplantario utilizando distintos materiales rehabilitadores, así mismo, conocer si estos materiales tenían la capacidad de absorción de la fuerza aplicada y se generaría una menor tensión en las distintas partes. Según lo expuesto anteriormente, si un exceso de tensión en el hueso periimplantario asociada a inflamación gingival puede producir una pérdida ósea alrededor del implante (2,9,10), consideramos pertinente conocer qué materiales tienen la capacidad de absorber las fuerzas aplicadas y minimizar la tensión transmitida al hueso periimplantario. Así mismo, es importante realizar el estudio en condiciones lo más parecidas posibles a las fisiológicas del paciente, dentro de las limitaciones propias de los estudios de elementos finitos. Es realmente complejo analizar *in vivo* las

tensiones que se producen en el hueso de un paciente producidas por un impacto determinado. Por ello, la investigación se realizó mediante el uso de análisis dinámico de elementos finitos, es decir, aplicando un impacto, en vez de una fuerza estática que es la más frecuentemente utilizada en la mayoría de estudios (41–43). Si aplicamos en distintos materiales una fuerza de intensidad predeterminada y constante (fuerza estática), sin llegar a provocar la fractura, las tensiones que se generaran en el implante y el hueso circundante serán las mismas para cualquiera de los materiales investigados, porque la fuerza resultante está predeterminada y su flujo a través del material (tensiones internas) también. Esto es debido, por un lado, al postulado de Euler-Cauchy y por otro lado, al principio de Saint Venant, que postula que "…la diferencia entre los efectos de dos sistemas de cargas estáticamente equivalentes se hace arbitrariamente pequeña a distancias suficientemente grandes de los puntos de aplicación de dichas cargas…" (44). Es por este motivo que el uso de impacto nos ayuda a dar una respuesta más cercana a la realidad fisiológica.

Una vez comprobado con la primera investigación que la tensión generada en la corona, el pilar y en el hueso cortical podía variar considerablemente dependiendo del material de rehabilitación utilizado, se quiso comprobar cuál sería la tensión en el hueso trabecular, sin la presencia del hueso cortical, dependiendo del material rehabilitador utilizado. Así mismo, siendo conocedores de que hay ciertas circunstancias en las que la ausencia de hueso cortical periimplantario puede suceder, como es el caso de pacientes con enfermedad periimplantaria activa, pacientes que llevan implantes en una zona en la que se ha realizado una regeneración ósea guiada con xenoinjerto o aloinjerto, en

implantes que se han colocado inmediatamente después de una extracción dental o en implantes con posición subcortical (45–49), quisimos conocer cuál sería la tensión recibida en el hueso trabecular en ausencia de la capa cortical y como repercutiría el hecho del uso de materiales menos rígidos para la rehabilitación sobre implantes unitarios.

La ausencia de hueso cortical puede conllevar un comportamiento distinto en el implante y la tensión generada en el hueso periimplantar debido a los impactos. Saber cuál es la tensión generada en el hueso trabecular en ausencia de hueso cortical dependiendo del material de rehabilitación que se está utilizando nos puede ayudar a decidir cuál es el material más adecuado para disminuir el riesgo de pérdida ósea.

III. HIPÓTESIS

Las tensiones transferidas a una prótesis implantosoportada y al hueso periimplantario cortical y trabecular por una fuerza oclusal de impacto varían según el material rehabilitador utilizado.

IV. OBJETIVOS

Objetivo general:

Estudiar las tensiones transferidas por fuerzas oclusales de impacto en prótesis unitarias implantosoportadas según el material rehabilitador.

Objetivos específicos

Evaluar las tensiones transferidas por una fuerza de impacto a la corona, al pilar y al hueso cortical periimplantario, según el material rehabilitador.

Evaluar las tensiones transferidas por una fuerza de impacto al hueso trabecular con presencia y ausencia de hueso cortical, según el material rehabilitador.

V. METODOLOGÍA

5.1.- Modelo

Se realizó un modelo 3D digital que simulaba una prótesis implantosoportada unitaria a nivel mandibular. El modelo estaba formado por una sección mandibular con hueso cortical y trabecular, un implante dental, un pilar protésico antirotatorio con un tornillo de fijación y una corona o rehabilitación protésica. Se asumió la total osteointegración del implante y la perfecta unión entre los distintos componentes de la rehabilitación. Por otro lado, se diseñó una superficie plana sobre la que impactaría el modelo (Fig.7).

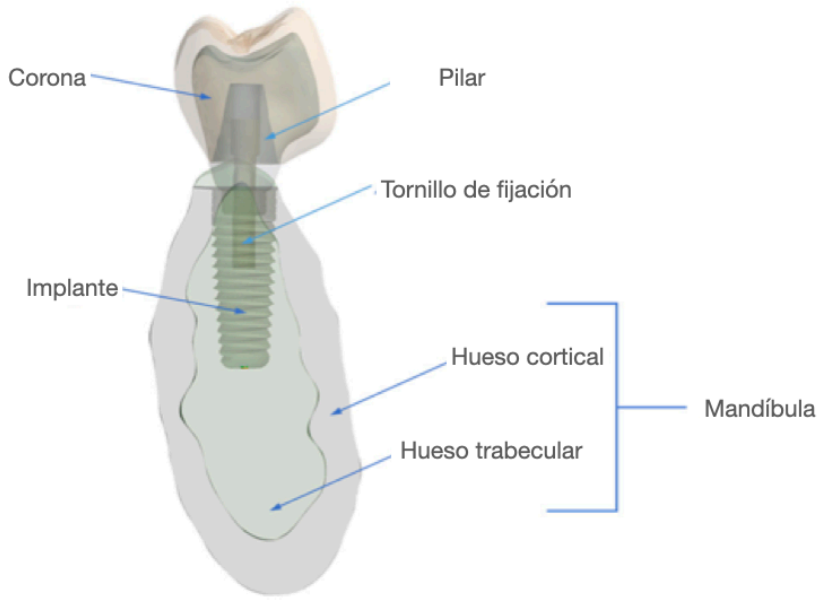

Fig. 7. Representación del modelo y partes.

5.1.1.- *La corona*

Para obtener un modelo sólido y poder realizar el análisis de elementos finitos, se diseñó un modelo 3D de una corona en el software Exocad (v3.0, Exocad GmbH, Darmstadt, Germany) y se importó al software SolidWorks (Dassault Systèmes, SolidWorks Corp., Waltham, MA, USA). Se crearon dos partes de la corona, el núcleo o estructura interna y el recubrimiento estético. El volumen total de la corona era de 411,5 mm^2, siendo la estructura interna el 51,3% del total y el otro 49,7% el recubrimiento estético (Fig.8).

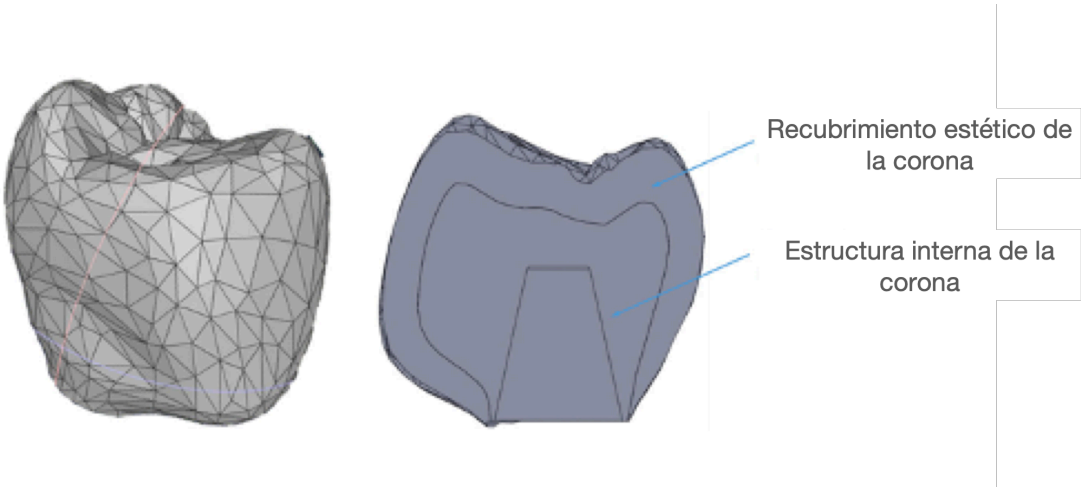

Fig.8. Representación del mallado 3D de la corona y sus partes.

5.1.2.- El pilar protésico y el tornillo de fijación

La función del pilar protésico es unir la corona con el implante. Se sujeta al implante mediante un tornillo. Además, el pilar tenía un mecanismo antirotatorio (un hexágono), para prevenir el movimiento rotacional entre el complejo pilar-

corona y el implante. Tanto el pilar como el tornillo de fijación fueron modelados mediante el software CAD de SolidWorks v.2021. El diseño original del pilar corresponde a un pilar protésico de la empresa MIS Implants Tech (MIS Implants Technology, Bar-Lev, Tel Aviv-Yafo, Israel), teniendo como sistema antirotatorio una conexión hexagonal interna (Fig.9).

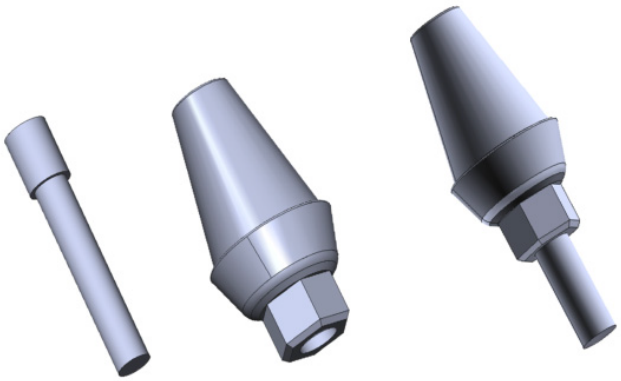

Fig. 9. Representación del pilar protésico con sistema antirotatorio y el tornillo de fijación.

5.1.3.- El implante

Se realizó el escaneado de un implante MIS SEVEN (MIS Implants Technology, Bar-Lev, Tel Aviv-Yafo, Israel) de 4,2x11,5 mm con conexión interna hexagonal mediante un escáner digital 3D (Visual Computing Lab, Pisa, Italy). El escaneado se convirtió a una malla en archivo STL (Standard Tessellation Language) y, posteriormente, a un modelo sólido con el software de SolidWorks. Así se obtuvieron las medidas del implante y finalmente se modeló con el software de

SolidWorks para garantizar la máxima precisión de la geometría de todos los componentes (Fig. 10).

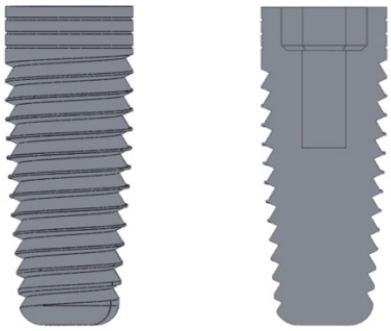

Fig.10. Esquema del implante.

5.1.4.- La mandíbula

La sección de hueso mandibular fue diseñada a través de la imagen de un CBCT (NewTom Giano, Newtom, Imola, Italia). Se dibujaron unos puntos de referencia a una distancia fija sobre la imagen de la sección mandibular para transferirlo al ordenador y la geometría se obtuvo con el software de SolidWorks midiendo las distancias de los distintos puntos. Con ello se crearon dos cuerpos sólidos: la estructura correspondiente al hueso cortical y la correspondiente al hueso trabecular o esponjoso (Fig.11).

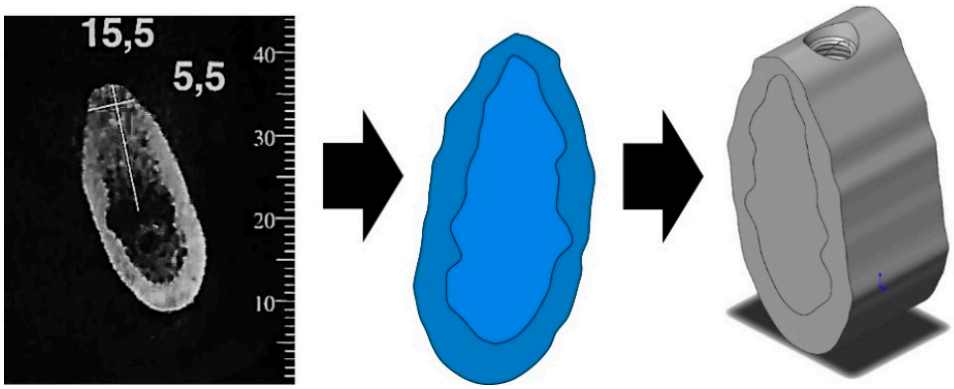

Fig. 11. CBCT de una sección mandibular transferida a la geometría 3D.

5.1.5.- La placa

Se necesitaba una superficie rígida sobre la que impactaría todo el conjunto corona-pilar-implante-hueso mandibular. Para ello se diseñó una superficie rectangular (w= 10mm, h= 12mm, e= 2mm) (Fig. 12). La distancia inicial entre la superficie y la corona fue de 0,01 mm y se consideró que el impacto sería sin fricción.

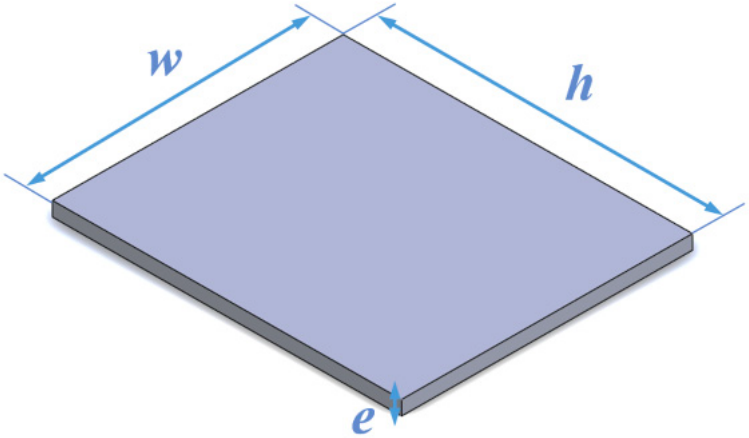

Fig.12. Representación de la placa sobre la que impacta el modelo.

5.2.- Opciones de rehabilitación estudiadas

Utilizando el mismo modelo de corona, se decidió comparar las distintas tensiones generadas en la corona, el pilar y el hueso periimplantar a partir de la aplicación de una fuerza de impacto a al modelo con los distintos materiales rehabilitadores.

Los materiales de rehabilitación y las combinaciones seleccionadas para el estudio fueron:

-FCOM: Corona con estructura interna de fibra de carbono (BioCarbon Bridge fibers. Microdemica, Italia) y recubrimiento estético de composite (Composite BioXfill. Micromedica, Italia).

-MCER: Corona con estructura interna de aleación de metal de Cr-Co (Renishaw, Gran Bretaña) y recubrimiento estético de cerámica (Ceramic VMK 95. Vita. Alemania).

-MCOM: Corona con estructura interna de aleación de metal (Renishaw. Gran Bretaña) y recubrimiento estético de composite (Composite BioXfill. Micromedica. Italia).

-MET: Corona completamente de aleación metálica de Cr-Co (Renishaw. Gran Bretaña).

-FCCER: Corona con estructura interna de fibra de carbono (BioCarbon Bridge fibers. Microdemica. Italia) y recubrimiento estético de cerámica (Ceramic VMK 95. Vita. Alemania).

-PKCOM: Corona con estructura interna de PEEK (Invibio. Alemania) y recubrimiento estético de composite (Composite BioXfill. Micromedica. Italia).

Con estos materiales se pretendía tener una representación de algunos de los distintos materiales existentes en el mercado, tanto clásicos como nuevos y que divergieran en sus propiedades físico-mecánicas.

5.3.- Propiedades de los materiales

Todos los materiales utilizados para el modelo se consideraron como isotrópicos y homogéneos. Los módulos de Young, el Coeficiente de Poisson y densidad se muestran en la Tabla 1. Las propiedades físicas y mecánicas de los diferentes materiales se consiguieron de los fabricantes de los mismos.

	Material	Fabricante	*E* Modulo de Young (MPa)	*v* Coeficiente Poisson	*ρ* Densidad (g/cm^3)
Corona	**FCOM** Corona de fibra de carbono-composite BioCarbon Bridge fibers Composite BioXfill	[86] Micro-Medica Micro-Medica	 300.000 22.000	 0,3 0,3	 1,40 8,30
	MCER Corona de Meta-Cerámica Aleación de Cr-Co Cerámica VMK 95	[87,88] Renishaw Vita	 208.000 69.000	 0,31 0,28	 8,90 2,50
	MCOM Corona de Metal-Composite Aleación de Cr-Co Composite BioXfill	[87,86] Renishaw Micro-Medica	 208.000 22.000	 0,31 0,3	 8,90 8,30
	MET Corona completamente metálica Aleación Cr-Co, Mo, W	[89] Heraeus Kulzer	 208.000	 0,31	 8,90
	FCCER Corona de Fibra de carbono-Cerámica Carbon Fiber Bridge Ceramic IPS e.max	[86,90] Micro-Medica Ivoclar Vivadent	 66.000 95.000	 0,3 0,2	 1,4 2,5
	PKCOM Corona de PEEK-composite PEEK Optima Composite BioXfill	[91,86] Invibio Micro-Medica	 4.100 22.000	 0,36 0,3	 1,3 8,30
Implante	Ti-6-Al-4V ELI	MIS [92]	113.800	0,34	4,43
Hueso	Hueso Cortical	[93,94]	15.000	0,3	1,79
	Hueso Trabecular	[93]	500	0,3	0,45

Tabla 1. Propiedades físicas y mecánicas de los materiales utilizadas en el estudio.

5.4.- Método numérico

Todos los modelos independientes se ensamblaron en un solo modelo, generando un modelo integrado por la prótesis, el implante y la sección de hueso mandibular. Este modelo geométrico fue convertido a un archivo IGS (Graphics Exchange Specification). Mediante el programa Ansys Workbrench Software (Ansys Inc., Canonsburg, PA, USA) se determinó la tensión transferida a la corona, al pilar protésico de titanio y al hueso cortical y esponjoso (dependiendo del estudio realizado), cambiando las características de los materiales de rehabilitación protésica.

Se simuló un impacto entre el modelo formado por el conjunto prótesis-implante-hueso contra la placa diseñada fijada y rígida a una velocidad de 1m/s y con un desplazamiento libre (*gap*) de 0,01mm.

Para tener un resultado preciso, el tamaño del modelo a nivel de nodos es muy importante. El modelo de elementos finitos tenía 96.160 nodos. En cuanto a las condiciones del contorno se consideró una serie de particularidades para el análisis de elementos finitos: todos los materiales eran isótropos y homogéneos, los desplazamientos se realizaban solo en dirección vertical, se asumió la perfecta osteointegración del implante en el hueso y que finalmente el impacto era contra un cuerpo rígido y no había fricción.

5.5.- Definición de la malla

Antes de realizar la simulación se tuvo que definir el tamaño de la malla y el tipo de elemento utilizado. La precisión de los resultados dependen directamente del tamaño de los elementos, es decir, a menor tamaño mayor precisión. Sin embargo, esto afecta al tiempo de trabajo computacional, no tan importante en un análisis estático, pero sí en un análisis dinámico, al repetirse el cálculo muchas veces, uno para cada instante de tiempo a lo largo del impacto.

En las zonas donde se requería mayor precisión, puntos de estudio y parte externa del implante (espiras), la distancia entre los elementos fue de 0,2 mm. En el resto de la corona e implante, la distancia variaba entre los 0,5 mm y los 2 mm. Aunque las diferentes partes estaban ensambladas se consideraron las partes por separado para el análisis de los resultados (fig.13).

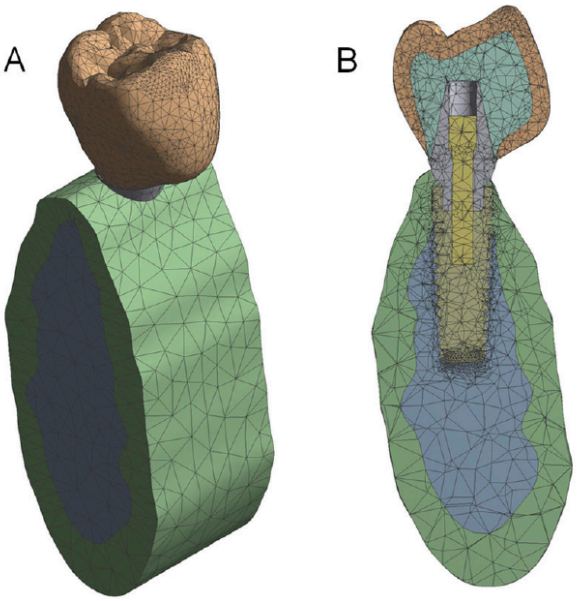

Fig.13. A. Imagen del modelo mallado 3D con sus nodos. B. Sección del mallado.

5.6.- Duración del impacto y de la simulación

Se estableció una duración de la simulación de 0,4 ms, para asegurar que fuera superior a la duración del impacto. Dentro de este tiempo se establecieron 53 momentos de valoración con un intervalo entre ellos de 7,55 µs. Si el tiempo hubiera sido más pequeño, el tiempo de trabajo del análisis computacional se hubiera incrementado mucho; si hubiera sido mayor la precisión hubiera sido disminuido.

5.7.- Configuración de la simulación

Inicialmente el complejo compuesto por la sección mandibular-implante-prótesis al impactar contra la superficie plana tiene una energía cinética que viene dada por la masa del modelo y su velocidad de acuerdo a la fórmula:

$$E_k = \sum \frac{1}{2} \cdot m_i \cdot v^2$$

Donde:

E_k es la energía cinética
m_i es la masa
v_i es la velocidad

Cuando el conjunto del modelo impacta contra la superficie de la placa rígida, la energía cinética se transforma en energía de deformación. Si la deformación ocurre dentro del rango elástico, la energía de deformación elástica puede obtenerse de la ecuación:

$$E_{def} = 1/2 \int_V \sigma_i \cdot \varepsilon_i \cdot dV$$

Donde:

E_{def} es la energía potencial elástica de deformación
σ_i es el estado de tensión
ε_i es el estado de deformación
dV es el diferencial de volumen

Las características dinámicas de un impacto están determinadas por la energía inicial del sistema ($0{,}5 \cdot m \cdot v^2$) y el momento lineal ($m \cdot v$). Ambas características deben tener el mismo valor para todos los modelos simulados, lo que se garantiza introduciendo la misma velocidad (v) y la misma masa total del sistema (m).

Como se observa en el cuadro de las propiedades de los materiales, cada uno de ellos tiene distinta densidad. Así pues, la masa inicial del sistema en cada uno de los casos propuestos de distinta rehabilitación sería diferente y en consecuencia también la energía cinética. A fin de igualar la energía cinética en cada uno de los casos, se añadió un valor de masa en los planos laterales de la sección mandibular (no en el implante) dependiendo de la densidad de cada uno de los materiales de los modelos. La tabla 2 muestra la masa adicional añadida en cada modelo.

Modelo	Masa Inicial (g)	Masa añadida (g)
MET	8.62	0
MCER	6.73	1.89
MCOM	6.63	1.99
FCOM	5.23	3.39
PKCOM	7.20	1.42
FCCER	5.07	3.55

Tabla.2. Compensación de la masa adicional añadida en cada modelo.

5.7.1.- Configuración de la simulación sin hueso cortical

Cuando se realizó el estudio sin hueso cortical se realizaron dos cambios en el modelo. En primer lugar, se suprimió del modelo la parte cortical del conjunto y se mantuvo intacto el resto de la malla y, en segundo lugar, se añadió masa para igualar la energía cinética del impacto y poder comparar con la situación de modelo con hueso cortical. Esta masa añadida corresponde al hueso cortical suprimido siendo constante para todos los modelos (2,27g). La Tabla 3 muestra la masa añadida para poder realizar la comparación. La masa se añadió en todo el conjunto del modelo.

Modelo	Masa añadida con cortical (g)	Masa añadida sin cortical (g)
MET	0	2.27
MCER	1.89	4.16
MCOM	1.99	4.26
FCOM	3.39	5.66
PKCOM	1.42	3.69
FCCER	3.55	5.82

Tabla 3. Compensación de la masa adicional añadida en los modelos con y sin cortical.

5.8.- Condiciones iniciales del contorno

En el análisis dinámico de elementos finitos la condición más relevante es la velocidad inicial que nos determina la energía cinética inicial del modelo.

Los distintos conceptos de energía nos permiten relacionar la masa del modelo y la velocidad aplicada como condiciones iniciales del contorno. Se calculó la masa de cada uno de los modelos, como se ha descrito anteriormente, y se compensaron sus

diferencias según las distintas densidades de los materiales. La velocidad aplicada al modelo fue de 1m/s como condición cinemática inicial.

Este dato importante en las condiciones iniciales de contorno se tomó de algunos estudios que se focalizan en la cinemática mandibular mediante acelerómetros y que dieron como resultado una aceleración máxima al abrir la boca de 2,5 m/s^2 (13,14,50). Considerando esto y teniendo en cuenta que estamos tratando con un movimiento controlado por el cerebro, se puede suponer la misma aceleración (*a*) durante la oclusión. De manera que mediante la siguiente fórmula podemos definir la velocidad (*v*):

$$v = a \cdot \Delta t \quad (1)$$

Donde:

v es la velocidad
a es la aceleración
Δt es el incremento el tiempo

Considerando que el contacto dental en la masticación dura menos de 0,5 segundos según la ecuación anterior podemos definir como un valor razonable para la velocidad de 1,25 m/s.

La placa utilizada para el impacto se supuso fija, es decir, que no podía moverse ni rotar en ninguna dirección. La distancia libre entre la placa y la corona fue de 0,01mm. Las superficies laterales del hueso cortical y trabecular estaban fijadas en el eje z y en el eje x de manera que solo se podían desplazar en el eje y ,es decir, de manera vertical.

5.9.- Selección de los nodos

Se decidió valorar las tensiones de von Mises obtenidas a través del tensor de tensiones de Cauchy en la corona (debajo del material estético de recubrimiento), el pilar, el hueso cortical y el hueso trabecular (dependiendo del estudio realizado).

VI. RESULTADOS DE LA INVESTIGACIÓN

1º Artículo publicado

"A 3D Finite Element Analysis Model of Single Implant-Supported Prosthesis under Dynamic Impact Loading for Evaluation of Stress in the Crown, Abutment and Cortical Bone Using Different Rehabilitation Materials"

Oriol Cantó-Navés, Raul Medina-Galvez, Xavier Marimon, Miquel Ferrer, Óscar Figueras-Álvarez y Josep Cabratosa-Termes

Citación:

Cantó-Navés O, Medina-Galvez R, Marimon X, Ferrer M, Figueras-Álvarez Ó, Cabratosa-Termes J. A 3D Finite Element Analysis Model of Single Implant-Supported Prosthesis under Dynamic Impact Loading for Evaluation of Stress in the Crown, Abutment and Cortical Bone Using Different Rehabilitation Materials. Materials (Basel). 2021 Jun 24;14(13):3519. doi: 10.3390/ma14133519. PMID: 34202625; PMCID: PMC8269525.

Rango de la revista: JCR - Q1 (*Metallurgy & Metallurgical Engineering*) / CiteScore - Q2 (*Condensed Matter Physics*) Q2 *(Dentistry)*

Factor de impacto: 3.623 (2020) ; 5-Años factor de impacto: 3.920 (2020)

Contribución del doctorando:

El doctorando ha contribuido en la conceptualización, investigación y validación; en la redacción del borrador original; articulo final, su revisión y edición.

A 3D Finite Element Analysis Model of Single Implant-Supported Prosthesis under Dynamic Impact Loading for Evaluation of Stress in the Crown, Abutment and Cortical Bone Using Different Rehabilitation Materials

Oriol Cantó-Navés [1], Raul Medina-Galvez [1], Xavier Marimon [2,3]*, Miquel Ferrer [4], Óscar Figueras-Álvarez [1] and Josep Cabratosa-Termes [1]

[1] Faculty of Dentistry, Universitat Internacional de Catalunya (UIC), 08017 Barcelona, Spain; oriolcanto@uic.es (O.C.); ruldoc@uic.es (R.M.G.); ofigueras@uic.es (O.F.A); cabratosa@uic.es (J.C.T.)
[2] Bioengineering Institute of Technology, Universitat Internacional de Catalunya (UIC), 08190 Barcelona, Spain
[3] Automatic Control Department, Universitat Politècnica de Catalunya (UPC-BarcelonaTECH), 08034 Barcelona, Spain
[4] Department of Strength of Materials and Structural Engineering, Universitat Politècnica de Catalunya (UPC-BarcelonaTECH), 08034 Barcelona, Spain; miquel.ferrer@upc.edu (M.F)
* Correspondence: xmarimon@uic.es (X.M)

Abstract: In the literature, many researchers investigated static loading effects on an implant. However, dynamic loading under impact loading has not been investigated formally using numerical methods. This study aims to evaluate, with 3D finite element analysis (3D FEA), the stress transferred (maximum peak and variation in time) from a dynamic impact force applied to a single implant-supported prosthesis made from different materials. A 3D implant-supported prosthesis model was created on a digital model of a mandible section using CAD and reverse engineering. By setting different mechanical properties, six implant-supported prostheses made from different materials were simulated: metal (MET), metal-ceramic (MCER), metal-composite (MCOM), carbon fiber-composite (FCOM), PEEK-composite (PKCOM), and carbon fiber-ceramic (FCCER). Three-dimensional FEA was conducted to simulate the collision of 8.62 g implant-supported prosthesis models with a rigid plate at a speed of 1 m/s after a displacement of 0.01 mm. The stress peak transferred to the crown, titanium abutment, and cortical bone, and the stress variation in time, were assessed.

Keywords: FEA; FEM; impact test; transient analysis; dynamical forces; biomechanical behavior; implant rehabilitation; rehabilitation materials; crown materials

1. Introduction

Currently, implant-supported prostheses are widely used for the rehabilitation of partially and fully edentulous patients. This type of treatment has undergone significant changes in the choice of materials since the first treatments carried out by Brånemark. The use of gold or gold alloys, with and without resin veneering (51,52), has been discarded for economic, esthetic, and functional reasons (53–55). The increase in the price of gold led to the use of much cheaper non-noble metals, although with different mechanical and biological characteristics (53–56). The composites and resins used at the end of the last century showed significant deficiencies in esthetics and wear; they were replaced by ceramics and, currently, by zirconia, (56–59) with different mechanical characteristics. The choice of the material used for implant-supported

prosthesis manufacturing is a crucial issue due to the dynamic characteristics of the stomatognathic system.[1]

Static forces are applied from the mandible to the maxilla, without mandibular movements, and the intensity remains constant over time. In contrast, dynamic forces are related to mandibular movements, and the intensity varies with time. The dynamic force magnitude is calculated by multiplying the mass of the moving object and its acceleration in that direction. Static (clenching) and dynamic forces (chewing, swallowing, and eccentric bruxism) occur in the masticatory system (12,14,20,50,60,61). The literature shows that forces are transferred to a lesser or greater extent to the peri-implant area (62) depending on whether the applied force is static or dynamic (63–70). Moreover, the results in recent publications showed that static loading, compared with dynamic loading, caused increased stress, which proves the need of transient analysis of dental implants (38,41).

The chosen material for single implant-supported prostheses manufacturing has little relevance in the transmission of static forces, as explained in the Saint-Venant principle, which states that the difference between the effects of two different but statically equivalent loads becomes minimal at sufficiently large distances from the load (44,71,72) Dynamic forces and the impact of the moving mandible against the maxilla are transferred very differently in single and multiple implant-supported prostheses, depending on the material that the prostheses are made from. Rigid materials, such as zirconia, ceramics, and metals, generate higher dynamic forces (63,65–67) than other materials used in veneering prosthetic frameworks (composites, hybrid composites, or resins) or in prosthetic framework manufacturing (carbon fiber, fiberglass, or polyether-ether-ketone (PEEK)), which absorb and dissipate the impact energy with lower dynamic forces [28–40].

There are different in vitro methods for studying the transmission of static and dynamic forces to the peri-implant area from single and partial implant-supported prostheses made from different materials, such as the use of photoelastic resins (44,64,83–85), digital image correlation (DIC) (44,86,87), strain gauges (65,88), loss coefficient (LC) (67), and finite element analysis (FEA) in two (2D FEA) and three dimensions (3D FEA) (43,68–70,89–92). All of them provide very similar results (44,93–95) in terms of stress.

Photoelastic resins allow visualizing the stress generated in the peri-implant area after the application of a static or dynamic force with isochromatic fringes. The color and number of the shown isochromatic fringes indicates the magnitude of the generated stress. Digital image correlation (DIC) is an optical-numerical system using resins with randomly colored microdots, where the displacement of these microdots is calculated after the application of a force, both vertically and horizontally. The magnitude of transferred forces is determined according to the magnitude of the displacements.

Magne et al. (67) used the Periometer (University of Southern California, Los Angeles, CA, USA) to calculate the energy absorbed by prostheses made with different frameworks and veneer materials, such as composite, ceramic, and zirconia. The Periometer is a handheld percussion probe that records the rebound suffered by the object of study, so the energy absorbed by the material can be calculated by subtracting the applied force and the rebound force.

Another system is the use of strain gauges, which are sensors that measure the material strain when loads are applied. Gracis (65) recorded the impact force transmitted by a steel ball rolled along a slope to discs made from different materials. Menini (63,66), used strain gauges to design a device that applied oscillating movements to monolithic prostheses of different materials (gold, zirconia, ceramics, composites, and resins) against an upper dental arch made of a Co-Cr alloy. The force transferred to the crowns (made from different materials) by the simulation of the mandibular movements was recorded.

Dental biomechanics based on finite element analysis (FEA) is attracting huge interest in many areas: biomedical sciences, anthropology and, odontology. However, several shortcomings

in FEA modeling exist, mainly due to unrealistic (static) loading imposition (96). FEA analysis is the most widely used numerical procedure today, since it allows reproducing mechanical behavior under a mechanical load based on the known properties of the material. Density, the Poisson coefficient, and Young's modulus values can be set in 2D or 3D FEA software, which also includes the depth dimension. Three-dimensional FEA permits the visualization of the stresses on the entire body of the implants. In the consulted dental literature, dynamic FEA studies are still scarce (34,38,41,96–98) compared to the large number of existing FEA studies with static loads. Moreover, very few studies that simulate dynamic forces under impact loading using 2D or 3D FEA have been found. Thus, this article is devoted exclusively to the study of the impacts on dental implants, which is minimally covered in the literature.

Knowledge about stress distribution in the peri-implant area may be essential for predicting the survival of dental implants, especially in patients with risk factors such as smoking, poor hygiene habits, previous periodontitis, or predisposing genetic factors (1,7,47,99,100). These patients present, to a greater or lesser extent, gingival inflammation that may cause peri-implant bone loss (2,6,9,10,45,101–104). This peri-implant bone loss may be directly affected by the stress generated in the implant-bone-prosthesis area; the higher the transferred force, the higher the risk of peri-implantitis (16,67,105–110). The amount of cortical bone could also be a factor to be considered when choosing the material for manufacturing the prosthesis, as this cortical bone is poorly vascularized, fragile, rigid, and regenerates slowly (48,111–114).

Numerous studies have shown, using 2D or 3D FEA, the behavior of implants rehabilitated with single crowns made with different materials. In these studies, all of them used a static force to simulate the oral environment. Our study has aimed to show, using dynamic 3D FEA, the dynamic impact forces related to oral function.

This in vitro study aims to evaluate, with three-dimensional finite element analysis (3D FEA), the stress transferred (time to peak, maximum peak, and variation in time) from an impact, a dynamic force, on a single implant-supported prosthesis made from different restorative materials (metal, metal-ceramic, metal-composite, carbon fiber-composite, PEEK-composite, and carbon fiber-ceramic), applied to the crown, titanium abutment, and cortical mandibular bone.

2. Materials and Methods

2.1. The Whole Implant Model

The 3D digital model simulated dental rehabilitation on the implants used in this study to evaluate the stress (von Mises stress) on the inner part of the crown, the external part of the neck of the titanium abutment, and the top of the cortical bone, using different implant crowns in a dynamic situation (chewing, swallowing, or eccentric bruxing). This was obtained from the integration of six independently developed models from real elements: (1) the crown, (2) an anti-rotatory abutment, (3) a fixation screw, (4) a single implant-supported prosthesis, (5) a section of the mandibular bone (cortical and cancellous bone), and (6) the plate. Total osseointegration of the implant was considered, assuming a perfect relation between the nodes at the interface of the implants and the bone.

2.1.1. The Crown

In order to obtain a solid model of the crown, a high-resolution 3D Exocad model was imported to SolidWorks. Then, two parts were created within the crown geometry (the core and the esthetic veneering), separated by an inner boundary. The framework and the veneering material were delimited from the single implant-supported prosthesis. The total volume of the crown was 411.5 mm^3. The framework core accounted for 51.3% of the total crown volume, and the remaining 39.7% was esthetic veneering.

2.1.2. The Abutment and Fixation Screw

The abutment's function is to join the crown and the implant with a thread mechanism. Also, an anti-rotation system must be available to prevent the relative movement between the implant and the abutment (in this case, a hexagonal anti-rotational system). The abutment and the fixation screw were fully modeled using the CAD software SolidWorks v.2021 (Dassault Systèmes, SolidWorks Corp., Waltham, MA, USA) [85] in order to reduce the typical surfaces of a 3D [2]scanning process to triangular forms, thus maintaining simpler geometries. The abutment used in this study was the MIS implant with an internal hexagonal connection.

2.1.3. The Implant

Accurate measurements of implant geometry were obtained by 3D digital scan (Visual Computing Lab, Pisa, Italy) of a 4.2 × 11.5 mm implant with an internal hexagon (MIS Implants Technology, Bar-Lev, Tel Aviv-Yafo, Israel), which was converted into an STL (Standard Tessellation Language) mesh. Then, it was converted into a solid with the SolidWorks Software (Dassault Systèmes, Vélizy-Villacoublay, France) in order to obtain the measurements of the implant. Finally, it was modeled with the CAD SolidWorks software in order to guarantee more precise geometry and to avoid too many surfaces being shown.

2.1.4. The Mandible

The section of the mandible bone was designed from a sectional image of cone-beam computed tomography (CBCT) (NewTom Giano, Newtom, Imola, Italy). Keypoints were drawn at a fixed distance over the section image of the CT scan in order to transfer it to the computer. The geometry of the mandible could be obtained with SolidWorks software by measuring the distances of the points and calculating the real value through the scanning scale. Two different bounded solids were created over the mandible geometry to apply the mechanical properties of both trabecular and cortical bone.

Kerrypnx	Material Name	Manufacturer	*E* Young Modulus (MPa)	*v* Poisson Ratio	*ρ* Density (g/cm^3)
Crown	**FCOM**				
	Carbon fiber-composite	[86]			
	BioCarbon Bridge fibers	Micro Medica	300,000	0.3	1.40
	Composite BioXfill	Micro Medica	22,000	0.3	8.30
	MCER				
	Metal-ceramic	[87,88]			
	Co-Cr alloy	Renishaw	208,000	0.31	8.90
	Ceramic VMK 95	Vita	69,000	0.28	2.50
	MCOM				
	Metal-composite	[87,86]			
	Co-Cr alloy	Renishaw	208,000	0.31	8.90
	Composite BioXfill	Micro-Medica	22,000	0.3	8.30
	MET	[89]			
	Full metal				
	Co-Cr Alloy, Mo, W	Heraeus Kulzer	208,000	0.31	8.90
	FCCER	[86,90]			
	Carbon fiber-ceramic				
	Carbon Fiber Bridge	Micro-Medica	66,000	0.3	1.4
	Ceramic IPS e.max	Ivoclar Vivadent	95,000	0.2	2.5
	PKCOM				
	PEEK-composite	[91,86]			
	PEEK Optima	Invibio	4100	0.36	1.3
	Composite BioXfill	Micro-Medica	22,000	0.3	8.30
Implant	Ti-6-Al-4V ELI	MIS [92]	113,800	0.34	4.43
Bone	Cortical bone	[93,94]	15,000	0.3	1.79
	Trabecular bone	[93]	500	0.3	0.45

2.1.5. The Plate

A fixed rigid body with a flat surface was required to simulate impact loads on the tooth during chewing. To this end, a rectangular-shaped plate (w = 10, h = 12, e = 2 mm) was set up to apply the impact load on the three parts of the whole model: the crown, the implant, and the mandible. The initial distance between the plate and the crown was only 0.01 mm. The collision with the plate was frictionless. This means that a zero coefficient of friction was assumed and allowed free sliding. In addition, normal pressure equaled zero if separation occurred.

2.2. Material Properties

All materials were modeled as linear elastic isotropic and homogeneous. Young's modulus and Poisson ratio of each material are shown in Table 1. The mechanical properties of the different materials of the crowns have been provided by the manufacturers.

Abbreviated names of the crown materials are the following: FCOM is a carbon fiber-composite crown, MCER is a metal-ceramic crown, MET is a metal crown alloy (Cr-Co, Mo, and W).

Table 1. Properties of materials used in the prothesis and the bone (trabecular and cortical).

2.3. Numerical Methods

All independent models were put together by assembly modeling, generating a unique prosthesis-implant-bone model (Figure 1). The geometry was converted to an IGES file, and Ansys Workbench Software (Ansys Inc., Canonsburg, PA, USA) was used to determine the stress transferred to the crown, titanium abutment, and cortical bone before the FEA simulation by the implant-supported prosthesis made from different materials.

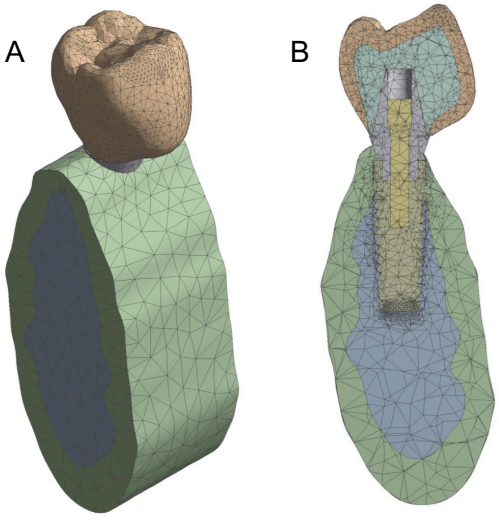

Figure 1. View of the whole 3D FEA model (**A**). Sectional model (**B**).

The prosthesis-implant-bone model was simulated to collide with a 10 × 12 × 2 mm fixed and rigid plate at a speed of 1 m/s after a displacement of 0.01 mm. For accurate results, the size of the elements is very important. The FEA model had 96,160 nodes and 62,606 elements to simulate the real models (prosthesis, implant, and bone) (see Figure 1). Young's modulus, Poisson's coefficient, and density were assigned to each material used in the manufacturing of the implant-supported prosthesis: CoCr (MET), CoCr-Ceramic (MCER), CoCr-Composite (MCOM), Carbon Fiber-Composite (FCOM), PEEK-Composite (PKCOM), Carbon Fiber-Ceramic (FCCER), the

titanium abutment, and the cortical bone of the model (Table 1). For the FEA, all materials were considered isotropic and homogeneous, displacements were only in the vertical direction, perfect osseointegration was assumed, the impact was carried out on a rigid object (plate), and, finally, the collision was frictionless.

2.3.1. Mesh Definition

Before performing the simulation with the finite element method, the mesh size and the element type must be defined. The accuracy of the results depends directly on the size of the elements. The smaller the elements, the more accurate the solution. Therefore, small elements were used in order to improve precision. However, this affected the computational time. While CPU time is not that important in static analyses, it is crucial in transient dynamic analyses.

The solid 3D element SOLID187 (Ansys Inc., Canonsburg, PA, USA) [85] was used, with 10 nodes and quadratic interpolation functions that are more suitable for irregular geometries. The element had three degrees of freedom per node, i.e., the three translations in the global coordinate directions x, y, z. Surface-to-surface contact was defined with the element CONTA174.

In the process of creating the mesh, a refinement process was carried out in order to obtain a stable solution independent of the mesh size, especially around the impact zone, thereby ensuring high accuracy in this area. Therefore, as this refinement had been done, it was not necessary to use an area to obtain an average solution, since the nodal solution was especially accurate. Thus, the corresponding mesh was then considered to be optimal.

In addition, Ansys software performs control of the aspect ratio systematically. The accuracy of the results depends directly on the size of the finite element mesh. The smaller the mesh, the more accurate the solution obtained. Near the loading point and the threaded part, where higher accuracy was needed, the size was 0.2 mm, but in the other parts it was larger, from 0.5 to 2 mm. Even if the different parts of the implant are assembled together, the finite element results can be analyzed independently. Six solids were considered individually: the crown, the abutment, the implant, the fixation screw, the mandible, and the plate.

2.3.2. Simulation Time

Regarding simulation time, 0.4 ms were simulated. The number of substeps is the number of intervals into which the simulation time is divided. That is to say, the calculation time-step between one instant to the next. If they are too small, the computing time increases considerably and, if they are set too high, the accuracy of the time-history response decreases. A value of 53 substeps, i.e., a time-step of 7.55 μs, was found to be reasonable.

3. Results

3.1. Stress Results

The von Mises stress value (obtained from a Cauchy stress tensor) was calculated over time in the dynamic FEA simulation and compared for each node (Figure 2) in a time interval of 0.4 ms. The stress peak values in the crown, titanium abutment, and cortical bone are summarized in Table 2.[3]

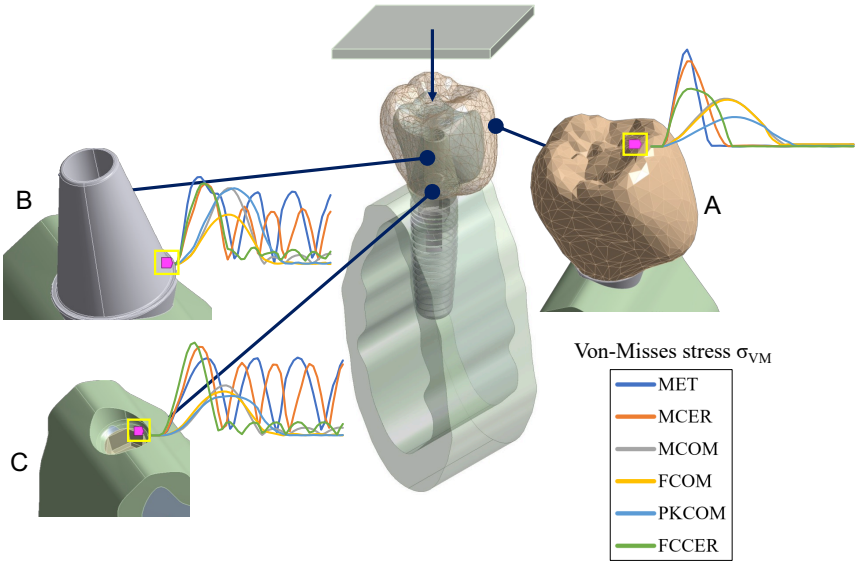

Figure 2. The nodes selected for numerical simulation. (**A**) Sectional view of the 3D FEA model at the crown node. (**B**) The abutment node. (**C**) The node on top of the cortical bone.

Table 2. Maximum equivalent von Mises stress transferred to the crown, the titanium abutment, and the cortical bone by the different prosthesis materials.

Node/Material	Maximum von Mises Stress σ_{VMmax} (MPa)					
	MET	**MCER**	**MCOM**	**FCOM**	**PKCOM**	**FCCER**
Crown	103.81	91.18	51.05	49.98	31.51	61.82
Abutment	89.27	81.91	77.82	50.80	77.78	82.80
Cortical	63.35	72.06	40.71	35.70	32.05	75.46

At the crown node (Figure 3) the maximum peaks were found at the MET and MCER crown, followed by that at FCCER. The lower values were found at MCOM and FCOM, and the lowest at the PKCOM crown.

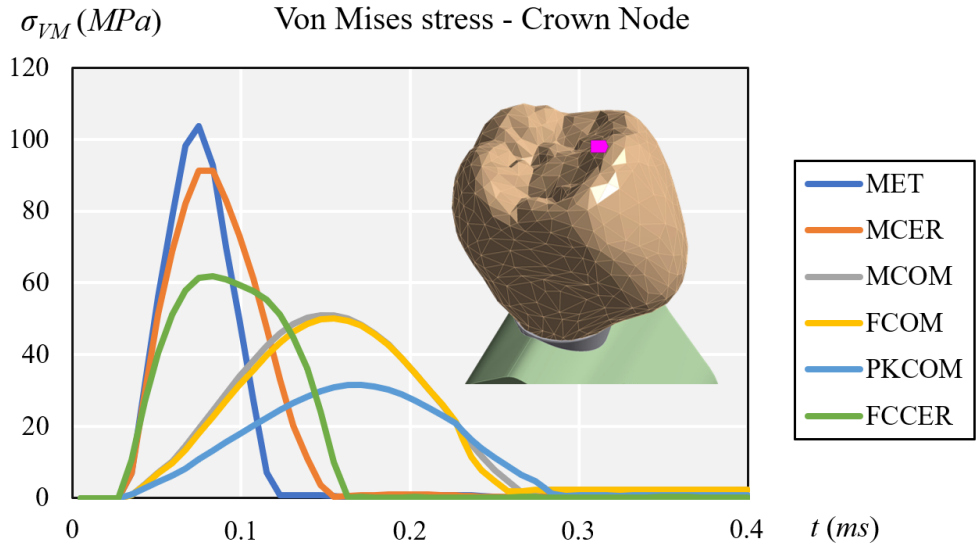

Figure 3. Comparison of equivalent von Mises stress at the crown node.

At the same time, Figure 4 compares the displacement of each crown during impact.

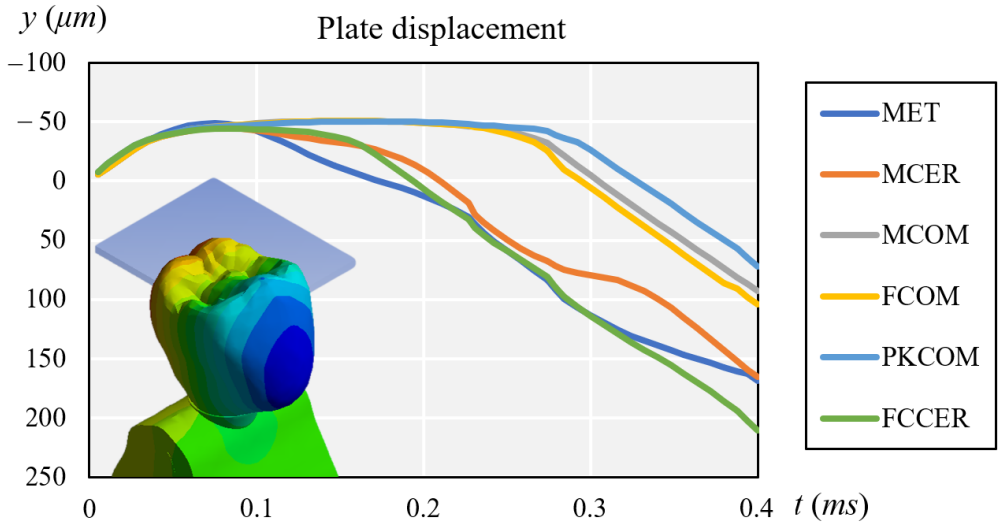

Figure 4. Comparison of plate displacement for each crown after impact.

All the crowns except FCOM showed high peak intensity values at the titanium abutment node (Figure 5). MET and MCER showed higher stress rebound over time, while MCOM, FCOM, PKCOM, and FCCER showed no rebound peaks after the impact (See Figure 5).

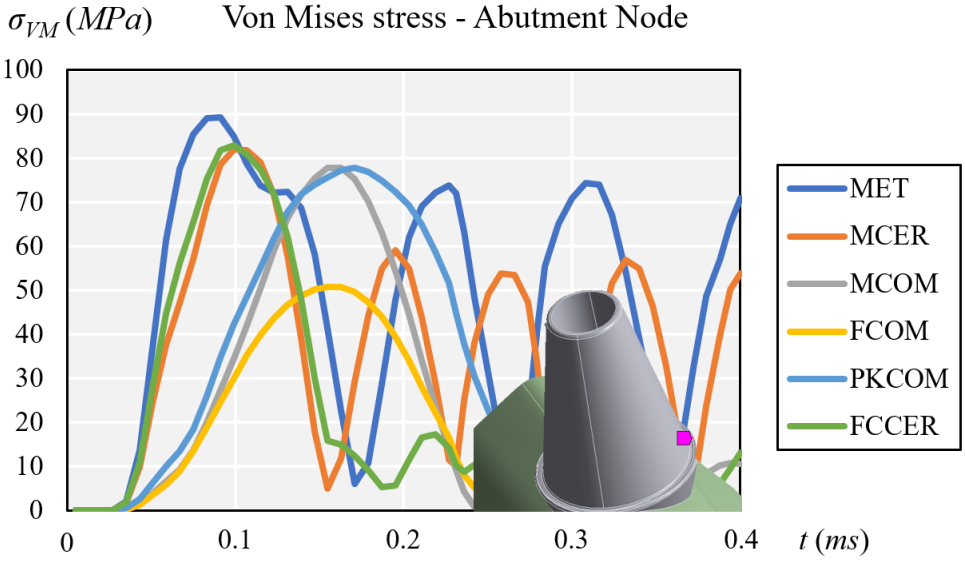

Figure 5. Comparison of equivalent von Mises stress at the titanium abutment node.

Composite-veneered implant-supported prostheses (MCOM, FCOM, and PKCOM) generated lower stress peaks at the cortical bone than ceramic-veneered (MCER and FCCER) or all-metal (MET) implant-supported prostheses. The implant-supported ceramic-veneered (MCER and FCCER) or all-metallic (MET) prostheses exhibited a more significant and earlier stress peak on the cortical bone than those veneered with composite (MCOM, PKCOM, and FCOM) (Figure 6). The highest stress rebound peaks happened in MET and MCER implant-supported prostheses. Implant-supported prostheses made of carbon fiber-ceramic (FCCER) showed the highest maximum peak of stress, but it dissipated quickly with rebound peaks of lower intensity. A rapid reduction in stress was observed in implant-supported prostheses

veneered with composite (MCOM, PKCOM, and FCOM) and in those made with carbon fiber-ceramic (FCCER) (Figure 6).[4]

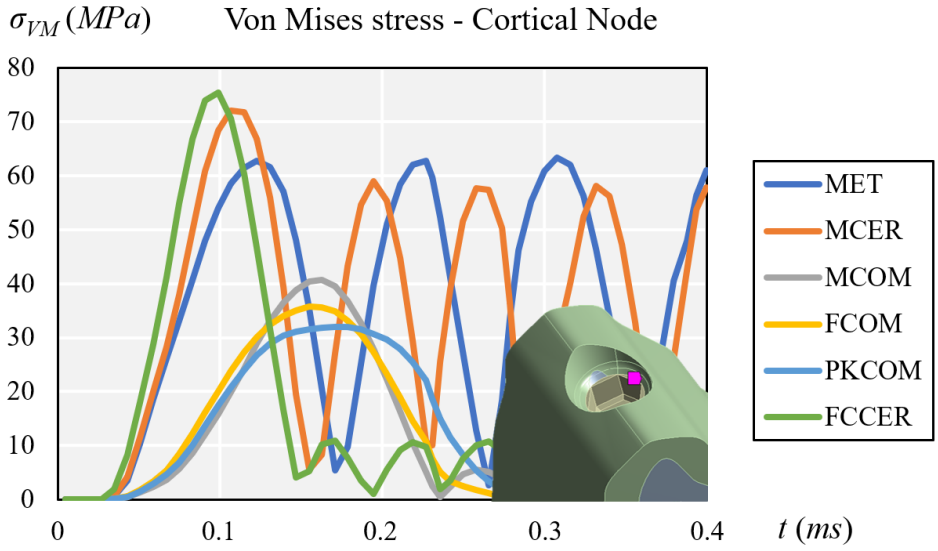

Figure 6. Comparison of equivalent von Mises stress at the cortical node.

3.2. Elastic Failure Test

A failure test was carried out to see if the dental implants could withstand the mechanical conditions to which they were subjected. Elastic failure criteria establish different approaches for different materials. In this case, the von Mises or maximum elastic distortion energy criterion was used. This criterion says that a structural element fails when at some point the distortion energy per unit volume exceeds a certain threshold. In stress terms, this means that the equivalent stress at a point, which is the von Mises stress, cannot exceed the elastic limit or the yield strength of the material, σ_y:

$$\sigma_{VM} \leq \sigma_y \tag{1}$$

Consequently, research on the elastic limits of the different materials was needed. After obtaining the values, a comparison was made for each model of the dental implant with each of the studied nodes used before. In Table 3, the yield stress, σ_y, and the maximum value of stress, σ_{VMmax}, are compared for each material and node. In this table, we can observe how the largest stresses occurred in the most rigid models.

[4] Materials 2021, 14, 3519. https://doi.org/10.3390/ma14133519

Table 3. Comparison of the yield stress, σ_y, and the maximum value of stress, σ_{VMmax}, for each material and node.

Material	Node	Yield Strength σ_y (MPa)	Maximum von Mises σ_{VMmax} (MPa)
MET	Crown	145–270	103.81
	Abutment	880–920	89.27
	Cortical	100–150	63.35
MCER	Crown	150	91.18
	Abutment	880–920	81.91
	Cortical	100–150	72.06
MCOM	Crown	280	51.05
	Abutment	880–920	77.82
	Cortical	100–150	40.71
FCOM	Crown	280	49.99
	Abutment	880–920	50.80
	Cortical	100–150	35.70
PKCOM	Crown	280	31.51
	Abutment	880–920	77.78
	Cortical	100–150	32.05
FCER	Crown	380	61.82
	Abutment	880–920	82.80
	Cortical	100–150	75.46

In order to prevent uncertainties that may occur when real loads act on the implant, a safety factor is used. The safety factor is defined as the ratio between the yield strength of the material and the maximum value of von Mises equivalent stress. A usually applied Safety Factor is 1.5.

$$\gamma_{SF} = \frac{\sigma_y}{\sigma_{VM}} = 1.5 \quad (2)$$

Taking yield strength as the 100% value and rearranging Equation (2):

$$\sigma_{VM} \leq \frac{100\% \cdot \sigma_y}{1.5} = 66.67\% \cdot \sigma_y \quad (3)$$

Figure 7 shows the yield strength ratio for each material and node. The red line indicates the 66.67% value of yield stress.

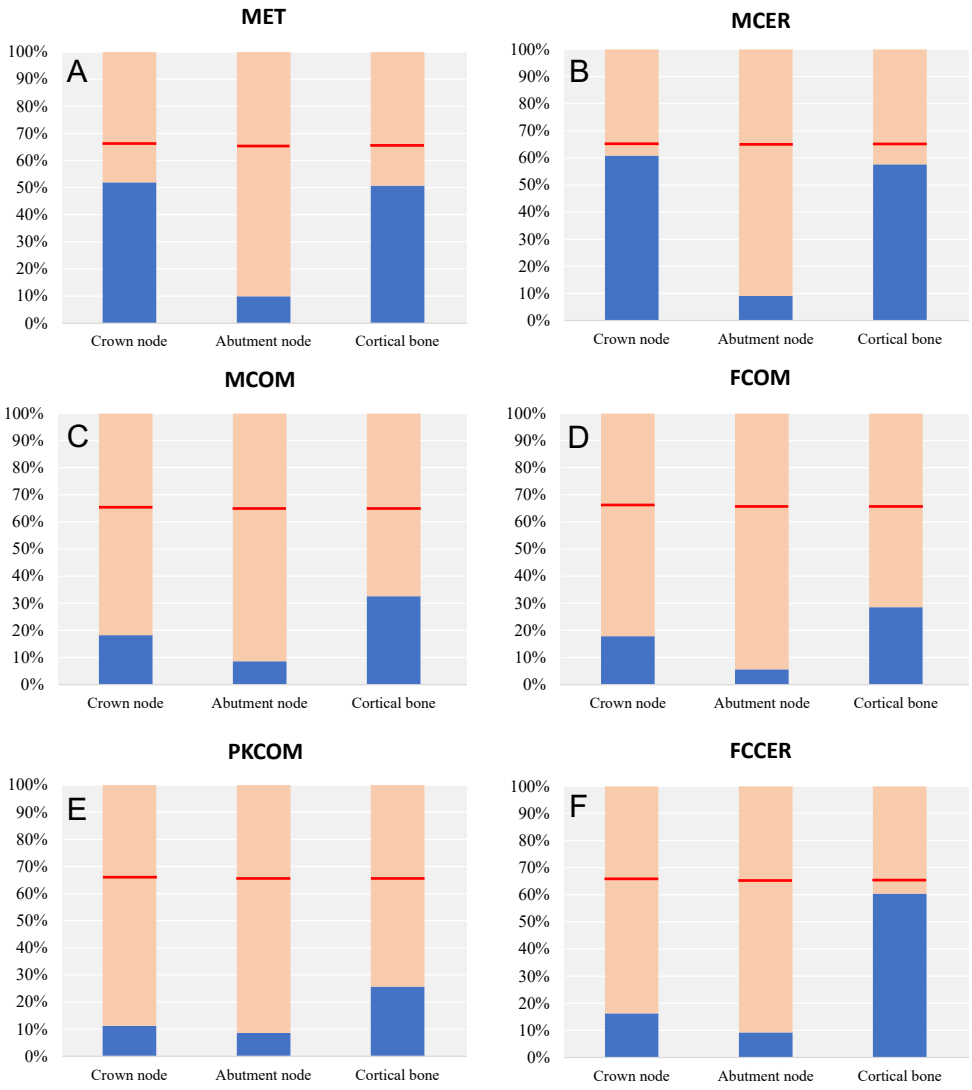

Figure 7. Comparison of the yield strength ratio depending on the node and crown material.

There was no elastic failure in any model, since all von Mises stresses were below the elastic limit, taking an arbitrary safety factor of 1.5. In the bar plots, we can observe how the von Mises stresses did not surpass 66.67% of the yield stress (red line). The most rigid models with the highest von Mises stresses were the ones closest to the 66.67% of the yield stress of each material.[5]

In summary, the assumption of linearity of the behavior of materials was fulfilled in the studied model, and the calculated stresses were below the yielding limits of the materials, so we can consider that there was no plasticization.

The spider plots of Figure 8 show a comparison between the yield strength, σ_y, of the materials and the maximum values of von Mises stress, σ_{VMmax}, obtained in the numerical simulations for each node.

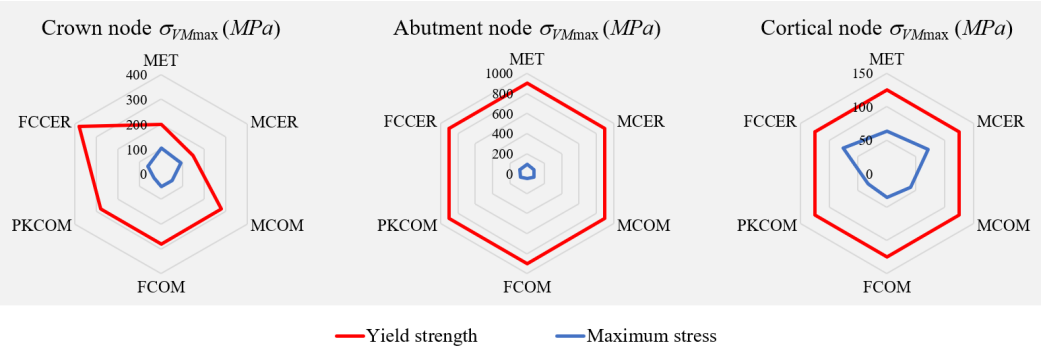

Figure 8. Spider plots comparing the yield strength of the materials and the maximum von Mises stress obtained for each node.

4. Conclusions

Denture forces, such as those from chewing, are transferred to implants and cause stress in the bone and the implant. That is why it is important to study the stresses (or strains) transferred to the implant and the bone in situations of maximum stress, modeled by dynamic forces under impact loading.

It can be concluded from the results of this study that the stress transferred to the crown, the abutment, and the peri-implant bone by an impact load on an implant-supported prosthesis varies according to the rigidity of the material and whether it is used as a framework or veneering material. It can also be stated that the more elastic material used for the crown, the lower the stresses generated in the bone. Too much stress induces bone resorption, which ultimately causes loosening of the implant, and overstrain can instigate bone failure. It turns out that the use of PEEK or carbon fibers as framework materials made stress dissipate faster than when using metal at the bone. By using these materials that can absorb and/or dissipate the stress transferred to the implant, we can reduce the risk of having bone resorption around the implant.

Therefore, with the use of more elastic materials that can better dissipate the impact energy and reduce the stress transferred to the implant, the risk of having bone resorption around the implant can also be reduced, especially in patients at risk of gingival inflammation that may cause peri-implant bone loss.

Author Contributions: Conceptualization, O.C.N., R.M.G., and J.C.T.; data curation, X.M.S.; formal analysis, X.M.S., M.F.B., and J.C.T.; funding acquisition, O.F.A. and J.C.T.; investigation, O.C.N. and X.M.S.; methodology, M.F.B.; project administration, J.C.T.; resources, O.C.N. and O.F.A.; software, X.M.S. and M.F.B.; supervision, O.F.A. and J.C.T.; validation, O.C.N., R.M.G., X.M.S., and O.F.A.; visualization, X.M.S.; writing—original draft, O.C.N. and X.M.S.; writing—review and editing, O.C.N., R.M.G., X.M.S., M.F.B., and J.C.T. All authors have read and agreed to the published version of the manuscript.

Funding: This research received no external funding.

Institutional Review Board Statement: Not applicable.

Informed Consent Statement: Not applicable.

Data Availability Statement: Not applicable.

Acknowledgments: We gratefully acknowledge the support of the NVIDIA Corporation with the donation of the Titan X Pascal GPU used for this numerical analysis.

Conflicts of Interest: The authors declare no conflicts of interests.

Abbreviations

MET	CoCr Metal
MCOM	CoCr Metal-Composite
MCER	CoCr Metal-Ceramic
FCOM	Carbon Fiber-Composite
PKCOM	PEEK-Composite
FCCER	Carbon Fiber-Ceramic

References

1. Jemt, T.; Lekholm, U.; Adell, R. Osseointegrated implants in the treatment of partially edentulous patients: a preliminary study on 876 consecutively placed fixtures. *Int. J. Oral Maxillofac. Implant* **1989**, *4*, 211–217.
2. Adell, R.; Eriksson, B.; Lekholm, U.; Branemark, P.I.; Jemt, T. Long-term follow-up study of osseointegrated implants in the treatment of totally edentulous jaws. *Int. J. Oral Maxillofac. Implant* **1990**, *5*, 347–359.
3. Roberts, H.W.; Berzins, D.W.; Moore, B.K.; Charlton, D.G. Metal-ceramic alloys in dentistry: A review. *J Prosthodont* **2009** ,*18* ,188–194.
4. Wataha, J.C. Biocompatibility of dental casting alloys: A review. *J. Prosthet. Dent*. **2000**, *83*, 223–234.
5. Tuna, S.H.; Pekmez, N.O.; Keyf, F.; Canli, F. The electrochemical propierties of four dental casting suprastructure alloys coupled with titanium implants. *J. App.l Oral Sci*. **2009**, *17*, 467–475.
6. Bagegni, A.; Abou-Ayash, S.; Rucker, G.; Algarny, A.; Att, W. The influence of prosthetic material on implant and prosthetic survival of implant-supported fixed complete dentures: A systematic review and meta-analysis. *J. Prosthodont. Res*. **2019**, *63*, 251–265.
7. Hu, M.L.; Lin, H.; Zhang, Y.D.; Han, J.M. Comparison of technical, biological, and esthetic parameters of ceramic and met-al-ceramic implant-supported fixed dental prostheses: A systematic review and meta-analysis. *J. Prosthet. Dent.* **2019**, *124*, 26–35.
8. Le, M.; Papia, E.; Larsson, C. The clinical success of tooth- and implant-supported zirconia-based fixed dental prostheses. A systematic review. *J. Oral Rehabil*. **2015**, *42*, 467–480.
9. Deany, I.L. Recent advances in ceramics for dentistry. *Crit Rev. Oral Biol. Med*. **1996**, *7*, 134–143.
10. Yamaguchi, S.; Okada, C.; Watanabe, Y.; Watanabe, M.; Hattori, Y. Analysis of masticatory muscle coordination during unilateral single-tooth clenching using muscle functional magnetic resonance imaging. *J. Oral Rehabil*. **2018**, *45*, 9–16.
11. Moss, R.A.; Villarosa, G.A.; Cooley, J.E.; Lombardo, T.W. Masticatory muscle activity as a function of parafunctional, active and passive oral behavioural patterns. *J. Oral Rehabil*. **1987**, *14*, 361–370.
12. Takeda, H.; Saitoh, K. Impact of proprioception during the oral phase on initiating the swallowing reflex. *Laryngoscope* **2016**, *126*, 1595–1599.
13. Safari, A.; Jowkar, Z.; Farzin, M. Evaluation of the relationship between bruxism and premature occlusal contacts. *J. Contemp. Dent. Pr*. **2013**, *14*, 616–621.
14. van der Bilt, A.; Engelen, L.; Pereira, L.J.; van der Glas, H.W.; Abbink, J.H. Oral physiology and mastication. *Physiol. Behav*. **2006**, *89*, 22–27.
15. Trulsson, M. Force encoding by human periodontal mechanoreceptors during mastication. *Arch. Oral Biol*. **2007**, 52, 357–360.
16. Cicciu, M.; Cervino, G.; Milone, D.; Risitano, G. FEM Investigation of the Stress Distribution over Mandibular Bone Due to Screwed Overdenture Positioned on Dental Implants. *Materials* **2018**, *11*, 1512, doi:10.3390/ma11091512.[6]
17. Menini, M.; Conserva, E.; Tealdo, T.; Bevilacqua, M.; Pera, F.; Signori, A.; Pera, P. Shock Absorption Capacity of Restorative Materials for Dental Implant Prostheses: An In Vitro Study. *Int. J. Prosthodont.* **2013**, *26*, 549–556, doi:10.11607/ijp.3241.[7]
18. Cehreli, M.; Duyck, J.; De Cooman, M.; Puers, R.; Naert, I. Implant design and interface force transfer. *Clin. Oral Implant. Res.* **2004**, *15*, 249–257, doi:10.1111/j.1600-0501.2004.00979.x.

9

19. Gracis, S.E.; Nicholls, J.I.; Chalupnik, J.D.; Yuodelis, R.A. Shock-absorbing behavior of five restorative materials used on im-plants. *Int. J. Prosthodont*. **1991**, *4*, 282–291.
20. Menini, M.; Conserva, E.; Tealdo, T.; Bevilacqua, M.; Pera, F.; Ravera, G.; Pera, P. The use of a masticatory robot to analyze the shock absorption capacity of different restorative materials for implant prosthesis. *J. Biol. Res.-Boll. Della Soc. Ital. di Biol. Sper.* **2011**, *84*, 118–119, doi:10.4081/jbr.2011.4636.
21. Magne, P.; Silva, M.; Oderich, E.; Boff, L.L.; Enciso, R. Damping behavior of implant-supported restorations. *Clin. Oral Implant. Res.* **2011**, *24*, 143–148, doi:10.1111/j.1600-0501.2011.02311.x.
22. Sevimay, M.; Turhan, F.; Kilicarslan, M.A.; Eskitascioglu, G. Three-dimensional finite element analysis of the effect of differ-ent bone quality on stress distribution in an implant-supported crown. *J. Prosthet. Dent.* **2005**, *93*, 227–234.
23. Mizusawa K; Shin C, Okada D; Ogura R, Komada W; Saleh O, et al. The investigation of the stress distribution in abutment teeth for connected crowns. *J. Dent Sci*. **2021**, 16, 929–36. doi:10.1016/j.jds.2020.11.005
24. Kaleli, N.; Sarac, D.; Külünk, S.; Öztürk, Özgür Effect of different restorative crown and customized abutment materials on stress distribution in single implants and peripheral bone: A three-dimensional finite element analysis study. *J. Prosthet. Dent.* **2018**, *119*, 437–445, doi:10.1016/j.prosdent.2017.03.008.
25. Geramizadeh, M.; Katoozian, H.; Amid, R.; Kadkhodazadeh, M. Static, Dynamic, and Fatigue Finite Element Analysis of Dental Implants with Different Thread Designs. *J. Autom. Inf. Sci.* **2016**, *26*, 347–355, doi:10.1615/jlongtermeffmedimplants.2017020008.
26. Geramizadeh, M.; Katoozian, H.; Amid, R.; Kadkhodazadeh, M. Finite Element Analysis of Dental Implants with and without Microthreads under Static and Dynamic Loading. *J. Autom. Inf. Sci.* **2017**, *27*, 25–35, doi:10.1615/jlongtermeffmedimplants.2017020007.
27. Karpov, E.G.; Danso, L.A.; Klein, J.T. Anomalous strain energy transformation pathways in mechanical metamaterials. *Proc. Math. Phys. Eng. Sci.* **2019**, *475*, 20190041.
28. King, H. *Basic Finite Element Method Apllied to Injury Biomechanics*; Academic Press: Cambridge, MA, USA, 2018. ISBN 9780128098318.
29. Cantó-Navés, O.; Marimon, X.; Ferrer, M.; Cabratosa-Termes, J. Comparison between experimental digital image processing and numerical methods for stress analysis in dental implants with different restorative materials. *J. Mech. Behav. Biomed. Mater.* **2021**, *113*, 104092, doi:10.1016/j.jmbbm.2020.104092.
30. Menini, M.; Pesce, P.; Pera, F.; Barberis, F.; Lagazzo, A.; Bertola, L.; Pera, P. Biological and mechanical characterization of carbon fiber frameworks for dental implant applications. *Mater. Sci. Eng. C* **2017**, *70*, 646–655, doi:10.1016/j.msec.2016.09.047.
31. Erkmen, E.; Meriç, G.; Kurt, A.; Tunç, Y.; Eser, A. Biomechanical comparison of implant retained fixed partial dentures with fiber reinforced composite versus conventional metal frameworks: A 3D FEA study. *J. Mech. Behav. Biomed. Mater.* **2011**, *4*, 107–116, doi:10.1016/j.jmbbm.2010.09.011.
32. Passaretti, A.; Petroni, G.; Miracolo, G.; Savoia, V.; Perpetuini, A.; Cicconetti, A. Metal free, full arch, fixed prosthesis for edentulous mandible rehabilitation on four implants. *J. Prosthodont. Res.* **2018**, *62*, 264–267, doi:10.1016/j.jpor.2017.10.002.
33. Zaparolli, D.; Peixoto, R.F.; Pupim, D.; Macedo, A.P.; Toniollo, M.B.; Mattos, M.D.G.C.D. Photoelastic analysis of mandibular full-arch implant-supported fixed dentures made with different bar materials and manufacturing techniques. *Mater. Sci. Eng. C* **2017**, *81*, 144–147, doi:10.1016/j.msec.2017.07.052.
34. Pera, F.; Pesce, P.; Solimano, F.; Tealdo, T.; Pera, P.; Menini, M. Carbon fibre versus metal framework in full-arch immediate loading rehabilitations of the maxilla-a cohort clinical study. *J. Oral Rehabil.* **2017**, *44*, 392–397.
35. Segerstrom, S.; Ruyter, I.E. Effect of thermal cycling on flexural properties of carbon-graphite fiber-reinforced polymers. *Dent. Mater.* **2009**, *25*, 845–851.
36. Segerstrom, S.; Ruyter, I.E. Adhesion properties in systems of laminated pigmented polymers, carbon-graphite fiber composite framework and titanium surfaces in implant suprastructures. *Dent. Mater.* **2009**, *25*, 1169–1177.
37. Segerstrom, S.; Sandborgh-Englund, G.; Ruyter, E.I. Biological and physicochemical properties of carbon-graphite fi-bre-reinforced polymers intended for implant suprastructures. *Eur. J. Oral Sci.* **2011**, *119*, 246–252.
38. Muhsin, S.A.; Hatton, P.; Johnson, A.; Sereno, N.; Wood, D.J. Determination of Polyetheretherketone (PEEK) mechanical properties as a denture material. *Saudi Dent. J.* **2019**, *31*, 382–391, doi:10.1016/j.sdentj.2019.03.005.
39. Schwitalla, A.D.; Spintig, T.; Kallage, I.; Müller, W.-D. Pressure behavior of different PEEK materials for dental implants. *J. Mech. Behav. Biomed. Mater.* **2016**, *54*, 295–304, doi:10.1016/j.jmbbm.2015.10.003.

40. Schwitalla, A.D.; Spintig, T.; Kallage, I.; Müller, W.-D. Flexural behavior of PEEK materials for dental application. *Dent. Mater.* **2015**, *31*, 1377–1384, doi:10.1016/j.dental.2015.08.151.
41. Gallucci, G.O.; Bernard, J.-P.; Bertosa, M.; Belser, U.C. Immediate loading with fixed screw-retained provisional restorations in edentulous jaws: The pickup technique. *Int. J. Oral Maxillofac. Implant.* **2004**, *19*, 524–533.
42. Norton, M.R. An in vitro evaluation of the strength of an internal conical interface compared to a butt joint interface in implant design. *Clin. Oral Implant. Res.* **1997**, *8*, 290–298, doi:10.1034/j.1600-0501.1997.080407.x.
43. Tonella, B.P.; Pellizzer, E.P.; Ferraço, R.; Falcón-Antenucci, R.M.; Carvalho, P.S.P.D.; Goiato, M.C. Photoelastic analysis of ce-mented or screwed implant-supported prostheses with different prosthetic connections. *J. Oral Implantol.* **2011**, *37*, 401–410.
44. Peixoto, R.F.; Tonin, B.S.H.; Martinelli, J.; Macedo, A.P.; Mattos, M.D.G.C.D. In vitro digital image correlation analysis of the strain transferred by screw-retained fixed partial dentures supported by short and conventional implants. *J. Mech. Behav. Biomed. Mater.* **2020**, *103*, 103556, doi:10.1016/j.jmbbm.2019.103556.
45. Hoult, N.A.; Take, W.A.; Lee, C.; Dutton, M. Experimental accuracy of two dimensional strain measurements using Digital Image Correlation. *Eng. Struct.* **2013**, *46*, 718–726.
46. Bassit, R.; Lindström, H.; Rangert, B. In vivo registration of force development with ceramic and acrylic resin occlusal materials on implant-supported prostheses. *Int. J. Oral Maxillofac. Implants.* **2002**, *17*, 17–23.
47. Bijjargi, S.; Chowdhary, R. Stress dissipation in the bone through various crown materials of dental implant restoration: A 2-D finite element analysis. *J. Investig. Clin. Dent.* **2012**, *4*, 172–177, doi:10.1111/j.2041-1626.2012.00149.x.
48. Sevimay, M.; Usumez, A.; Eskitascioglu, G. The influence of various occlusal materials on stresses transferred to im-plant-supported prostheses and supporting bone: A three-dimensional finite-element study. *J. Biomed. Mater. Res. B Appl. Biomater.* **2005**, *73*, 140–147.
49. Bacchi, A.; Consani, R.L.; Mesquita, M.F.; dos Santos, M.B. Stress distribution in fixed-partial prosthesis and peri-implant bone tissue with different framework materials and vertical misfit levels: A three-dimensional finite element analysis. *J. Oral Sci.* **2013**, *55*, 239–244. Available from: http://www.ncbi.nlm.nih.gov/pubmed/24042591 (accessed on 15 May 2019).
50. Merz, B.R.; Hunenbart, S.; Belser, U.C. Mechanics of the implant-abutment connection: An 8-degree taper compared to a butt joint connection. *Int. J. Oral Maxillofac. Implant.* **2000**, *15*, 519–526.
51. Valera-Jiménez, J.; Burgueño-Barris, G.; Gómez-González, S.; López-López, J.; Valmaseda-Castellón, E.; Fernández-Aguado, E. Finite element analysis of narrow dental implants. *Dent. Mater.* **2020**, *36*, 927–935, doi:10.1016/j.dental.2020.04.013.
52. Anami, L.C.; Lima, J.M.D.C.; Takahashi, F.E.; Neisser, M.P.; Noritomi, P.Y.; Bottino, M.A. Stress Distribution Around Osseointegrated Implants With Different Internal-Cone Connections: Photoelastic and Finite Element Analysis. *J. Oral Implant.* **2015**, *41*, 155–162, doi:10.1563/aaid-joi-d-12-00260.
53. Carvalho, L.; Roriz, P.; Simões, J.; Frazão, O. New Trends in Dental Biomechanics with Photonics Technologies. *Appl. Sci.* **2015**, *5*, 1350–1378, doi:10.3390/app5041350.
54. Karl M, Dickinson A, Holst S, Holst A. Biomechanical methods applied in dentistry: A comparative overview of photoelastic examinations, strain gauge measurements, finite element analysis and three-dimensional deformation analysis. *Eur. J. Prosthodont. Restor. Dent.* **2009**, *17*, 50–57.
55. Benazzi, S.; Nguyen, H.N.; Kullmer, O.; Kupczik, K. Dynamic Modelling of Tooth Deformation Using Occlusal Kinematics and Finite Element Analysis. *PLoS One* **2016**, *11*, e0152663.
56. Razaghi, R.; Haghpanahi, M. Dynamic simulation and finite element analysis of the maxillary bone injury around dental implant during chewing different food. *Biomed. Eng. Appl. Basis. Commun.* **2016**, *28*, 1–10.
57. Kayabaşı, O.; Yüzbasıoğlu, E.; Erzincanlı, F. Static, dynamic and fatigue behaviors of dental implant using finite element method. *Adv. Eng. Softw.* **2006**, *37*, 649–658, doi:10.1016/j.advengsoft.2006.02.004.
58. Chang, Y.; Tambe, A.A.; Maeda, Y.; Wada, M.; Gonda, T. Finite element analysis of dental implants with validation: To what extent can we expect the model to predict biological phenomena? A literature review and proposal for classification of a validation process. *Int. J. Implant Dent.* **2018**, *4*, 1–14, doi:10.1186/s40729-018-0119-5.[8]

59. Lindhe, J.; Meyle, J.; on behalf of Group D of the European Workshop on Periodontology Peri-implant diseases: Consensus Report of the Sixth European Workshop on Periodontology. *J. Clin. Periodontol.* **2008**, *35*, 282–285, doi:10.1111/j.1600-051x.2008.01283.x.
60. Sanz, M.; Lang, N.P.; Kinane, D.F.; Berglundh, T.; Chapple, I.; Tonetti, M.S. Seventh European Workshop on Periodontol-ogy of the European Academy of Periodontology at the Parador at la Granja, Segovia, Spain. *J. Clin. Periodontol.* **2011**, *38 (Suppl 11)*, 1–2.
61. Ramseier, C.A.; Needleman, I.G.; Gallagher, J.E.; Lahtinen, A.; Ainamo, A.; Alajbeg, I.; Albert, D.; Al-Hazmi, N.; Antohé, M.E.; Beck-Mannagetta, J.; et al. Consensus Report: 2nd European Workshop on Tobacco Use Prevention and Cessation for Oral Health Professionals. *Int. Dent. J.* **2010**, *60*, 3–6.
62. Mazel, A.; Belkacemi, S.; Tavitian, P.; Stéphan, G.; Tardivo, D.; Catherine, J.H.; Aboudharam, G. Peri-implantitis risk factors: A pro-spective evaluation. *J. Investig. Clin. Dent.* **2019**, *10*, e12398.
63. Tsigarida, A.; Dabdoub, S.; Nagaraja, H.; Kumar, P. The Influence of Smoking on the Peri-Implant Microbiome. *J. Dent. Res.* **2015**, *94*, 1202–1217, doi:10.1177/0022034515590581.
64. Derks, J.; Tomasi, C. Peri-implant health and disease. A systematic review of current epidemiology. *J. Clin. Periodontol.* **2015**, *42*, S158–S171, doi:10.1111/jcpe.12334.
65. Duyck, J.; Vandamme, K. The effect of loading on peri-implant bone: A critical review of the literature. *J. Oral Rehabil.* **2014**, *41*, 783–794, doi:10.1111/joor.12195.
66. Naert, I.; Duyck, J.; Vandamme, K. Occlusal overload and bone/implant loss. *Clin. Oral Implant Res.* **2012**, *23*, 95–107, doi:10.1111/j.1600-0501.2012.02550.x.
67. Klinge, B.; Meyle, J.; Working Group 2. Peri-implant tissue destruction. The Third EAO Consensus Conference 2012. *Clin. Oral Implants Res.* 2012, *23 (SUPPL.6)*, 108–110.
68. Mombelli, A.; van Oosten, M.A.; Schurch, E., Jr.; Land, N.P. The microbiota associated with successful or failing osseointe-grated titanium implants. *Oral Microbiol. Immunol.* **1987**, *2*, 145–151.
69. Kozlovsky, A.; Tal, H.; Laufer, B.Z.; Leshem, R.; Rohrer, M.D.; Weinreb, M.; Artzi, Z. Impact of implant overloading on the pe-ri-implant bone in inflamed and non-inflamed peri-implant mucosa. *Clin. Oral Implants Res.* **2007**, *18*, 601–610.
70. Afrashtehfar, K.I.; Afrashtehfar, C.D. Lack of association between overload and peri-implant tissue loss in healthy conditions. *Evid. Based Dent.* **2016**, *17*, 92–93.
71. Esposito, M.; Hirsch, J.-M.; Lekholm, U.; Thomsen, P. Biological factors contributing to failures of osseointegrated oral implants, (I). Success criteria and epidemiology. *Eur. J. Oral Sci.* **1998**, *106*, 527–551, doi:10.1046/j.0909-8836. t01-2-.x.
72. Mattheos, N.; Collier, S.; Walmsley, A.D. Specialists' management decisions and attitudes towards mucositis and peri-implantitis. *Br. Dent. J.* **2012**, *212*, E1.
73. Hermann Schoolfield, J.D.; Schenk, R.K.; Buser, D.; Cochran, D.L.J.S. Influence of the size of the microgap on crestal bone changes around titanium implants. A histometric evaluation of unloaded non-submerged implants in the canine mandible. *J. Periodontol.* **2001**, *72*, 1372–1383.
74. VanSchoiack Wu, J.C.; Sheets, C.G.; Earthma, J.C.L.R. Effect of bonedensity on thedampingbehavior of dental implants: An in vitro method. *Mater. Sci. Eng.* **2006**, *26*, 1307–1311.
75. Lima de Andrade, C.; Carvalho, M.A.; Bordin, D.; da Silva, W.J.; Del Bel Cury, A.A.; Sotto-Maior, B.S. Biomechanical Behavior of the Dental Implant Macrodesign. *Int. J. Oral Maxillofac. Implants.* **2017**, *32*, 264–270.
76. Coltro, M.P.L.; Ozkomur, A.; Villarinho, E.A.; Teixeira, E.R.; Vigo, A.; Shinkai, R.S.A. Risk factor model of mechanical complica-tions in implant-supported fixed complete dentures: A prospective cohort study. *Clin. Oral Implants Res.* **2018**, *29*, 915–921.
77. Karakis, D.; Dogan, A. The craniofacial morphology and maximum bite force in sleep bruxism patients with signs and symptoms of temporomandibular disorders. *CRANIO®* **2014**, *33*, 32–37, doi:10.1179/2151090314y.0000000009.
78. Mengatto, C.M.; Coelho-de-Souza, F.H.; de Souza Junior, O.B. Sleep bruxism: Challenges and restorative solutions. *Clin. Cosmet. Investig. Dent.* **2016**, *8*, 71–77, doi:10.2147/ccide.s70715.
79. Mikeli, A.; Walter, M.H. Impact of Bruxism on Ceramic Defects in Implant-Borne Fixed Dental Prostheses: A Retrospective Study. *Int. J. Prosthodont*. **2016**, *29*, 296–298.
80. Insua, A.; Monje, A.; Wang, H.-L.; Miron, R.J. Basis of bone metabolism around dental implants during osseointegration and peri-implant bone loss. *J. Biomed. Mater. Res. Part A* **2017**, *105*, 2075–2089, doi:10.1002/jbm.a.36060.
81. Sathapana, S.; Monsour, P.; Naser-ud-Din, S.F.A. Age-related changes in maxillary and mandibular cortical bone thickness in relation to temporary anchorage device placement. *Aust. Dent. J.* **2013**, *8*, 67–74.

82. Tomar, V. Modeling of Dynamic Fracture and Damage in Two-Dimensional Trabecular Bone Microstructures Using the Cohesive Finite Element Method. *J. Biomech. Eng.* **2008**, *130*, 021021, doi:10.1115/1.2903434.
83. Li, J.; Yin, X.; Huang, L.; Mouraret, S.; Brunski, J.; Cordova, L.; Salmon, B.; Helms, J. Relationships among Bone Quality, Implant Osseointegration, and Wnt Signaling. *J. Dent. Res.* **2017**, *96*, 822–831, doi:10.1177/0022034517700131.
84. Asa'Ad, F.; Monje, A.; Larsson, L. Role of epigenetics in alveolar bone resorption and regeneration around periodontal and peri-implant tissues. *Eur. J. Oral Sci.* **2019**, *127*, 477–493, doi:10.1111/eos.12657.
85. Solidworks Dassault Systemes 2020. Available online: http://www.solidworks.com(accessed on 15 May 2019).
86. Micro Medica Srl 2021. Italy. Available online: http://micromedicasrl.it (accessed on 15 May 2019).
87. Renishaw 2021. United Kingdom. Available online: https://www.renishaw.com (accessed on 15 May 2019).
88. VITA Zahnfabrik H. Rauter GmbH & Co 2021. Germany. Available online: www.vita-zahnfabrik.com (accessed on 15 May 2019).
89. Heraeus Kulzer GmbH 2021. Germany. Available online: https://www.kulzer.de (accessed on 15 May 2019).
90. Ivoclar Vivadent 2021. Spain. Available online: https://www.ivoclarvivadent.es (accessed on 15 May 2019).
91. Invibio 2021. United Kingdom. Available online: https://invibio.com (accessed on 15 May 2019).
92. MIS Implants Technologies Ltd 2021. Israel. Available online: https://www.mis-implants.com (accessed on 15 May 2019).
93. Lakatos, É.; Magyar, L.; Bojtár, I. Material Properties of the Mandibular Trabecular Bone. *J. Med Eng.* **2014**, *2014*, 1–7, doi:10.1155/2014/470539
94. Geng, J.P.; Tan, K.B.; Liu, G.R. Application of finite element analysis in implant dentistry: A review of the literature. *J. Pros-thet. Dent.* **2001**, *85*, 585–598.[9]

2º Artículo publicado

"Bone Stress Evaluation with and without Cortical Bone Using Several Dental Restorative Materials Subjected to Impact Load: A Fully 3D Transient Finite-Element Study"

Raul Medina-Galvez, Oriol Cantó-Navés, Xavier Marimon, Miguel Cerrolaza, Miquel Ferrer y Josep Cabratosa-Termes

Citación:

Medina-Galvez R, Cantó-Navés O, Marimon X, Cerrolaza M, Ferrer M, Cabratosa-Termes J. Bone Stress Evaluation with and without Cortical Bone Using Several Dental Restorative Materials Subjected to Impact Load: A Fully 3D Transient Finite-Element Study. Materials (Basel). 2021 Oct 4;14(19):5801. doi: 10.3390/ma14195801. PMID: 34640200; PMCID: PMC8510134.

Rango de la revista: JCR - Q1 (*Metallurgy & Metallurgical Engineering*) / CiteScore - Q2 (*Condensed Matter Physics*) Q2 *(Dentistry)*

Factor de impacto: 3.623 (2020) ; 5-Años factor de impacto: 3.920 (2020)

Contribución del doctorando:

El doctorando ha contribuido en la conceptualización, investigación y validación; en el borrador origina; escritura, revisión y edición del articulo final.

Bone Stress Evaluation with and without Cortical Bone Using Several Dental Restorative Materials Subjected to Impact Load: A Fully 3D Transient Finite-Element Study

Raul Medina-Galvez [1], Oriol Cantó-Navés [1], Xavier Marimon [2,3,*], Miguel Cerrolaza [2,4], Miquel Ferrer [5] and Josep Cabratosa-Termes [1]

[1] Faculty of Dentistry, Universitat Internacional de Catalunya (UIC), 08017 Barcelona, Spain; ruldoc@uic.es (R.M.-G.); oriolcanto@uic.es (O.C.-N.); cabratosa@uic.es (J.C.-T.)
[2] Bioengineering Institute of Technology, Universitat Internacional de Catalunya (UIC), 08190 Barcelona, Spain; mcerrolaza@uic.es
[3] Automatic Control Department, Universitat Politècnica de Catalunya (UPC-BarcelonaTECH), 08034 Barcelona, Spain
[4] School of Engineering, Science & Technology, Valencian International University, 46002 Valencia, Spain
[5] Department of Strength of Materials and Structural Engineering, Universitat Politècnica de Catalunya (UPC-BarcelonaTECH), 08034 Barcelona, Spain; miquel.ferrer@upc.edu
* Correspondence: xmarimon@uic.es

Abstract: Statement of problem. Previous peri-implantitis, peri-implant bone regeneration, or immediate implant placement postextraction may be responsible for the absence of cortical bone. Single crown materials are then relevant when dynamic forces are transferred into bone tissue and, therefore, the presence (or absence) of cortical bone can affect the long-term survival of the implant. **Purpose**: the purpose of this study is to assess the biomechanical response of dental rehabilitation when selecting different crown materials in models with and without cortical bone. **Methods**: several crown materials were considered for modeling six types of crown rehabilitation: full metal (MET), metal-ceramic (MCER), metal-composite (MCOM), peek-composite (PKCOM), carbon fiber-composite (FCOM), and carbon fiber-ceramic (FCCER). An impact-load dynamic finite-element analysis was carried out on all the 3D models of crowns mentioned above to assess their mechanical behavior against dynamic excitation. Implant-crown rehabilitation models with and without cortical bone were analyzed to compare how the load-impact actions affect both type of models. **Results**: numerical simulation results showed important differences in bone tissue stresses. The results show that flexible restorative materials reduce the stress on the bone and would be especially recommendable in the absence of cortical bone. **Conclusions:** this study demonstrated that more stress is transferred to the bone when stiffer materials (metal and/or ceramic) are used in implant supported rehabilitations; conversely, more flexible materials transfer less stress to the implant connection. Also, in implant-supported rehabilitations, more stress is transferred to the bone by dynamic forces when cortical bone is absent.

Keywords: FEA; FEM; impact test; transient analysis; dynamical forces; biomechanical behavior; implant rehabilitation; rehabilitation materials; crown materials; bone loss

1. Introduction

The quantity and quality of bone tissue around a rehabilitated implant play a key role in its long-term survival [1]. After peri-implantitis, immediate implant placement, or regenerated bone, cortical bone is missing for a variable period [2]. Moreover, the absence of cortical bone can affect the biomechanical behavior of both the bone tissue and its ability to withstand impact loads [3].

Different models and techniques are used to analyze the behavior of dental implants [4] including two-dimensional (2D) or three-dimensional (3D) finite element analyses (FEA), photo-elastic studies, or digital image-correlations (DIC). Also, ultrasonic wave analysis [5,6] can be used successfully in dental implant analysis [7].

FEA, whether in 2D or 3D, is a numerical and approximate technique that yields results depending on both the geometry and mechanical properties of the materials. Regarding photo-elastic techniques, when either static or dynamic forces are applied, isochromatic fringes appear in photo-elastic studies [8], thereby allowing the stress distribution at implants to be calculated. The DIC is an image-based analysis that shows how points inside resin blocks move when static or dynamic forces are applied [9]. On the other hand, the analysis of implant behavior requires that the difference between static forces (due to clenching) and dynamic forces (due to mastication or eccentric bruxism) be very clear, particularly when selecting the rehabilitation materials [10,11].

Other works reported similar results for implant behavior [4,8]. These authors showed that the main differences are due to variables such as the type of implant connection, the diameter/length of the implant, the type of rehabilitation material or whether the load was applied statically or dynamically [8,12]. However, the presence or absence of cortical bone is an issue that, to date, was not studied or quantified sufficiently. The absence of cortical bone can lead to the implant loosening and eventually to implant failure [13–17].

From a mechanical perspective, and according to some previous works [18–22], static analysis is not completely enough to get precise and reliable results. Several authors agreed that it is needed to perform dynamic analysis. Dynamic analysis can be found in literature [18,22] but addressing fatigue analysis and not impact dynamic loading.

In previous works [23] the authors analyzed the mechanical behavior of implants with different restorative materials subjected to static loads by three different methods: finite element method (FEM), digital photoelasticity (DP), and digital image correlation (DIC). They concluded that (1) all 3 methods provide very close solutions; (2) FEM is enough reliable and robust for predicting the tooth-implant mechanical behavior, and (3) dynamic impact analysis is mandatory for getting more accurate and closer results to the problem's physical reality.

Therefore, in this work a fully 3D dynamic FEA study of the influence of different crown materials on the implant behavior with and without cortical bone when subjected to impact dynamic loads is performed. Moreover, we also discuss two clinical cases: (a) both trabecular and cortical bone, and (b) only trabecular bone.

Significant differences in the mechanical response when the peri-implantitis generated a loss of cortical bone were encountered. The study concludes with a comparative dynamic analysis of crowns made with different restorative materials.

2. Materials and Methods

2.1. The Model

A 3D dynamic finite-element model comprising a crown, an abutment screw, an abutment, an implant, and the surrounding bone was set up to evaluate the von Mises stresses at both the cortical and trabecular bone (See Figure 1). Ethics approval was not required for this in-vitro study. All the parts of the model are described hereafter.

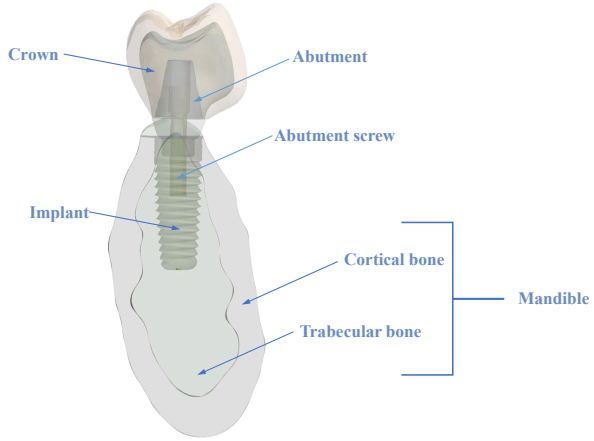

Figure 1. Cross-sectional view of 3D model.

2.1.1. The Crown

The crown model was processed using Solidworks (version 2021, Dassault Systèmes, Waltham, Massachusetts , USA) [24] by importing a CAD model generated by Exocad-3D (v3.0, Exocad GmbH, Darmstadt, Germany). The model was built by assembling two components: the core (51% of the total volume) and the aesthetic veneering (40% of the total volume), as displayed in Figure 2. The volume of the resulting crown model is 411.5 mm^3.

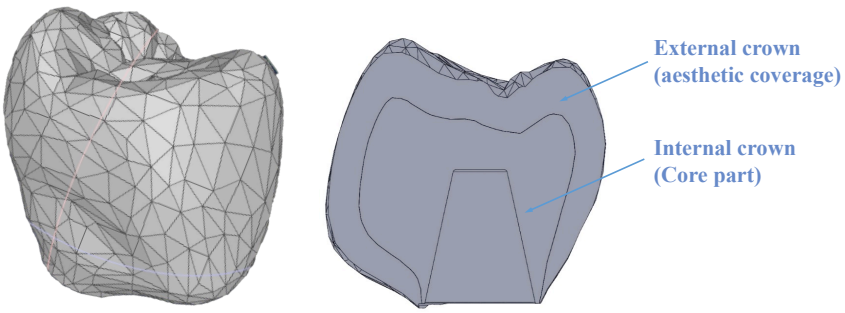

Figure 2. Crown model. Left: cross section showing both internal and external crown.

2.1.2. The Abutment and Screw

The abutment is a metal component whose function is to attach the crown and the implant. Also, a hexagonal antirotation system prevents the relative movement between the abutment and the implant. The screw allows the connection between the abutment and the implant.
Solidworks was also used to model the abutment and the screw, thus reducing the classical surfaces to a simpler triangular shapes (see Figure 3). The model corresponds to the hexagonal-connection abutment of the MIS implant [25].

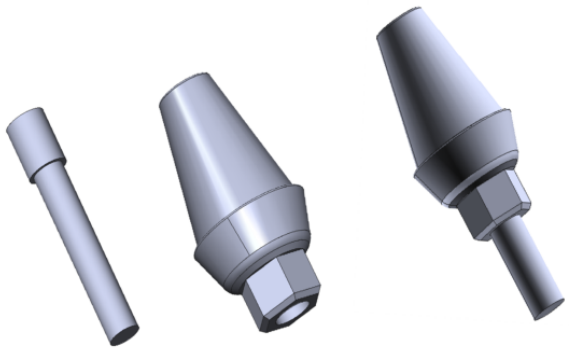

Figure 3. Left: abutment screw; center: abutment with hexagonal antirotational system; right: screw-abutment assembly.

2.1.3. The Implant

Figure 4 displays the implant created with Solidworks to obtain more accurate geometric shapes. The implant used in this study was a 4.2 × 11.5 mm^2 MIS implant [25], because it is a well-known and reliable implant used in the area of restorative dentistry and world-wide commercialized.

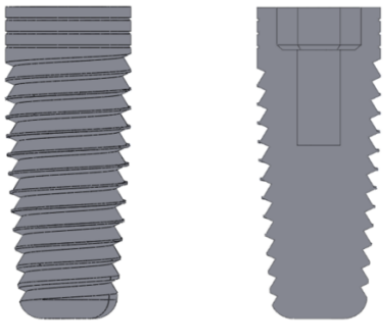

Figure 4. Implant. Left: lateral view; right: cross section.

2.1.4. The Mandible

The mandible section was made from a CT scan section [26]. The mandible's geometry was generated by following two steps: (a) some key points were defined at a known distance at the CT-scan section, and (b) the scan scale was then used to compute the actual distances at the real mandible. The 3D geometry of the mandible was split into an external region of cortical bone and an internal one of trabecular bone, each one with its specific mechanical properties (see Figure 5).

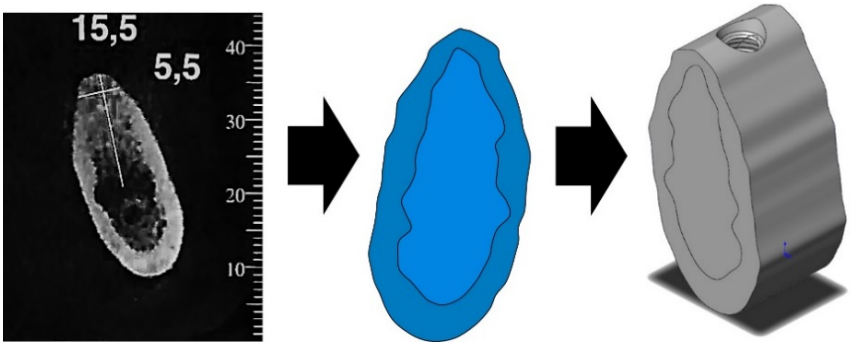

Figure 5. Left: CT scan. Center: mandible section obtained from CT scan. Right: isometric view of mandible's model.

2.1.5. The Loading Plate

The impact loads produced by chewing were applied to the model (crown, implant, and mandible) by using a rectangular rigid plate dimensioned as shown in Figure 6. Some boundary conditions were considered: (a) the initial separation between the plate and the crown was set to 0.01 mm; (b) free sliding is assumed, i.e., the impact of the plate on the model is frictionless; (c) normal stresses were considered null if the plate loses contact with the model.

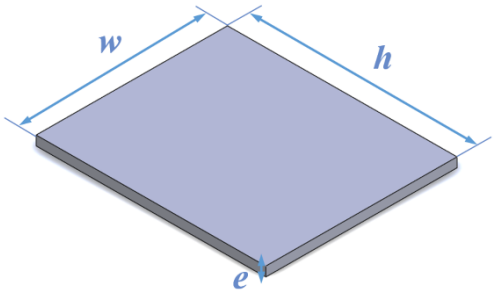

Figure 6. Dimensions of rigid plate (w = 10 mm, h = 12 mm, e = 2 mm).

2.2. Geometry of the Assembled Model

After all the individual parts were independently built, they were assembled together as shown in Figure 7.

Before conducting the FEA simulation, the assembled geometry was converted to IGES format, which was imported into Ansys Workbench Design Modeler (version 2021, ANSYS, Inc, Canonsburg, Pennsylvania, USA)]. Perfect osseointegration between the implant and the bone was assumed. This means that the bone is integrated into all slots of the placed implant, although this does not always happen in clinical cases

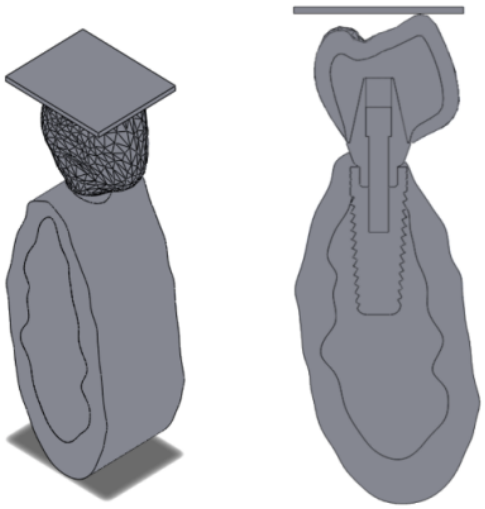

Figure 7. Assembled geometry. **Left**: isometric view; r**ight**: cross section.

2.3. Materials of the Model

The mechanical properties of the materials have a direct influence on the calculation of the stress response and its deformations. All materials were considered elastic, homogeneous, and isotropic. Mandible bone mechanical properties can be found elsewhere [27]. Different materials were used in the crown, to discover if the crown material has a direct effect on the implant stress distribution and mechanical performance (see Table 1 below):

	Material Name	Manufacturer	Young Modulus [MPa]	Poisson Ratio	Density [g/cm^3]
Crown	**FCOM** *Carbon fiber-composite* BioCarbon Bridge fibers Composite BioXfill	 Micro Medica Micro Medica	 300,000 22,000	 0.3 0.3	 1.40 8.30
	MCER *Metal-ceramic* Co-Cr alloy Ceramic VMK 95	 Renishaw Vita	 208,000 69,000	 0.31 0.28	 8.90 2.50
	MCOM *Metal-composite* Co-Cr alloy Composite BioXfill	 Renishaw Micro-Medica	 208,000 22,000	 0.31 0.3	 8.90 8.30
	MET *Full metal* Co-Cr Alloy, Mo, W	 Heraeus Kulzer	 208,000	 0.31	 8.90
	FCCER *Carbon fiber-ceramic* Carbon Fiber Bridge Ceramic IPS e.max	 Micro-Medica Ivoclar Vivadent	 66,000 95,000	 0.3 0.2	 1.4 2.5
	PKCOM *PEEK-composite* PEEK Optima Composite BioXfill	 Invibio Micro-Medica	 4,100 22,000	 0.36 0.3	 1.3 8.30
Implant	Ti-6-Al-4V ELI	MIS	113,800	0.34	4.43
Bone	Cortical bone	[27,28]	15,000	0.3	1.79
	Trabecular bone	[28]	500	0.3	0.45

Table 1. Crown materials and manufactures. Acronyms used in this study.

A total of six crown rehabilitation materials were analyzed: the carbon fiber-composite crown (FCOM) had an aesthetic layer of a BioXfill composite [29] and carbon fiber framework of BioCarbon Bridge; the metal-ceramic crown (MCER) had a framework of LaserPFM Co-Cr metal alloy and aesthetic veneering of VITA VMK 95 ceramic material [30,31]; the metal-composite crown (MCOM) had a framework of LaserPFM Co-Cr metal alloy [30] and BioXfill composite [29]; the metal crown (MET) is made entirely of melted Co-Cr alloy [32]; the carbon fiber-ceramic crown (FCCER) had a framework of BioCarbon Bridge carbon fibers [29] and lithium disilicate ceramic aesthetic covering [33]; finally, the PEEK-composite crown (PKCOM) is made in the inner part of polymer polyetheretherketone (PEEK) and the aesthetic veneering with BioXfill composite [34].
All the mechanical properties of each crown, the implant, and both bone tissues (cortical and trabecular) used in the numerical simulation are listed in Table 1. The mechanical properties of the materials were obtained from the manufacturer datasheets indicated in the table.

2.4. Numerical Simulation

Although there are numerous studies centered on static forces, there are few studies of the dynamic forces applied during physiological functions. Some biomechanical estimated values can be obtained in the literature [35,36]. Therefore, a simulated impact between the rigid plate and the whole implant geometry was carried out. **Results were analyzed over time due to the dynamic response of the model**. The simulation was performed with ANSYS (version 2021, ANSYS, Inc, Canonsburg, Pennsylvania, USA) [37] using the mechanical APDL solver and the Transient Structural analysis system.

2.4.1. Simulation Setup

A first simulation was performed to check that all the materials, hypotheses, and boundary conditions of the model were correctly defined. All the results were coherent, but the computational time was very high for two main reasons: there was a very large number of nodes and elements and the time set for analysis was more than was needed. Therefore, the time and number of elements and nodes were reduced. The distance between the plate and the crown was also shortened. Furthermore, to carry out reasonable comparisons, the dynamic characteristics of the impact, i.e., initial kinetic energy and linear momentum, should be the same in all the simulations.
Initially, all the mass particles of the dental implant have the same velocity as well as the kinetic energy due to the movement of the whole structure (mandible, implant, crown, and abutment), as shown below:

$$E_k = \sum \frac{1}{2} \cdot m_i \cdot v^2 \quad (1)$$

where
E_k is the kinetic energy
m_i is the particle mass
v_i is the particle velocity

When the dental implant collides with the plate the kinetic energy is transformed into strain energy. The strain energy for a deformable solid can be determined through the stress and strain tensors time-history.
If the deformation occurs within the linear-elastic range, the potential elastic deformation energy can be obtained from Equation (2):

$$E_{def} = \int_V \sigma_i \cdot \varepsilon_i \cdot dV \quad (2)$$

where
E_{def} is the potential elastic deformation energy
σ_i is the stress state
ε_i is the strain state
dV is the volume differential

The dynamic characteristics of an impact are determined by the system's initial energy ($0.5 \cdot m \cdot v^2$) and linear momentum ($m \cdot v$). Both features must have the same value in any case, which is guaranteed by introducing the same speed (v) and the same mass (m). On the other hand, the effect of the mandible's mass is not so significant because it is externally fixed.
Since each crown material has a different density, the initial mass of the system and, consequently, its initial kinetic energy would be different for every combination case. Then, the base mass (implant + mandible) was leveled in all models to balance the crown's mass changes. Note that the base mass represents the whole mass of the mandible, which should be assumed to be the same in all cases. Therefore, a uniformly distributed mass was added to the models to make the impacts equivalent energetically. Table 2 shows the additional mass added to each model.

Table 2. Initial and added masses to each model.

Model	Initial Mass (g)	Added Mass (g)
MET	8.62	0
MCER	6.73	1.89
MCOM	6.63	1.99
FCOM	5.23	3.39
PKCOM	7.20	1.42
FCCER	5.07	3.55

Two changes were made to the whole model to simulate the absence of cortical bone, as in peri-implantitis, peri-implant bone regeneration, or immediate implant placement. Firstly, the cortical part of the assembly was suppressed, and the rest of the mesh is kept intact. Therefore, the nodes chosen (see section 'Node selection') are the same and can be compared. Secondly, some mass was added to equal the impact energy. This added mass corresponds to the suppressed cortical bone and is obtained by multiplying the volume by its density. It is constant for all models, and the value is 2.27 g. Table 3 lists the added mass in the lateral surface for each crown material:

Table 3. Added mass for both analyses: with and without cortical bone.

Model	Added Mass with Cortical (g)	Added Mass without Cortical (g)
MET	0	2.27
MCER	1.89	4.16
MCOM	1.99	4.26
FCOM	3.39	5.66
PKCOM	1.42	3.69
FCCER	3.55	5.82

2.4.2. Finite Element Mesh

Now, the next step is to generate a suitable finite element mesh, which must be done carefully since the precision of the results depends largely on how refined the mesh is. Then, if greater precision is needed, smaller elements should be used. The more refined the mesh, the more computer time is required. This does not have a large impact in finite element (FE) static analysis but, nevertheless, it is a key aspect in FE transient dynamic analysis.

A mesh sensitivity analysis was done to ensure a reliable model mesh. The refining process started from an initial mesh of 57,330 nodes until reaching a final mesh of 96,160 nodes, where the difference between stress values at some selected nodes did not exceed 5%. Figure 8 shows the finite elements mesh.

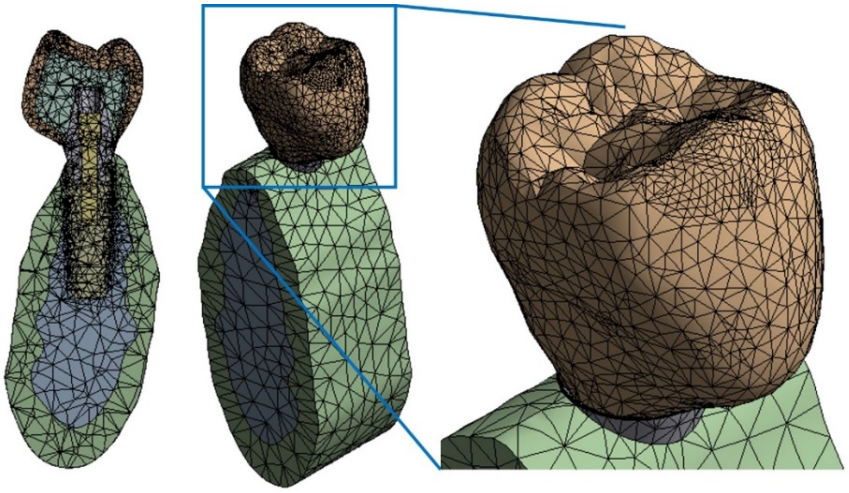

Figure 8. Model mesh (96,160 nodes and 62,606 elements). **Left**: cross section; c**enter**: isometric view; r**ight**: details on top of crown.

The Ansys 3D solid element type SOLID187 was used, with 10 nodes and quadratic interpolation functions, which fits better to irregular geometries. The element has three degrees of freedom per node, i.e., the three translations in the global coordinate directions x, y, z. The surface-to-surface contact was defined with the element CONTA174.

Also, a refinement was set for the impact zone, thereby ensuring better accuracy in this area. Therefore, as this refinement was done, it is not necessary to use an area to obtain an average solution, since the nodal solution is especially accurate. In addition, Ansys software performs a control of the aspect ratio systematically.

The size of the finite element mesh, related to its accuracy, is smaller at the loading point and the threaded part (0.2 mm), where higher accuracy is needed, but larger in the other parts (from 0.5 to 2 mm). To find the optimal mesh and an acceptable computational time, a sensitivity analysis of the mesh was also carried out. First of all, a coarse mesh was used, and subsequently, finer meshes were tested. The refining process was stopped when results became stabilized.

2.4.3. Initial and Boundary Conditions

In dynamic analysis, the boundary conditions (BC) are displacements, velocities, and accelerations instead of static forces and displacements as in static analysis. There are many publications and studies offering strategies on how to configure the loads to obtain a realistic simulation in static analysis. But in dynamic analysis the loads are the result of the calculation, i.e., the input for an impact simulation is the model's initial energy, not an applied load.

Energy concepts allow us to relate the model mass (bone-implant-abutment-crown) and the velocity applied as an initial boundary condition. The mass was calculated according to a density

and volume of 411.5 mm^3 for each crown (see Table 1). The model was also subjected to an initial velocity of 1 m/s as the initial kinematic condition.
Some studies focus on the mandibular kinematics by using small accelerometers [33]. The peak peripheral acceleration when opening the mouth can reach an average of 2.5 m/s^2. Considering this and keeping in mind that we are dealing with a brain-controlled occlusally system, the same acceleration (a) during occlusion can be assumed. An estimated velocity (v) can now be obtained using this value and the formula of the constant acceleration movement:

$$1\ v = a \cdot \Delta t \tag{3}$$

where
v is the velocity
a is the acceleration
Δt is the time increment
Considering that the mastication occlusion lasts less than 0.5 s, according to Equation (3) we can write: $v = a \cdot \Delta t = 2.5 \cdot 0.5 = 1.25$ m/s. Therefore, a reasonable value for the velocity condition would be 1.25 m/s.
Note that the bottom surface of the plate was fixed. This means that it cannot move or rotate in any direction. During the impact, certain forces appear to counteract the vertical displacement of the rest of the bodies. The distance between the plate and the external crown is 0.01 mm. The lateral surfaces of the cortical and trabecular bones were fixed in the normal (z-axis) and tangential (x-axis) directions, thereby having a degree of freedom in the direction of the displacement (y-axis). As a result, the bones only move in the direction of the vertical axis and do not rotate in any direction.

2.4.4. Simulation Time

The simulation time-limit also has to be set. The impacts happen in a very short period. Some previous works in other scientific fields found that the impact lasts less than one millisecond [38, 39], but there is very little (or almost no) published work on dynamic impact loads in dental applications. On the one hand, the duration of the simulations should be as short as possible to reduce the CPU computation time; but on the other, it should be longer than the impact duration and its further effects. Finally, the simulation time was set at 0.4 ms.
Now, the time interval between two analysis steps (known as time-step or Δt) needs to be defined. Similar to what was discussed about mesh's size, the shorter the time-step, the more accurate the results and the more computer time is required. After some sensibility numerical analyses, a time-step of $\Delta t = 7.55$ μs was found to lead to sufficiently accurate results.

2.4.5. Node Selection

To conduct this study, the energy of the object was computed over two benchmark nodes: one at the top of the cortical bone, and the other at the top of the trabecular bone (see Figure 9). The dynamic simulation was run on the six types of crown, with and without cortical bone. As the mesh is the same for all the models, the selected nodes are also the same.

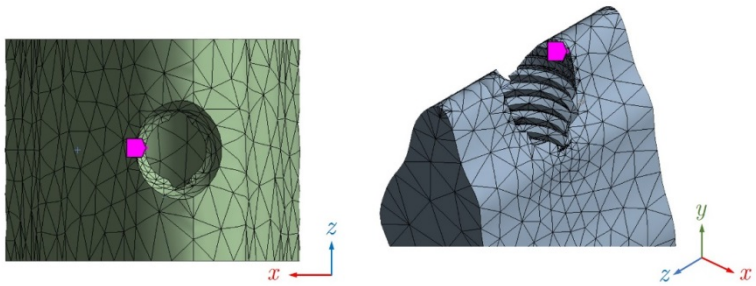

Figure 9. Benchmark nodes shown with a purple marker. **Left**: node at top of cortical bone; **right**: node at top of trabecular bone.

Two simulations were performed. In the first simulation, a healthy bone was considered, with a cortical and trabecular part, where the stresses at the cortical node and the trabecular node were measured. In the second simulation, a cortical bone absence was considered; this is only containing trabecular part, so stresses were measured only at the trabecular node (See Table 4).

Table 4. Bone part considered in each simulation.

	Node	Cortical Bone	Trabecular Bone
Simulation 1	Trabecular	X	X
	Cortical	X	X
Simulation 2	Trabecular		X

3. Results

The von Mises stress value was calculated and compared for each node. Table 5 shows the values of maximum von Mises stress obtained over time in the dynamic FEA simulation, with cortical bone at both nodes (cortical and trabecular) and the trabecular node without cortical bone.

Table 5. Maximum von Mises stresses obtained in cortical bone node (cortical and trabecular) and trabecular node without cortical bon[10]e.

		Maximum Von Mises Stress (MPa)					
Node	**Bone**	**MET**	**MCER**	**MCOM**	**FCOM**	**PKCOM**	**FCCER**
Cortical	trab + cort	63.35	72.06	40.71	35.70	32.05	75.46
Trabecular	trab + cort	12.09	15.23	10.30	10.01	9.15	16.69
Trabecular	Trab	30.80	33.87	29.30	31.14	22.80	43.33
trab vs. Trab + cort $\Delta\sigma_{vM}$ (%)		60.75%	55.03%	64.85%	67.85%	59.87%	61.48%

The von Mises stresses increase of trabecular bone without cortical with respect to the trabecular bone with cortical were calculated as follows:

$$\Delta\sigma_{vM}(\%) = \frac{\sigma_{vM\ trab+cort} - \sigma_{vM\ trab}}{\sigma_{vM\ trab+cort}} \cdot 100 \quad (4)$$

where σ_{vM} is the von Mises stress. The distribution of stress varies according to the time, reaching the maximum values of stress during the impact (see Figure 10).

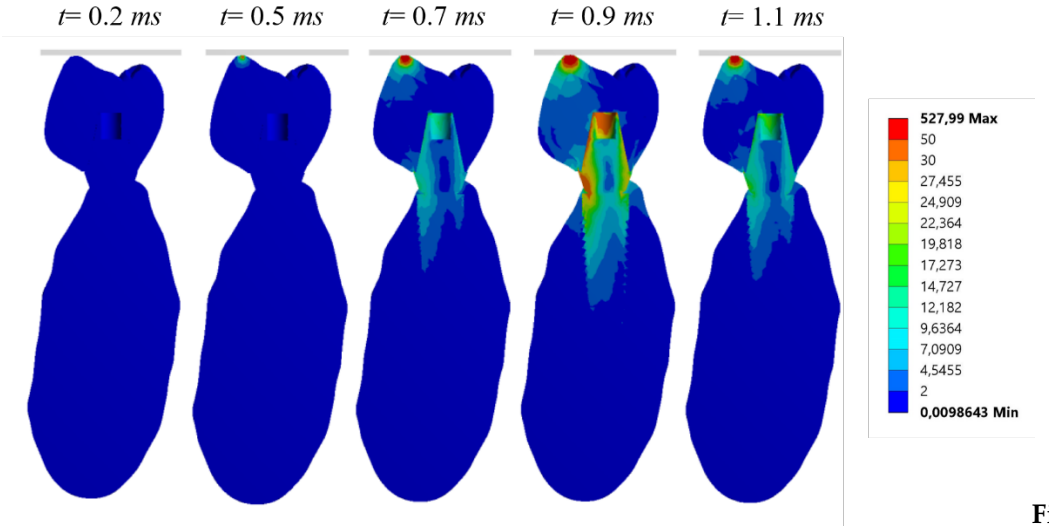

Figure 10. Von Mises stress distribution over time at a cross section using the Carbon Fiber-Ceramic crown (FCCER), considering both trabecular and cortical bone.

3.1. Cortical Node (with Cortical and Trabecular Bone)

Figure 11 shows the evolution of the von Mises stress of the dynamic simulation over time for the different models at the cortical node. The results obtained at the cortical node were (units in MPa): 32.05 (PKCOM), 35.70 (FCOM), 40.71 (MCOM), 63.35 (MET), 72.06 (MCER), and 75.46 (FCCER).

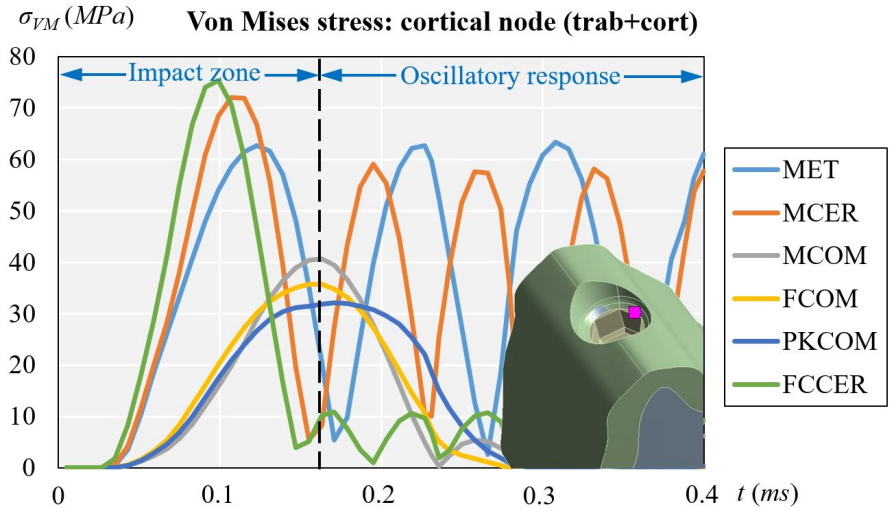

Figure 11. Comparison of equivalent von Misses stress over time on all crown materials at cortical node, considering both trabecular and cortical bone.

3.2. Trabecular Node (with Cortical and Trabecular Bone)

Figure 12 displays the evolution of the von Mises stress of the dynamic simulation over time for the different models at the trabecular node. The results obtained at the trabecular node (units in MPa) were: 9.15 (PKCOM), 10.01 (FCOM), 10.30 (MCOM), 12.09 (MET), 15.23 (MCER), and 16.69 (FCCER).

The evolution of the stress in the trabecular node displays the same pattern as in the cortical node but the stress values are considerably lower, since the trabecular bone is not very dense and is less rigid than cortical bone. Moreover, the trabecular bone receives the effects of the impact-load later. The shape of the function is almost equal to that of the cortical node, with more irregular oscillations at the end. Similar as the case of cortical node the maximum stress is in FCCER.

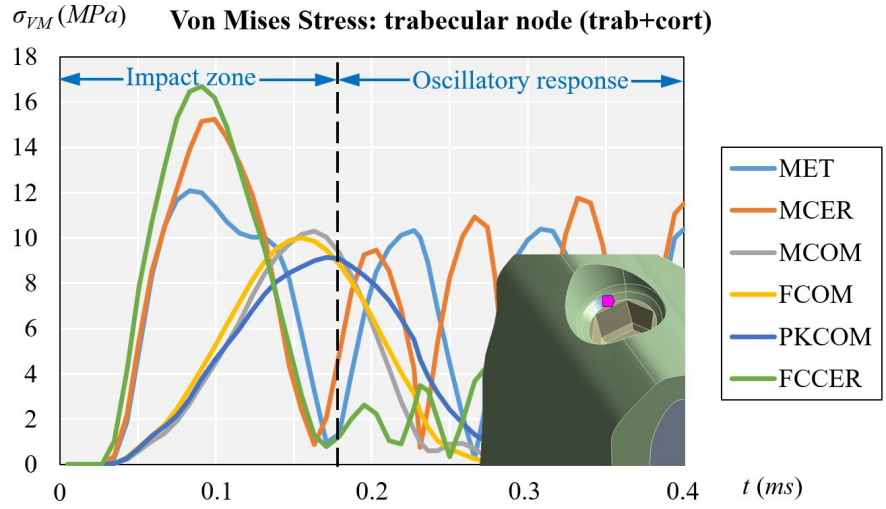

Figure 12. Comparison of equivalent von Mises stress over time depending on all crown materials at trabecular node, considering both trabecular and cortical bone.

Figure 11 (cortical node) and Figure 12 (trabecular node) show the high peak of stress and the duration over time for FCCER and MCER, which were much longer than for the composite-coated crowns, MCOM, FCOM, and PKCOM. The stress fluctuations due to the eccentricity of

the impact load with respect to the implant longitudinal axis can also be observed. The maximum stress values in the ceramic models (MCER and FCCER) are notably higher than in the rest of the models.

3.3. Trabecular Node (with Trabecular Bone Only)

This section is devoted to analyzing the effects of the pathological bone without cortical bone (peri-implantitis, bone regeneration, or immediate implant placement). Figure 13 displays the evolution of the von Mises stress of the dynamic simulation over time for the different models at the trabecular node. The results obtained trabecular node (units in *MPa*) were: 22.80 (PKCOM), 31.14 (FCOM), 29.30 (MCOM), 30.80 (MET), 33.87 (MCER), and 43.33 (FCCER). Figure 12 shows, like Figure 11, a similar behavior of the oscillations after the first peak happens. In Figure 13 the frequency of the oscillations is lower as a result of a more damped impact. Results at the cortical node (see Figure 11) showed that the behavior of the stress in the trabecular node is the same as the cortical but the values are much lower. Since the trabecular bone is not very dense, it is more flexible and works as a stress reducer.

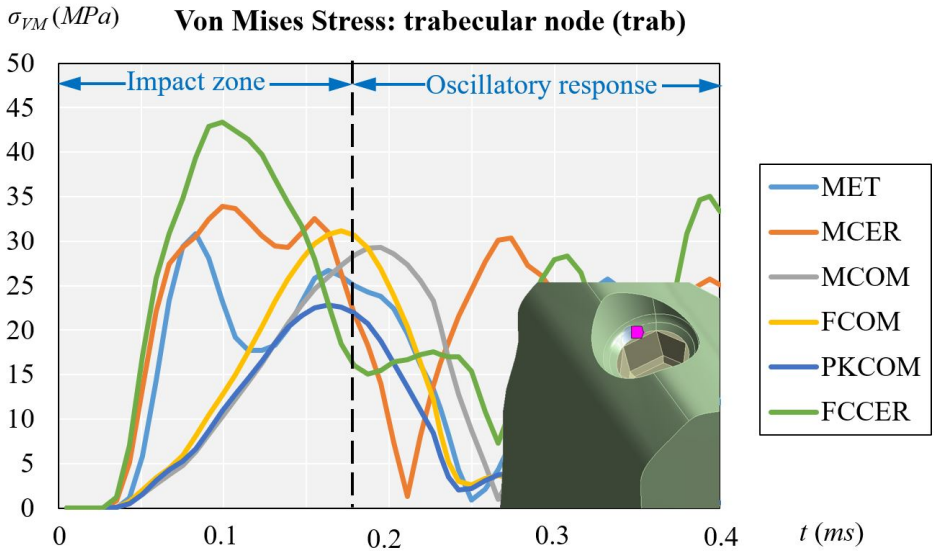

Figure 13. Comparison of equivalent von Mises stress over time at trabecular node, considering trabecular bone only.

Figure 14 shows a comparison between the maximum von Mises stress obtained in trabecular node with and without cortical bone.

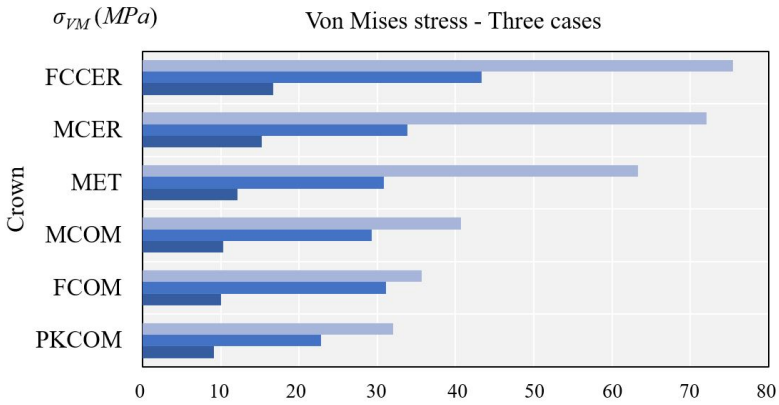

		PKCOM	FCOM	MCOM	MET	MCER	FCCER
Node cortical	trab+cort bone	32,05	35,70	40,71	63,35	72,06	75,46
Node trabecular	trab bone	22,80	31,14	29,30	30,81	33,87	43,33
	trab+cort bone	9,14	10,01	10,30	12,09	15,23	16,69

Figure 14. Comparison of maximum von Mises stress obtained at different nodes.

Figure 14 also shows a significant decrease of the von Mises equivalent stress at the trabecular bone with cortical compared to the case without cortical bone. The reason is that in the case with cortical bone, the impact was affecting the whole jawbone and cortical and trabecular bones, so the stress was divided into the two parts. The biggest increase in absolute value was observed in the MCER, with approximately 19 MPa difference.

4. Discussion

This study focused on comparing the stresses generated on cortical bone using six types of crown materials placed on a specific implant under impact-load conditions, so the same implant was maintained in all simulations. Therefore, the same methodology can be used to analyze the dynamic response of other implant models.

Since the forces applied in the masticatory process and eccentric bruxism are dynamic, it is important not only to study the mechanical behavior of the restorative materials in static forces, but also to know the mechanical behavior produced by dynamic forces. The rehabilitation materials used in the oral cavity could absorb impacts that may vary according to their mechanical properties [10,40–42]. Therefore, the evaluation of the mechanical behavior of the most widely-used materials in implant supported rehabilitations becomes a key issue. Moreover, the morphological, elemental, and biochemical structure without cortical bone is different to healthy bone structure [2].

Figures 11 and 12 (healthy bone) show that over time the reaction of the crown veneered with ceramic was different to that of the crown veneered with composite or with peek as a core. Many fluctuations in the MCER can be observed over time, and the results of the rebound produced by the material's stiffness, whereas in the crowns with less rigid materials (MCOM, PKCOM, or FCOM), only one fluctuation was observed.

Figure 13 (trabecular node: only trab.) does not have the damping effect of Figure 11 (cortical node: cort. and trab. bone) and Figure 12 (trabecular node: cort. and trab. bone). On the other hand, Figures 11 and 12 can be analyzed through the type of bone they represent, although the shape and location of the oscillations are similar, the Figure 12 has lower amplitudes.

The implant-crown rehabilitation materials made from a combination of metals and ceramics (FCCER, MET, MCER) are more rigid. In those materials, an initial stress peak of higher magnitude is observed, as compared to polymeric materials (PKCOM) that are less rigid. On the other hand, FCOM and PKCOM composites (less rigid) presented very low oscillations which were quickly damped.

It is important to transfer less stress to bone in cases of immediate implant placement, bone regeneration, or after peri-implantitis healing, given that there is no bone for some time in those cases. Hence, using materials that transfer less stress to the bone could avoid problems. In short, crowns made of rigid materials present a greater risk over time of bone loss around implants in the presence of gingival inflammation, since these materials transfer more stress to the bone, whether cortical or trabecular.

5. Conclusions

Our study demonstrated that more stress is transferred to the bone when stiffer materials (metal and/or ceramic) are used in implant supported rehabilitations and, conversely, more flexible materials transfer less stress to the implant connection. These relationships between materials' elastic properties and the dynamic force transmission are in accordance with the findings of different authors [10,40–43].

The presence (or absence) of cortical bone around the implant connection generates different behavior in rehabilitation implants when dynamic forces are applied, such as grinding, swallowing, or eccentric movements. Such transferred force, on the other hand, varies according to the rehabilitation material (more with ceramic than with composite), which is even more pronounced if cortical bone is present than if it is not.

The absence of cortical bone, in peri-implantitis, bone regeneration, or immediate implant placement cases, must be considered when choosing the crown material for the rehabilitation.

Author Contributions: Conceptualization, O.C.-N., R.M.-G. and J.C.-T.; data curation, X.M., M.C.; formal analysis, X.M., M.F., M.C. and J.C.-T.; funding acquisition, J.C.-T.; investigation, R.M.-G., X.M.; methodology, M.F.; project administration, J.C.-T.; resources, O.C.-N., J.C.-T.; software, X.M., M.F.; supervision, J.C.-T.; validation, O.C.-N., R.M.-G., X.M. and M.C.; visualization, X.M.; writing—original draft, R.M.-G., X.M., M.C.; writing—review and editing, O.C.-N., R.M.-G., X.M., M.F., M.C. and J.C.-T. All authors have read and agreed to the published version of the manuscript.

Funding: This research received no external funding.

Institutional Review Board Statement: Not applicable.

Informed Consent Statement: Not applicable.

Data Availability Statement: Not applicable.

Acknowledgments: We gratefully acknowledge the support of the NVIDIA Corporation with the donation of the Titan X Pascal GPU used for this numerical analysis.

Conflicts of Interest: The authors declare no conflict of interests.

Abbreviations

MET	Metal crown
MCER	Metal-Ceramic crown
MCOM	Metal-Composite crown
FCOM	Carbon fiber-Composite crown
PKCOM	Peek-Composite crown
FCCER	Carbon Fiber-Ceramic crown
FEA	Finite Element Analysis
DIC	Digital Image Correlation
CAD	Computer-Aided Design
CT Scan	Computer Tomography Scanner

References

1. Esposito, M.; Hirsch, J.M.; Lekholm, U.; Thomsen, P. Biological factors contributing to failures of osseointegrated oral implants. (I): Success criteria and epidemiology. *Eur. J. Oral Sci.* **1998**, *106*, 527–551. [CrossRef]
2. Maglione, M.; Vaccari, L.; Mancini, L.; Ciancio, R.; Bedolla, D.; Bevilacqua, L.; Tonellato, P. Micro-ATR FTIR, SEM-EDS, and X-ray Micro-CT: An Innovative Multitechnique Approach to Investigate Bone Affected by Peri-implantitis. *Int. J. Oral Maxillofac. Implants* **2019**, *34*, 631–641. [CrossRef]
3. Earthman, J.C.; Li, Y.; Van Schoiack, L.R.; Sheets, C.G.; Wu, J.C. Reconstructive Materials and Bone Tissue Engineering in Implant Dentistry. *Dent. Clin. N. Am.* **2006**, *50*, 229. [CrossRef]
4. Tribst, J.; Piva, A.D.; Borges, A. Biomechanical tools to study dental implants: A literature review. *Braz. Dent Sci.* **2016**, *19*, 5. [CrossRef]
5. Tang, Q.; Du, C.; Hu, J.; Wang, X.; Yu, T. Surface rust detection using ultrasonic waves in a cylindrical geometry by finite element simulation. *Infrastructures* **2018**, *3*, 29. [CrossRef]
6. Jerban, S.; Ma, Y.; Nazaran, A.; Dorthe, E.; Cory, E.; Carl, M.; D'Lima, D.; Sah, R.; Chang, E.; Du, J. Detecting stress injury (fatigue fracture) in fibular cortical bone using quantitative ultrashort echo time-magnetization transfer (UTE-MT): An ex vivo study. *NMR Biomed.* **2018**, *31*, e3994. [CrossRef] [PubMed]
7. Hériveaux, E.; Audoin, B.; Biateau, C.; Nguyen, V.H.; Haïat, G. Ultrasonic Propagation in a Dental Implant. *Ultrasound Med. Biol.* **2020**, *46*, 1464–1473. [CrossRef] [PubMed]
8. Pesqueira, A.; Goiato, M.; Filho, H.; Monteiro, D.; Dos Santos, D.; Haddad, M. Use of stress analysis methods to evaluate the biomechanics of oral rehabilitation with implants. *J. Oral Implantol.* **2014**, *40*, 217–228. [CrossRef]
9. McCormick, N.; Lord, J. Digital image correlation. *Materials Today* **2010**, *13*, 52–54. [CrossRef]
10. Magne, P.; Silva, M.; Oderich, E.; Boff, L.; Enciso, R. Damping behavior of implant-supported restorations. *Clin. Oral Implants Res.* **2013**, *24*, 143–148. [CrossRef] [PubMed]
11. Duyck, J.; Rønold, H.J.; Van Oosterwyck, H.; Naert, I.; Vander Sloten, J.; Ellingsen, J.E. The influence of static and dynamic loading on marginal bone reactions around osseointegrated implants: An animal experimental study. *Clin. Oral Implants Res.* **2001**, *12*, 207–218. [CrossRef]
12. Galindo-Moreno, P.; Fernández-Jiménez, A.; Avila-Ortiz, G.; Silvestre, F.J.; Hernández-Cortés, P.; Wang, H.L. Marginal bone loss around implants placed in maxillary native bone or grafted sinuses: A retrospective cohort study. *Clin. Oral Implants Res.* **2014**, *25*, 378–384. [CrossRef]
13. Lin, D.; Li, Q.; Li, W.; Swain, M. Dental implant induced bone remodeling and associated algorithms. *J. Mech. Behav. Biomed. Mater.* **2009**, *2*, 410–432. [CrossRef] [PubMed]
14. Cicciu, M.; Cervino, G.; Milone, D.; Risitano, G. FEM Investigation of the Stress Distribution over Mandibular Bone Due to Screwed Overdenture Positioned on Dental Implants. *Materials* **2018**, *11*, 1512. [CrossRef] [PubMed]
15. Li, J.; Jansen, J.; Walboomers, F.; van den Beucken, J. Mechanical aspects of dental implants and osseointegration: A narrative review. *J. Mech. Behav. Biomed. Mater.* **2020**, *103*, 103574. [CrossRef]
16. Kitagawa, T.; Tanimoto, Y.; Nemoto, K.; Aida, M. Influence of cortical bone quality on stress distribution in bone around dental implant. *Dent. Materials J.* **2005**, *24*, 219–224. [CrossRef] [PubMed]
17. Wachter, N.J.; Krischak, G.D.; Mentzel, M.; Sarkar, M.R.; Ebinger, T.; Kinzl, L.; Claes, L.; Augat, P. Correlation of bone mineral density with strength and microstructural parameters of cortical bone in vitro. *Bone* **2002**, *31*, 90–95. [CrossRef]
18. Kayabasi, O.; Yuzbasıoglu, E.; Erzincanli, F. Static, dynamic and fatigue behaviors of dental implant using finite element method. *J. Adv. Eng. Softw.* **2006**, *37*, 649–658. [CrossRef]
19. Benazzi, S.; Nguyen, H.N.; Kullmer, O.; Kupczik, K. Dynamic Modelling of Tooth Deformation Using Occlusal Kinematics and Finite Element Analysis. *PLoS ONE* **2016**, *11*, e0152663. [CrossRef]
20. Razaghi, R.; Mallakzadeh, M.; Haghpanahi, M. Dynamic simulation and finite Element analysis of the maxillary bone injury around dental implant during chewing different food. *Biomed. Eng. Appl. BasisCommun.* **2016**, *28*, 1650014. [CrossRef]
21. Chang, Y.; Tambe, A.; Maeda, Y.; Wada, M.; Gonda, T. Finite element analysis of dental implants with validation: To what extent can we expect the model to predict biological phenomena? A literature review and proposal for classification of a validation process. *Implant Dent.* **2018**, *4*, 7–12. [CrossRef]

22. Geramizadeh, M.; Katoozian, H.; Amid, R.; Kadkhodazadeh, M. Finite Element Analysis of Dental Implants with and without Microthreads under Static and Dynamic Loading. *J. Long-Term Eff. Med. Implants* **2017**, *27*, 25–35. [CrossRef]
23. Canto-Naves, O.; Marimon, X.; Ferrer, M.; Cabratosa-Termes, J. Comparison between experimental digital image processing and numerical methods for stress analysis in dental implants with different restorative materials. *J. Mech. Behav. Biomed. Mater.* **2021**, *113*, 104092. [CrossRef]
24. Solidworks Dassault Systemes. 2020. Available online: www.solidworks.com (accessed on 3 August 2021).
25. MIS Implants Tech. Ltd. 2021. Available online: https://www.mis-implants.com (accessed on 3 August 2021).
26. NewTom. 2021. Available online: https://www.newtom.it (accessed on 3 August 2021).
27. Lakatos, É.; Magyar, L.; Bojtár, I. Material Properties of the Mandibular Trabecular Bone. *J. Med. Eng.* **2014**, *2014*, 470539. [CrossRef]
28. Geng, J.P.; Tan, K.B.; Liu, G.R. Application of finite element analysis in implant dentistry: A review of the literature. *J. Prosthet. Dent.* **2001**, *85*, 585–598. [CrossRef]
29. Micro Medica Srl. 2021. Available online: http://micromedicasrl.it (accessed on 3 August 2021).
30. Renishaw. 2021. Available online: https://www.renishaw.com (accessed on 3 August 2021).
31. VITA Zahnfabrik, H. Rauter GmbH & Co. 2021. Available online: www.vita-zahnfabrik.com (accessed on 3 August 2021).
32. Heraeus Kulzer GmbH. 2021. Available online: https://www.kulzer.de (accessed on 3 August 2021).
33. Ivoclar Vivadent. 2021. Available online: https://www.ivoclarvivadent.es (accessed on 3 August 2021).
34. Invibio. 2021. Available online: https://invibio.com (accessed on 3 August 2021).
35. Van Eijden, T.M. Biomechanics of the Mandible. *Crit. Rev. Oral Biol. Med.* **2000**, *11*, 123–136. [CrossRef]
36. Peck, C.C. Biomechanics of occlusion—Implications for oral rehabilitation. *J. Oral Rehabil.* **2016**, *43*, 205–214. [CrossRef] [PubMed]
37. Ansys®Academic Research Mechanical, Release 18.1. 2020. Available online: www.ansys.com (accessed on 3 August 2021).
38. Minami, I.; Oogai, K.; Nemoto, T.; Nakamura, T.; Igarashi, Y.; Wakabayashi, N. Measurement of jerk-cost using a triaxial piezoelectric accelerometer for the evaluation of jaw movement smoothness. *J. Oral Rehabil.* **2010**, *37*, 590–595. [CrossRef] [PubMed]
39. Dattakumar, S.S.; Ganeshan, V. Converting Dynamic Impact Events to Equivalent Static Loads in Vehicle Chassis. Master Thesis, Chalmers University of Technology, Gothenburg, Sweden, 2017.
40. Conserva, E.; Menini, M.; Tealdo, T.; Bevilacqua, M.; Pera, F.; Ravera, G.; Pera, P. Robotic chewing simulator for dental materials testing on a sensor-equipped implant setup. *Int. J. Prosthodont.* **2008**, *21*, 501–508. [PubMed]
41. Menini, M.; Conserva, E.; Tealdo, T.; Bevilacqua, M.; Pera, F.; Ravera, G.; Pera, P. The use of a masticatory robot to analyze the shock absorption capacity of different restorative materials for implant prosthesis. *J. Biol. Res.* **2011**, *84*, 118–119. [CrossRef]
42. Menini, M.; Conserva, E.; Tealdo, T.; Bevilacqua, M.; Pera, F.; Signori, A. Shock Absorption Capacity of Restorative Materials for Dental Implant Prostheses: An In Vitro Study. *Int. J. Prosthodont.* **2013**, *26*, 549–556. [CrossRef] [PubMed]
43. Vigolo, P.; Gracis, S.; Carboncini, F.; Mutinelli, S. Internal- vs External-Connection Single Implants: A Retrospective Study in an Italian Population Treated by Certified Prosthodontists. *Int. J. Oral Maxillofac. Implants* **2016**, *31*, 1385–1396. [CrossRef] [PubMed]

VII. DISCUSIÓN

Es importante conocer las propiedades físico-mecánicas de los materiales utilizados en las rehabilitaciones implantológicas. Hay diversas investigaciones que valoran y analizan las propiedades mecánicas de los materiales de rehabilitación. Una de las valoraciones mecánicas que se halla habitualmente en las investigaciones, es la respuesta de los materiales de rehabilitación a las cargas o fuerzas estáticas. Constatamos que la mayoría de investigaciones realizadas con fuerzas estáticas no encuentran diferencias significativas entre materiales de distinta rigidez cuando se someten a una fuerza constante, tanto en estudios *in vitro* de laboratorio (115), como en estudios de elementos finitos (116). Como indican Cantó-Navés et al. (44) y Juodzbalys et al. (117), esto es debido a que cuando se somete un material de rehabilitación a una fuerza constante, una vez se ha producido la deformación correspondiente, la tensión transmitida a través del material no varía para materiales de distinta rigidez.

Como hemos visto, en la fisiología oral no todas las fuerzas que pueden recibir nuestras rehabilitaciones son siempre fuerzas constantes o estáticas, de manera que es importante valorar también el comportamiento de los materiales de rehabilitación cuando están sujetos a fuerzas dinámicas. Así, durante la masticación se producen fuerzas de impacto, resultado de la entrada en contacto de dos cuerpos (bien diente-alimento o diente-diente) a cierta velocidad. Las fuerzas de impacto han sido muy

frecuentemente utilizadas para evaluar el comportamiento de los materiales de rehabilitación a las fuerzas oclusales. Se han utilizado distintas metodologías para su determinación.

Gracis et al. (65) realizaron un estudio *in vitro* en el que analizaron la capacidad de absorber los impactos de distintos materiales de rehabilitación: oro, cromo-cobalto, metal-cerámica, metal-composite y metal-resina. Mediante una rampa, impactaron una bola de acero sobre unas muestras cilíndricas de las distintas combinaciones de los materiales indicados. Debajo de las muestras se posicionó una galga extensiométrica conectada a un transductor y este a un osciloscopio digital que reproducía una curva en la que se podía medir la tensión transmitida.

Magne et al. (67) analizaron la capacidad de absorción de fuerzas de impacto de rehabilitaciones implantosoportadas de resina compuesta CAD/CAM monolítica, resina compuesta-cerámica, zirconia-resina compuesta, zirconia-cerámica, utilizando el Periometer®. El Periometer® (Perimetrics, Newport Beach, CA, EE. UU.) es un instrumento aprobado por la FDA que proporciona datos del coeficiente de pérdida (comportamiento de amortiguamiento) y la energía que retorna después de haberse realizado el impacto.

Bassit et al. (88) realizaron un estudio *in vivo* para evaluar la capacidad de absorción de las fuerzas de masticación de coronas implantosoportadas de oro-cerámica y oro-resina, mediante galgas extensiométricas. A cinco pacientes les emplazaron a realizar un

cierre bucal rápido y posteriormente varios cierres rápidos continuados sobre los dos tipos de coronas. En la misma investigación, también realizaron un estudio *in vitro* en el que se hacía impactar un peso de 164 gr desde una altura (no concretada) sobre estas mismas muestras.

Destacar el estudio de Conserva et al. (115). Estos autores diseñaron un simulador de masticación mecánico que era capaz de reproducir los movimientos mandibulares en tres dimensiones. Además, lo validaron para determinar la transmisión de la tensión de materiales con distinto módulo elástico. Aparte de simular los movimientos tridimensionalmente con una precisión de 0,1 mm, el sistema estaba provisto de una base con sensores (8 galgas extensiométricas activas, 2 galgas pasivas en la superficie y 2 galgas activas en la base) que permitían detectar las tensiones de las muestras cada 100 ms, mediante un conversor analógico-digital.

También cabe mencionar el estudio *in vivo* de Hobkirk et al. (116). Colocaron en cinco pacientes dos tipos de rehabilitaciones completas sobre implantes (resina acrílica y cerámica). Con unos transductores fijados a la prótesis evaluaron la trasmisión de las fuerzas de masticación a través de las prótesis al masticar diferentes tipos de comida.

Por otro lado Juodzbalys et al. (42) utilizaron como metodología el análisis de elementos finitos. Mediante el diseño de una sección mandibular con una corona sobre un implante unitario se aplicaron, primeramente, fuerzas estáticas y posteriormente fuerzas a lo largo de un periodo de tiempo, a las que denominó fuerza transicional o de

impacto. Sin embargo, al ser una fuerza que iba en aumento en el tiempo podemos decir que era una fuerza dinámica pero no una fuerza de impacto.

No hemos hallado en la literatura investigaciones con elementos finitos 3D dinámicos que utilicen fuerzas de impacto en el estudio de materiales de rehabilitación sobre implantes.

Por otra parte, Geng et al. en el 2001 (31) en su revisión bibliográfica sobre el análisis de elementos finitos en implantología, recomienda el uso de estudios dinámicos, ya que hay una tensión mayor cuando se aplican fuerzas dinámicas que cuando se aplican fuerzas estáticas.

Así pues, la metodología aplicada en nuestros estudios es novedosa al utilizar una fuerza dinámica mediante un impacto con elementos finitos 3D. De esta forma, podemos evaluar la tensión generada y transferida a distintos niveles de la rehabilitación sobre implantes, es decir, a nivel del material de recubrimiento estético, del pilar y del hueso, lo cual creemos que es dificultoso o no es posible mediante otros métodos.

Los estudios que hemos realizado demuestran que las fuerzas dinámicas generadas por un impacto se distribuyen a lo largo de la rehabilitación implantológica unitaria hasta el hueso y que este recibe una determinada tensión. Esta tensión puede variar de acuerdo con las propiedades físico-mecánicas de los materiales utilizados en la

rehabilitación, ya sea el recubrimiento estético de las coronas sobre implantes como el material interno de las mismas.

En el primer estudio publicado se observó que las fuerzas de impacto en las coronas con recubrimiento estético de materiales rígidos (cerámica) y las coronas metálicas generaban, a nivel de la cortical ósea y a nivel del material de recubrimiento estético, mayores tensiones que las coronas con recubrimiento estético menos rígido (composite) y, además, esta tensión en el nodo de la corona y en la cortical aparecía de manera más inmediata en las coronas con recubrimiento rígido que en las coronas con recubrimiento menos rígido. Así, a nivel de la corona MET se generaba una tensión de 103,81 MPa y en la MCER de 91,18 MPa. Por el contrario, en la corona FCOM se observó una tensión de 49,98 MPa, en la de PKCOM de 31,51 MPa y en la de FCCER una tensión de 61,82 MPa. Por lo tanto, se reducía la tensión con el uso de materiales menos rígidos y más aún si estos materiales estaban en el recubrimiento estético. Estos resultados no pueden ser comparados con otros estudios de impactos dinámicos, ya que solo es posible obtener estas tensiones mediante el análisis de una fuerza de impacto con un estudio dinámico de elementos finitos.

En el nodo del pilar, las tensiones obtenidas fueron similares en todas las coronas (entre 89,27 MPa y 77,82 MPa), excepto en la de FCOM que fue de 50,80 MPa. Con la corona de FCCER se generaba, a nivel de la cortical, una tensión de 75,46 MPa, mientras que con la de PKCOM la tensión fue de 32,05 MPa, lo cual supone una reducción de la tensión de un 42,5%. Estos resultados se corresponden con los resultados obtenidos

por Gracis et al. (65) en su estudio *in vitro*, en el que se midió una trasmisión de las fuerzas de impacto de 148,38 N para las muestras de metal-cerámica y de 64,28 N para las muestras de metal-composite. O sea, se observó una absorción del impacto generado del 43,3 % con el uso de metal-composite respecto a las muestras metal-cerámica. Este resultado es altamente similar al que hemos obtenido con nuestro estudio de impacto mediante análisis dinámico de elementos finitos 3D.

Así mismo, Magne et al. (67) en su estudio *in vitro* utilizando el Periometer® y el coeficiente de pérdida de energía, obtuvieron como resultado que las coronas sobre implantes que utilizaban composite, ya fuera en el pilar o en la rehabilitación, tenían una capacidad de absorción de los impactos parecido al diente natural simulado que utilizaron. Y además, el cambio de material en cualquiera de los componentes (pilar, estructura interna o estructura externa) tenía un efecto significativo, siendo la corona sobre implante con núcleo de composite y composite en la rehabilitación la que tenía más coeficiente de pérdida de energía (LC = 0,068) y la corona con núcleo de zirconia y cerámica en la rehabilitación la que menos (LC= 0,042). Por tanto, se observa que los valores altos de LC (composites), corresponden a los materiales que presentan mayor absorción de la energía. Debemos tener en cuenta que en este estudio los autores evalúan el efecto de amortiguación con el Periometer®. La capacidad de amortiguación está relacionada con la viscosidad del material y esta a la velocidad de deformación y, por tanto, a la velocidad de impacto. A pesar de las diferencias metodológicas, las conclusiones que obtuvieron son similares a las de nuestros estudios.

Bassit et al.(88), en su estudio *in vivo,* no encontraron diferencias significativas entre el uso de coronas con recubrimiento cerámico (rígido) y coronas con recubrimiento de resina (menos rígido). Hallaron una gran variabilidad en los resultados, tanto entre pacientes como en cada uno de ellos. Así pues, la falta de significancia podría ser debida a esta variabilidad y al tamaño muestral (n=5). Por otro lado, cuando realizaron la parte *in vitro* de su estudio mediante la caída de un peso sobre las muestras, sí observaron diferencias significativas entre las coronas con recubrimiento cerámico (n1: 310 N; n2: 3025 N; n3: 1197; n4: 3668 N; n5: 2164 N) y las coronas con recubrimiento de resina (n1: 110 N; n2: 315; n3: 403 N; n4: 530 N; n5: 344 N) cuyos valores presentan una variación de porcentaje que oscila de entre un 10% y un 35%. Aún observando los resultados del estudio, los autores discrepan de la idea de que las fuerzas de la masticación puedan generar, en una situación fisiológica real, más tensiones sobre el implante cuando se utilizan rehabilitaciones cerámicas que cuando se utilizan rehabilitaciones de resina acrílica, ya que, según ellos mismos, la velocidad del movimiento de cierre o de oclusión y la masa de la mandíbula pueden no ser suficientes para introducir una generación de choque significativa y que la diferencia de elasticidad entre los diferentes materiales oclusales puede ser anulada por la flexibilidad del hueso. Ahora bien, nuestros estudios han demostrado que la masa de la mandíbula y la velocidad de movimiento de la mandíbula es suficiente para apreciar diferencias significativas en cuanto a las tensiones generadas en el hueso periimplantario.

En el estudio *in vitro* de Menini et al. (66), utilizando el robot descrito por Conserva et al. (117) que simulaba los movimientos masticatorios, determinaron que una corona

de cerámica Empress 2 (Ivoclar Vivadent, Liechtenstein) transmitía una fuerza de 484,5 N (5,5 SD (Standard Deviation)) y una corona de composite Signum (Heraeus Kulzer, Alemania) 187,4 N (4,2 SD); por lo tanto, se producía una reducción de la fuerza transmitida entre ellos de un 38,7% (63). Como se puede observar en la reducción de la fuerza transmitida al hueso según el material de rehabilitación utilizado, aún usando distintos parámetros, hay resultados similares entre nuestro estudio dinámico de elementos finitos 3D y los estudios realizados por Menini et al. (63,66).

Teniendo en consideración las limitaciones de una comparación de resultados obtenidos mediante distintas metodologías y evaluando distintos materiales, se constata en todos ellos el efecto de reducción de tensiones que tienen los materiales con menor rigidez.

Se ha podido constatar con los resultados obtenidos en nuestros estudios, que el material estético de recubrimiento de la corona es el que más influye en la absorción de la energía del impacto. Así, cuanto menos rígido es el material de recubrimiento menores son las tensiones en la superficie de la corona y en la zona periimplantar. Las prótesis unitarias implantosoportadas con recubrimiento de cerámica o totalmente metálicas mostraron un pico de tensión más significativo y más temprano, tanto en la corona como en el hueso cortical que aquellas con recubrimiento de composite.

En el estudio en el que valoramos las tensiones en ausencia de hueso cortical se observó que la tensión que recibía el hueso trabecular era mucho mayor cuando hay

ausencia de hueso cortical. En la corona de PKCOM se pasa de tensiones en el nodo trabecular de 9,14 MPa en presencia de cortical a 22,8 MPa en ausencia de cortical; en la corona de FCOM se pasaba de 10,01 MPa a 31,14 MPa; en la corona de MCOM se pasaba de 10,3 MPa a 29,30 MPa; en la corona de MET se pasaba de 12,09 MPa a 30,82 MPa; en la corona de MCER se pasaba de 15,23 MPa a 33,87 MPa y finalmente en la corona de FCCER se pasaba de 16,64 MPa a 43,33 MPa; es decir había un incremento de las tensiones de entre 2,23 y 3 veces. También se constató que el uso de materiales menos rígidos en la parte de recubrimiento estético disminuye sustancialmente la tensión generada en el hueso trabecular en ausencia de hueso cortical. Así, la tensión en el hueso trabecular en ausencia de cortical en el caso de la corona de FCCER fue de 43,33 MPa donde contrasta con la tensión de la corona de PKCOM de 22,8 MPa.

En el estudio de Juodzbalys et al. (42) los autores compararon una rehabilitación unitaria sobre implante con un recubrimiento estético de cerámica Vita VMK 68 Vident (Vita, Alemania) con una con recubrimiento estético de composite GC Gradia (GC, Japón). Se observó una reducción de la fuerza de impacto en más de un 6.75% con el uso del recubrimiento de composite. Aún observándose en estos resultados una reducción de la tensión obtenida no se asemeja mucho a nuestros resultados. Creemos que esto puede ser debido a que en este estudio se utilizó un tiempo de 5 ms, cuando nosotros utilizamos una duración de la simulación de 0,4 ms y 53 puntos de valoración con un intervalo entre ellos de 7,55 µs siendo más concisos Así mismo, teniendo en cuenta que Juodzbalys et al. (42) emplearon fuerzas que llegaron hasta los 1000N en sentido oblicuo sus resultados pueden diferir de los nuestros en gran medida. Además,

en nuestro estudio, se utilizaron fuerzas de impacto creadas por una masa a una velocidad de 1,25 m/s y entendemos que en su estudio no se realizó un impacto sino que se utilizó un estudio de fuerzas dinámicas en el que se incrementaba la fuerza aplicada de forma constante hasta llegar a los 1000 N.

Por otro lado, Wakabayashi et al. (118) recomiendan utilizar los datos de los materiales de forma adecuada, es decir, en el caso de los materiales que presentan una curva de tensión-deformación, los llamados materiales no-lineales, utilizar estos valores no-lineales para mejorar la precisión del estudio. En el primero de nuestros estudios, a pesar de ser dinámico, se comprobó que las tensiones a las que se sometían los materiales en nuestra investigación no llegaban al punto de deformación plástica, por lo tanto, las tensiones aplicadas no podían crear una deformación permanente en los materiales, de manera que usar condiciones de los materiales no lineales no tendría consecuencias en nuestros resultados.

Nuestros estudios presentan las limitaciones propias de los estudios de simulación numérica, debido a sus posibles diferencias con la realidad clínica, a pesar que intentamos reproducirlas en la medida de lo posible.

Los resultados obtenidos nos indican que los materiales de rehabilitación menos rígidos tienen la capacidad de absorber más las fuerzas de impacto que los materiales más rígidos. Así mismo podemos afirmar que en ausencia de hueso cortical las tensiones transmitidas al hueso trabecular son mayores que en su presencia. Por tanto, estos

resultados están de acuerdo con la hipótesis de que las tensiones transferidas a una prótesis unitaria implantosoportada y al hueso periimplantario cortical y trabecular por una fuerza oclusal de impacto varían según el material rehabilitador utilizado.

Al analizar los resultados a nivel de la cortical ósea, se observó que el material utilizado en la estructura interna de la corona también influye ya que aparecen unas oscilaciones a lo largo de los 4 ms. que no se observan cuando analizamos el nodo de la corona. En las coronas con materiales rígidos en la superficie (MET, MCER y FCCER) se aprecia un pico alto, mientras que las restauraciones con materiales menos rígidos en la superficie (MCOM, FCOM y PKCOM) presentan un pico de tensión menor. Podemos observar, además, que las coronas MET y MCER presentan unas oscilaciones con picos altos de tensión, mientras que la corona FCCER estas oscilaciones desaparecen casi por completo. Las coronas MCOM, FCOM y PKCOM, casi no presentan oscilaciones. No se han encontrado estudios que refieran dichas oscilaciones, de manera que no podemos contrastarlas.

En nuestro estudio, en las situaciones con ausencia de hueso cortical se observo, así mismo, que esas oscilaciones a las que nos hemos referido eran erráticas.

Las revisiones sobre elementos finitos en implantología de Reddy et al. (119), Jian-Ping et al.(31) y Chang et al. (34) sugieren que las investigaciones de elementos finitos deberían tener una validación con estudios *in vitro*. En las investigaciones realizadas en esta tesis, donde queríamos conocer como repercutía el uso de distintos materiales de

rehabilitación sobre un implante en la tensión recibida en el hueso, no teníamos la capacidad de realizar un estudio *in vitro* o *in vivo* que nos permitiera conocer la tensión en el hueso. Este es el motivo por el que se realizó solo mediante análisis dinámico de elementos finitos. No obstante, actualmente, estamos trabajando dentro de esta línea de investigación en un estudio *in vitro,* que nos permitirá determinar la capacidad de absorción de un impacto con distintos materiales de restauración, aunque no la tensión generada a nivel óseo. El estudio *in vitro* que estamos realizando, refleja nuestro interés de proseguir con esta línea de investigación. Las características de los materiales de restauración utilizados y el desarrollo de metodologías estandarizadas para la valoración de la tensión generada por las fuerzas oclusales en la prótesis y en el hueso periimplantario son nuestro objetivo. Este interés se basa en las posibles consecuencias que pudieran derivarse del uso de un material u otro en las rehabilitaciones, especialmente en situaciones en las que hay inflamación de los tejidos blandos periimplantarios o ausencia de hueso cortical. La industria va generando nuevos materiales que deberán ir siendo estudiados.

VIII. CONCLUSIONES

Las fuerzas oclusales se transfieren a la corona, al pilar y al implante causando tensión en el hueso periimplantario, tanto cortical como trabecular. Por este motivo es importante estudiar las tensiones transferidas al hueso periimplantar dependiendo de los materiales de rehabilitación utilizados.

Teniendo en consideración las limitaciones de nuestros estudios, se puede concluir que la tensión que se transfiere al hueso periimplantario a través de la corona, el pilar y el implante con la aplicación de una fuerza de impacto depende del material rehabilitador. Dicha tensión varía según la rigidez del material utilizado en la rehabilitación, tanto del material de la estructura interna de la corona como del material estético de recubrimiento.

Se puede observar en nuestro estudio que el uso de materiales menos rígidos utilizados como recubrimiento estético reduce las tensiones a nivel de la corona (nodo dispuesto por debajo del recubrimiento estético).

También podemos concluir que, cuanto menos rígido es el material usado en la corona, tanto en la parte externa como en la interna, menor es la tensión generada en la superficie de la corona y en el hueso periimplantario. El uso de materiales

menos rígidos en el recubrimiento estético de la corona protésica es más recomendable que el uso de materiales rígidos, aunque tengamos en la estructura interna materiales menos rígidos. Por lo tanto, podría deducirse que se puede reducir el riesgo de pérdida ósea periimplantaria, especialmente en pacientes de riesgo de presentar inflamación gingival, usando materiales menos rígidos, ya que se reduce la tensión generada en el hueso.

En ausencia de hueso cortical, como podemos encontrar en los pacientes con regeneraciones óseas, periimplantitis previa, colocación de implantes inmediatos post-extracción o en implantes colocados a nivel subcortical, la transmisión de la tensión en el hueso trabecular varía considerablemente según el material utilizado en la rehabilitación, presentando en todos los casos mayor tensión que en las situaciones en que sí hay cortical ósea.

En ausencia de hueso cortical el uso de materiales con menor rigidez reduce considerablemente la tensión en el hueso trabecular, comparándolo con el uso de materiales más rígidos y se debería considerar su uso cuando se realiza la elección del material de rehabilitación.

IX. BIBLIOGRAFÍA

1. Sanz M, Lang NP, Kinane DF, Berglundh T, Chapple I, Tonetti MS. Seventh European Workshop on Periodontology of the European Academy of Periodontology at the Parador at la Granja, Segovia, Spain. J Clin Periodontol. 2011 Mar;38 Suppl 1:1–2.
2. Klinge B, Meyle J, Claffey N, Flemmig T, Flemming I, Mombelli A, et al. Peri-implant tissue destruction. The Third EAO Consensus Conference 2012. Clin Oral Implants Res. 2012;23(SUPPL.6):108–10.
3. S Calderon P, M C Dantas P, C L Montenegro S, F P Carreiro A, G R C Oliveira A, M Dantas E, et al. Technical complications with implant-supported dental prostheses. J Oral Sci [Internet]. 2014;56(2):179–84.
4. Chang M, Chronopoulos V, Mattheos N. Impact of excessive occlusal load on successfully-osseointegrated dental implants: a literature review. J Investig Clin Dent. 2013 Aug;4(3):142–50.
5. Mattheos N, Schittek Janda M, Zampelis A, Chronopoulos V. Reversible, Non-plaque-induced loss of osseointegration of successfully loaded dental implants. Clin Oral Implants Res. 2013;24(3):347–54.
6. Afrashtehfar KI, Afrashtehfar CD. Lack of association between overload and peri-implant tissue loss in healthy conditions. Evid Based Dent. 2016 Sep;17(3):92–3.
7. Mazel A, Belkacemi S, Tavitian P, Stephan G, Tardivo D, Catherine JH, et al. Peri-implantitis risk factors: A prospective evaluation. J Investig Clin Dent. 2019 May;10(2):e12398.
8. Duyck J, Rønold HJ, Van Oosterwyck H, Naert I, Sloten J Vander, Ellingsen JE. The influence of static and dynamic loading on marginal bone reactions around osseointegrated implants: An animal experimental study. Clin Oral Implants Res. 2001;12(3):207–18.
9. Naert I, Duyck J, Vandamme K. Occlusal overload and bone/implant loss. Clin Oral Implants Res. 2012;23(SUPPL.6):95–107.
10. Duyck J, Vandamme K. The effect of loading on peri-implant bone: A critical review of the literature. J Oral Rehabil. 2014;41(10):783–94.
11. Carl F. Driscoll, Martin A. Freilich, Albert D. Guckes, Kent L. Knoernschild and Thomas J. McGarry, Members G of PTC. The Glossary of Prosthodontic Terms [Internet]. MISCELLANEOUS| VOLUME 117, ISSUE 5, SUPPLEMENT , E1-E105, MAY 01, 2017. 2017. Availablefrom:https://www.thejpd.org/pb/assets/raw/HealthAdvance/journals/ympr/index.htm
12. Trulsson M. Force encoding by human periodontal mechanoreceptors during mastication. Arch Oral Biol. 2007 Apr;52(4):357–60.
13. Peck CC. Biomechanics of occlusion - implications for oral rehabilitation. J Oral Rehabil. 2016;43(3):205–14.
14. van der Bilt A, Engelen L, Pereira LJ, van der Glas HW, Abbink JH. Oral physiology

and mastication. Physiol Behav. 2006;89(1):22–7.
15. Rovira-Lastra B, Flores-Orozco EI, Ayuso-Montero R, Peraire M, Martinez-Gomis J. Peripheral, functional and postural asymmetries related to the preferred chewing side in adults with natural dentition. J Oral Rehabil. 2016;43(4):279–85.
16. Karakis D, Dogan A. The craniofacial morphology and maximum bite force in sleep bruxism patients with signs and symptoms of temporomandibular disorders. Cranio. 2015 Jan;33(1):32–7.
17. Lujan-Climent M, Martinez-Gomis J, Palau S, Ayuso-Montero R, Salsench J, Peraire M. Influence of static and dynamic occlusal characteristics and muscle force on masticatory performance in dentate adults. Eur J Oral Sci. 2008;116(3):229–36.
18. Hattori Y, Satoh C, Kunieda T, Endoh R, Hisamatsu H, Watanabe M. Bite forces and their resultants during forceful intercuspal clenching in humans. J Biomech. 2009;42(10):1533–8.
19. Varga S, Spalj S, Lapter Varga M, Anic Milosevic S, Mestrovic S, Slaj M. Maximum voluntary molar bite force in subjects with normal occlusion. Eur J Orthod. 2011;33(4):427–33.
20. Yamaguchi S, Okada C, Watanabe Y, Watanabe M, Hattori Y. Analysis of masticatory muscle coordination during unilateral single-tooth clenching using muscle functional magnetic resonance imaging. J Oral Rehabil. 2018 Jan;45(1):9–16.
21. Wang L, D'Alpino PHP, Lopes LG, Pereira JC. Mechanical properties of dental restorative materials: relative contribution of laboratory tests. J Appl Oral Sci. 2003;11(3):162–7.
22. Anusavice KJ. Recent developments in restorative dental ceramics. J Am Dent Assoc. 1993 Feb;124(2):72-74,76-78,80-84.
23. RG C. Mechanical properties. In: Restorative dental materials. 1997. p. 56-103.
24. Ayneto Gubert X, Ferrer Balles M. Mecánica del medio continuo en la ingeniería: Teoría y problemas resueltos [Internet]. Universitat Politecnica de Catalunya. Iniciativa Digital Politecnica; 2012. (Libros UPC en acceso abierto). Available from: https://books.google.es/books?id=tQBqBQAAQBAJ
25. Landau LD, Lifshitz EM, Berestetskii VB, Pitaevskii LP, D'Alessio JT. Física teórica.Teoría de la elasticidad [Internet]. Reverte; 2021. (Física teórica de Landau). Available from: https://books.google.es/books?id=vpAXEAAAQBAJ
26. Callister WD. Introducción a la ciencia e ingeniería de los materiales. Volumen I [Internet].Reverte;2020.Availablefrom:https://books.google.es/books?id=38n7DwAAQBAJ
27. The International Organization for Standardization [Internet]. Available from: https://www.iso.org/standard/59936.html
28. Timoshenko S. Elements Of Strength Of Materials 5ed [Internet]. Affiliated East West Press Pvt. Limited; 1968.
29. Williams PD, Smith DC. Measurement of the tensile strength of dental restorative materials by use of a diametral compression test. J Dent Res. 1971;50(2):436–42.
30. Welch-Phillips A, Gibbons D, Ahern DP, Butler JS. What Is Finite Element Analysis? Clin spine Surg. 2020 Oct;33(8):323–4.
31. Geng JPA, Tan KBC, Liu GR. Application of finite element analysis in implant

dentistry: A review of the literature. J Prosthet Dent. 2001 Jun;85(6):585–98.
32. Trivedi S. Finite element analysis: A boon to dentistry. J Oral Biol Craniofacial Res [Internet]. 2014;4(3):200–3.
33. Silva NRFA, Bonfante E, Rafferty BT, Zavanelli RA, Martins LL, Rekow ED, et al. Conventional and Modified Veneered Zirconia vs. Metalloceramic: Fatigue and Finite Element Analysis. J Prosthodont. 2012;21(6):433–9.
34. Chang Y, Tambe AA, Maeda Y, Wada M, Gonda T. Finite element analysis of dental implants with validation: to what extent can we expect the model to predict biological phenomena? A literature review and proposal for classification of a validation process. Int J Implant Dent. 2018 Mar 8;4(1):5–7.
35. Poojar B, Ommurugan B, Adiga S, Thomas H, Sori RK, Poojar B, et al. Application of Finite Element Model in Implant Dentistry: A Systematic Review. Asian J Pharm Clin Res. 2017;7(10):1–5.
36. Menini M, Pesce P, Bevilacqua M, Pera F, Tealdo T, Barberis F, et al. Effect of Framework in an Implant-Supported Full-Arch Fixed Prosthesis: 3D Finite Element Analysis. Int J Prosthodont [Internet]. 2015;28(6):627–30.
37. Alvarez-Arenal A, Lasheras FS, Fernández EM, González I. A jaw model for the study of the mandibular flexure taking into account the anisotropy of the bone. Math Comput Model [Internet]. 2009;50(5–6):695–704.
38. Geramizadeh M, Katoozian H, Amid R, Kadkhodazadeh M. Finite Element Analysis of Dental Implants with and without Microthreads under Static and Dynamic Loading. J Long Term Eff Med Implants. 2017;27(1):25–35.
39. Cantó-Navés O, Medina-Galvez R, Marimon X, Ferrer M, Figueras-Álvarez Ó, Cabratosa-Termes J. A 3D Finite Element Analysis Model of Single Implant-Supported Prosthesis under Dynamic Impact Loading for Evaluation of Stress in the Crown, Abutment and Cortical Bone Using Different Rehabilitation Materials. Mater (Basel, Switzerland). 2021 Jun;14(13).
40. Medina-Galvez R, Cantó-Navés O, Marimon X, Cerrolaza M, Ferrer M, Cabratosa-Termes J. Bone Stress Evaluation with and without Cortical Bone Using Several Dental Restorative Materials Subjected to Impact Load: A Fully 3D Transient Finite-Element Study. Mater (Basel, Switzerland). 2021 Oct;14(19).
41. Geramizadeh M, Katoozian H, Amid R, Kadkhodazadeh M. Static, Dynamic, and Fatigue Finite Element Analysis of Dental Implants with Different Thread Designs. J Long Term Eff Med Implants. 2016;26(4):347–55.
42. Juodzbalys G, Kubilius R, Eidukynas V, Raustia AM. Stress distribution in bone: Single-unit implant prostheses veneered with porcelain or a new composite material. Implant Dent. 2005;14(2):166–75.
43. Erkmen E, Meriç G, Kurt A, Tunç Y, Eser A. Biomechanical comparison of implant retained fixed partial dentures with fiber reinforced composite versus conventional metal frameworks: A 3D FEA study. J Mech Behav Biomed Mater [Internet]. 2011 [cited 2017 Jul 1];4(2):107–16.
44. Cantó-Navés O, Marimon X, Ferrer M, Cabratosa-Termes J. Comparison between experimental digital image processing and numerical methods for stress analysis in dental implants with different restorative materials. J Mech Behav Biomed Mater. 2021 Jan;113:104092.

45. Esposito M, Hirsch JM, Lekholm U, Thomsen P. Biological factors contributing to failures of osseointegrated oral implants. (I): Success criteria and epidemiology. Eur J Oral Sci [Internet]. 1998;106(106(1):527-551):527.
46. Roos-Jansaker AM, Renvert S, Egelberg J. Treatment of peri-implant infections: a literature review. J Clin Periodontol. 2003 Jun;30(6):467–85.
47. Lindhe J, Meyle J, Periodontology GD of EW on. Peri-implant diseases: Consensus Report of the Sixth European Workshop on Periodontology. J Clin Periodontol. 2008 Sep;35(8 Suppl):282–5.
48. Insua A, Monje A, Wang HL, Miron RJ. Basis of bone metabolism around dental implants during osseointegration and peri-implant bone loss. J Biomed Mater Res A. 2017 Jul;105(7):2075–89.
49. Muñoz M, Busoms E, Vilarrasa J, Albertini M, Ruíz-Magaz V, Nart J. Bone-level changes around implants with 1- or 3-mm-high abutments and their relation to crestal mucosal thickness: A 1-year randomized clinical trial. J Clin Periodontol. 2021;48(10):1302–11.
50. Moss RA, VILLAROSA GA, COOLEY JE, LOMBARDO TW. Masticatory muscle activity as a function of parafunctional, active and passive oral behavioural patterns. J Oral Rehabil. 1987 Jul;14(4):361–70.
51. Jemt T, Lekholm U, Adell R. Osseointegrated implants in the treatment of partially edentulous patients: a preliminary study on 876 consecutively placed fixtures. Int J Oral Maxillofac Implants. 1989;4(3):211–7.
52. Adell R, Eriksson B, Lekholm U, Branemark PI, Jemt T. Long-term follow-up study of osseointegrated implants in the treatment of totally edentulous jaws. Int J Oral Maxillofac Implants. 1990;5(4):347–59.
53. Roberts HW, Berzins DW, Moore BK, Charlton DG. Metal-ceramic alloys in dentistry: a review. J Prosthodont. 2009 Feb;18(2):188–94.
54. Wataha JC. Biocompatibility of dental casting alloys: a review. J Prosthet Dent. 2000 Feb;83(2):223–34.
55. Hakan Tuna S OPN. The electrochemical propierties of four dental casting suprastructure alloys coupled with titanium implants. J Appl Oral Sci. 2009 Oct;17(5):467–75.
56. Bagegni A, Abou-Ayash S, Rucker G, Algarny A, Att W. The influence of prosthetic material on implant and prosthetic survival of implant-supported fixed complete dentures: a systematic review and meta-analysis. J Prosthodont Res. 2019 Jul;63(3):251–65.
57. Zhou L, Wang Q. Comparison of fracture resistance between cast posts and fiber posts: a meta-analysis of literature. J Endod. 2013 Jan;39(1):11–5.
58. Le M, Papia E, Larsson C. The clinical success of tooth- and implant-supported zirconia-based fixed dental prostheses. A systematic review. J Oral Rehabil. 2015 Jun;42(6):467–80.
59. Deany IL. Recent advances in ceramics for dentistry. Crit Rev Oral Biol Med. 1996;7(2):134–43.
60. Takeda H, Saitoh K. Impact of proprioception during the oral phase on initiating the swallowing reflex. Laryngoscope. 2016 Jul;126(7):1595–9.
61. Safari A, Jowkar Z, Farzin M. Evaluation of the relationship between bruxism and

premature occlusal contacts. J Contemp Dent Pract. 2013;14(4):616–21.
62. Cicciu M, Cervino G, Milone D, Risitano G. FEM Investigation of the Stress Distribution over Mandibular Bone Due to Screwed Overdenture Positioned on Dental Implants. Mater (Basel, Switzerland). 2018 Aug 23;11(9):10.3390/ma11091512.
63. Menini M, Conserva E, Tealdo T, Bevilacqua M, Pera F, Signori A, et al. Shock Absorption Capacity of Restorative Materials for Dental Implant Prostheses: An In Vitro Study. Int J Prosthodont [Internet]. 2013;26(6):549–56.
64. Cehreli M, Duyck J, De Cooman M, Puers R, Naert I. Implant design and interface force transfer. A photoelastic and strain-gauge analysis. Clin Oral Implants Res. 2004 Apr;15(2):249–57.
65. Gracis SE, Nicholls JI, Chalupnik JD, Yuodelis R a. Shock-absorbing behavior of five restorative materials used on implants. Int J Prosthodont. 1991;4(3):282–91.
66. Menini M, Conserva E, Tealdo T, Bevilacqua M, Pera F, Ravera G, et al. The use of a masticatory robot to analyze the shock absorption capacity of different restorative materials for implant prosthesis. J Biol Res. 2011;84(1):118–9.
67. Magne P, Silva M, Oderich E, Boff LL, Enciso R. Damping behavior of implant-supported restorations. Clin Oral Implants Res. 2013 Feb;24(2):143–8.
68. Sevimay M, Turhan F, Kilicarslan MA, Eskitascioglu G. Three-dimensional finite element analysis of the effect of different bone quality on stress distribution in an implant-supported crown. J Prosthet Dent. 2005 Mar;93(3):227–34.
69. Bijjargi S, Chowdhary R. Stress dissipation in the bone through various crown materials of dental implant restoration: a 2-D finite element analysis. J Investig Clin Dent [Internet]. 2013 Aug;4(3):172–7.
70. Kaleli N, Sarac D, Kulunk S, Ozturk O. Effect of different restorative crown and customized abutment materials on stress distribution in single implants and peripheral bone: A three-dimensional finite element analysis study. J Prosthet Dent. 2018 Mar;119(3):437–45.
71. Karpov EG Klein JT DLA. Anomalous strain energy trasnformation pathways in mechanical metamaterials. Proc Math Phys Eng Sci. 2019 Jun;
72. King H. Basic finite element method apllied to injury biomechanics. In 2018.
73. Muhsin SA, Hatton P V, Johnson A, Sereno N, Wood DJ. Determination of Polyetheretherketone (PEEK) mechanical properties as a denture material. Saudi Dent J. 2019 Jul;31(3):382–91.
74. Schwitalla AD, Spintig T, Kallage I, Muller WD. Pressure behavior of different PEEK materials for dental implants. J Mech Behav Biomed Mater. 2016 Feb;54:295–304.
75. Schwitalla AD, Spintig T, Kallage I, Müller WD. Flexural behavior of PEEK materials for dental application. Dent Mater [Internet]. 2015;31(11):1377–84.
76. Menini M, Pesce P, Pera F, Barberis F, Lagazzo A, Bertola L, et al. Biological and mechanical characterization of carbon fiber frameworks for dental implant applications. Mater Sci Eng Mater Biol Appl. 2017 Jan 1;70(Pt 1):646–55.
77. Passaretti A, Petroni G, Miracolo G, Savoia V, Perpetuini A, Cicconetti A. Metal free, full arch, fixed prosthesis for edentulous mandible rehabilitation on four implants. J Prosthodont Res. 2018 Apr;62(2):264–7.

78. Zaparolli D, Peixoto RF, Pupim D, Macedo AP, Toniollo MB, Mattos MDGC. Photoelastic analysis of mandibular full-arch implant-supported fixed dentures made with different bar materials and manufacturing techniques. Mater Sci Eng Mater Biol Appl. 2017 Dec 1;81:144–7.
79. Pera F Solimano F, Tealdo T, Pera P, Menini M PP. Carbon Fiber vs. metal framework in full-arch immediate loading rehabilitations of the maxilla- a cohort clinical study. J Oral Rehabil. 2017 May;44(5):392–7.
80. Segerstrom S, Ruyter IE. Effect of thermal cycling on flexural properties of carbon-graphite fiber-reinforced polymers. Dent Mater. 2009 Jul;25(7):845–51.
81. Segerstrom S, Ruyter IE. Adhesion properties in systems of laminated pigmented polymers, carbon-graphite fiber composite framework and titanium surfaces in implant suprastructures. Dent Mater. 2009 Sep;25(9):1169–77.
82. Segerstrom S, Sandborgh-Englund G, Ruyter EI. Biological and physicochemical properties of carbon-graphite fibre-reinforced polymers intended for implant suprastructures. Eur J Oral Sci. 2011 Jun;119(3):246–52.
83. Gallucci GO, Bernard JP, Bertosa M, Belser UC. Immediate loading with fixed screw-retained provisional restorations in edentulous jaws: the pickup technique. Int J Oral Maxillofac Implants. 2004;19(4):524–33.
84. Norton MR. An in vitro evaluation of the strength of an internal conical interface compared to a butt joint interface in implant design. Clin Oral Implants Res. 1997 Aug;8(4):290–8.
85. Tonella BP, Pellizzer EP, Ferraço R, Falcón-Antenucci RM, Carvalho PSP de, Goiato MC. Photoelastic analysis of cemented or screwed implant-supported prostheses with different prosthetic connections. J Oral Implantol. 2011 Aug;37(4):401–10.
86. Peixoto RF, Tonin BSH, Martinelli J, Macedo AP, de Mattos M da GC. In vitro digital image correlation analysis of the strain transferred by screw-retained fixed partial dentures supported by short and conventional implants. J Mech Behav Biomed Mater. 2020 Mar;103:103556.
87. Hoult NA, Andy Take W, Lee C, Dutton M. Experimental accuracy of two dimensional strain measurements using Digital Image Correlation. Eng Struct. 2013 Jan;46:718–26.
88. Bassit R, Lindström H, Rangert B. In vivo registration of force development with ceramic and acrylic resin occlusal materials on implant-supported prostheses. Int J Oral Maxillofac Implants. 2002;17(1):17–23.
89. Sevimay M, Usumez A, Eskitascioglu G. The influence of various occlusal materials on stresses transferred to implant-supported prostheses and supporting bone: a three-dimensional finite-element study. J Biomed Mater Res B, Appl Biomater. 2005 Apr;73(1):140–7.
90. Bacchi a, R LXC, M FM, M BFDS. Stress distribution in fixed-partial prosthesis and peri-implant bone tissue with different framework materials and vertical misfit levels: a three-dimensional finite element analysis. J Oral Sci [Internet]. 2013;55(3):239–44.
91. Merz BR, Hunenbart S, Belser UC. Mechanics of the implant-abutment connection: an 8-degree taper compared to a butt joint connection. Int J Oral Maxillofac Implants. 2000;15(4):519–26.

92. Valera-Jimenez JF, Burgueno-Barris G, Gomez-Gonzalez S, Lopez-Lopez J, Valmaseda-Castellon E, Fernandez-Aguado E. Finite element analysis of narrow dental implants. Dent Mater. 2020 Jul;36(7):927–35.
93. Anami LC, da Costa Lima JM, Takahashi FE, Neisser MP, Noritomi PY, Bottino MA. Stress distribution around osseointegrated implants with different internal-cone connections: photoelastic and finite element analysis. J Oral Implantol. 2015 Apr;41(2):155–62.
94. Carvalho L. Simões J., Frazão O RP. New Trends in Dental Biomechanics with Photonics Technologies. Appl Sci. 2015;
95. Karl M, Dickinson A, Holst S, Holst A. Biomechanical methods applied in dentistry: a comparative overview of photoelastic examinations, strain gauge measurements, finite element analysis and three-dimensional deformation analysis. Eur J Prosthodont Restor Dent. 2009;17(2):50–7.
96. Benazzi S, Nguyen HN, Kullmer O, Kupczik K. Dynamic Modelling of Tooth Deformation Using Occlusal Kinematics and Finite Element Analysis. PLoS One. 2016 Mar 31;11(3):e0152663.
97. Razaghi R Haghpanahi M MM. Dynamic simulation and finite element analysis of the maxillary bone injury around dental implant during chewing different food. Biomed Eng Appl Basis Commun. 2016;28(2):1–10.
98. Kayabasi O Erzincanlı F YE. Static, dynamic and fatigue behaviors of dental implant using finite element method. Adv Eng Softw. 2006;37:649–58.
99. Ramseier CA, Warnakulasuriya S, Needleman IG, Gallagher JE, Lahtinen A, Ainamo A, et al. Consensus Report: 2nd European Workshop on Tobacco Use Prevention and Cessation for Oral Health Professionals. Int Dent J. 2010 Feb;60(1):3–6.
100. Tsigarida AA, Dabdoub SM, Nagaraja HN, Kumar PS. The Influence of Smoking on the Peri-Implant Microbiome. J Dent Res. 2015 Sep;94(9):1202–17.
101. Derks J, Tomasi C. Peri-implant health and disease. A systematic review of current epidemiology. J Clin Periodontol. 2015 Apr;42 Suppl 1:S158-71.
102. Mombelli A, van Oosten MA, Schurch Jr E, Land NP. The microbiota associated with successful or failing osseointegrated titanium implants. Oral Microbiol Immunol. 1987 Dec;2(4):145–51.
103. Kozlovsky A, Tal H, Laufer BZ, Leshem R, Rohrer MD, Weinreb M, et al. Impact of implant overloading on the peri-implant bone in inflamed and non-inflamed peri-implant mucosa. Clin Oral Implants Res. 2007 Oct;18(5):601–10.
104. Mattheos N, Collier S, Walmsley AD. Specialists' management decisions and attitudes towards mucositis and peri-implantitis. Br Dent J. 2012 Jan 13;212(1):E1.
105. Hermann Schoolfield, J.D., Schenk, R.K., Buser, D. & Cochran, D.L. JS. Influence of the size of the microgap on crestal bone changes around titanium implants. A histometric evaluation of unloaded non-submerged implants in the canine mandible. J Periodontol. 2001;72:1372–1383.
106. VanSchoiack Wu, J.C., Sheets, C.G. & Earthma, J.C. LR. Effect of bonedensity on thedampingbehavior of dental implants: an in vitro method. . Mater Sci Eng. 2006;26:1307–1311.
107. Lima de Andrade C, Carvalho MA, Bordin D, da Silva WJ, Del Bel Cury AA, Sotto-Maior BS. Biomechanical Behavior of the Dental Implant Macrodesign. Int J Oral

Maxillofac Implants. 2017;32(2):264–70.
108. Coltro MPL, Ozkomur A, Villarinho EA, Teixeira ER, Vigo A, Shinkai RSA. Risk factor model of mechanical complications in implant-supported fixed complete dentures: A prospective cohort study. Clin Oral Implants Res. 2018 Sep;29(9):915–21.
109. Mengatto CM, Coelho-de-Souza FH, de Souza Junior OB. Sleep bruxism: challenges and restorative solutions. Clin Cosmet Investig Dent. 2016 Apr 22;8:71–7.
110. Mikeli A, Walter MH. Impact of Bruxism on Ceramic Defects in Implant-Borne Fixed Dental Prostheses: A Retrospective Study. Int J Prosthodont. 2016;29(3):296–8.
111. Sathapana S Monsour P, Naser-ud-Din S FA. Age-related changes in maxillary and mandibular cortical bone thickness in relation to temporary anchorage device placement. Aust Dent J. 2013;
112. Tomar V. Modeling of dynamic fracture and damage in two-dimensional trabecular bone microstructures using the cohesive finite element method. J Biomech Eng. 2008 Apr;130(2):21021.
113. Li J, Yin X, Huang L, Mouraret S, Brunski JB, Cordova L, et al. Relationships among Bone Quality, Implant Osseointegration, and Wnt Signaling. J Dent Res. 2017 Jul;96(7):822–31.
114. Asa'ad F, Monje A, Larsson L. Role of epigenetics in alveolar bone resorption and regeneration around periodontal and peri-implant tissues. Eur J Oral Sci. 2019 Dec;127(6):477–93.
115. Conserva E, Menini M, Tealdo T, Bevilacqua M, Pera F, Ravera G, et al. Robotic chewing simulator for dental materials testing on a sensor-equipped implant setup. Int J Prosthodont. 2008;21(6):501–8.
116. Hobkirk JA, Psarros KJ. The influence of occlusal surface material on peak masticatory forces using osseointegrated implant-supported prostheses. Int J Oral Maxillofac Implants [Internet]. 1992;7(3):345–52.
117. Conserva E, Menini M, Tealdo T, Bevilacqua M, Ravera G, Pera F, et al. The use of a masticatory robot to analyze the shock absorption capacity of different restorative materials for prosthetic implants: a preliminary report. Int J Prosthodont. 2009;22(1):53–5.
118. Wakabayashi N, Ona M, Suzuki T, Igarashi Y. Nonlinear finite element analyses: Advances and challenges in dental applications. J Dent. 2008;36(7):463–71.
119. Reddy MS, Sundram R, Eid Abdemagyd HA. Application of Finite Element Model in Implant Dentistry: A Systematic Review. J Pharm Bioallied Sci. 2019 May;11(Suppl 2):S85–91.

X. ANEXOS

materials

an Open Access Journal by MDPI

Indexed in: PubMed | Indexed in: Ei Compendex | CITESCORE 4.2 SCOPUS | IMPACT FACTOR 3.623

CERTIFICATE OF PUBLICATION

Certificate of publication for the article titled:

A 3D Finite Element Analysis Model of Single Implant-Supported Prosthesis under Dynamic Impact Loading for Evaluation of Stress in the Crown, Abutment and Cortical Bone Using Different Rehabilitation Materials

Authored by:

Oriol Cantó-Navés; Raul Medina-Galvez; Xavier Marimon; Miquel Ferrer; Óscar Figueras-Álvarez; Josep Cabratosa-Termes

Published in:

Materials **2021**, Volume 14, Issue 13, 3519

MDPI Academic Open Access Publishing since 1996

Basel, October 2021

materials

an Open Access Journal by MDPI

Indexed in: PubMed | Indexed in: Ei Compendex | CITESCORE 4.2 SCOPUS | IMPACT FACTOR 3.623

CERTIFICATE OF ACCEPTANCE

Certificate of acceptance for the manuscript (**materials-1369846**) titled:

Bone stress evaluation with and without cortical bone using several dental restorative materials subjected to impact load: a fully 3D transient finite-element study

Authored by:

Raul Medina-Galvez; Oriol Cantó-Navés; Xavier Marimon; Miguel Cerrolaza; Miquel Ferrer; Josep Cabratosa-Termes

has been accepted in *Materials* (ISSN 1996-1944) on 01 October 2021

MDPI Academic Open Access Publishing since 1996

Basel, October 2021

CER

ComitéUniversitat d'ÉticaInternacional de Recerca de Catalunya

APROVACIÓ PROJECTE PEL CERI APROBACIÓN PROYECTO POR EL CER

Codi de l'estudi / Código del estudio: REST-ELM-2017-05
Versió del protocol / Versión del protocolo: 1 .O
Data de la versió / Fecha de la versión: 19/10/18
Títol / Título: Estudio sobre la absorción de las fuerzas oclusales dinámicas en prótesis implantoportadas según el material rehabilitador. Elementos Finitos 3D Dinámicos

Sant Cugat del Vallés, 30 d'octubre de 2018

Doctorand/o: Raul Medina Galvez
Dicrector: Josep Cabratosa Termes

Títol de l'estudi I Título del estudio: Estudio sobre la absorción de las fuerzas oclusales dinámicas en prótesis implantoportadas según el material rehabilitador. Elementos Finitos 3D Dinámicos

Benvolgut/da,

Valorat el projecte presentat, el CER de la Universitat Internacional de Catalunya, considera que, el contingut de la investigació, no implica cap inconvenient relacionat amb la dignitat humana, tracte ¿tic per als animals ni atempta contra el medi ambient, ni té implicacions econàmiques ni conflicte d'interessos, però no s'han valorat eis aspectes metodològics del projecte de recerca degut a que tal anàlisis correspon a d'altres instàncies.

Per aquests motius, el Comité d'Ética de Recerca, RESOLT FAVORABLEMENT, emetre aquest CERTIFICAT D'APROVACIÓ, per que pugui ser presentat a les instàncies que així ho requereixin.

Em permeto recordar•li que si en el procés d'execució es produís algun canvi significatiu en els seus plantejaments, hauria de ser sotmàs novament a la revisió i aprovació del CER.
Atentament,

Apreciado/a,

Valorado el proyecto presentado, el CER de la Universidad Internacional de Catalunya, considera que, el contenido de la investigación, no implica ningún inconveniente relacionado con la dignidad humana, trato ético para los animales, ni atenta contra el medio ambiente, ni tiene implicaciones económicas ni conflicto

de intereses, pero no se han valorado aspectos metodológicos del proyecto de investigación debido a que tal análisis corresponde a otras instancias.

Por estos motivos, el Comité d'Êtica de Recerca, RESUELVE FAVORABLEMENTE, emitir este CERTIFICADO DE APROBACIÓN, para que pueda ser presentado a las instancias que así lo requieran.

Me permito recordade que si el proceso de ejecución se produjera algún cambio significativo en sus planteamientos, debería ser sometido nuevamente a la revisión y aprobación del CER.

Atentamente,

Dr. Josep Argemí
President CER-UIC

materials

MDPI

Article

A 3D Finite Element Analysis Model of Single Implant-Supported Prosthesis under Dynamic Impact Loading for Evaluation of Stress in the Crown, Abutment and Cortical Bone Using Different Rehabilitation Materials

Oriol Cantó-Navés [1], Raul Medina-Galvez [1], Xavier Marimon [2,3,*], Miquel Ferrer [4], Óscar Figueras-Álvarez [1] and Josep Cabratosa-Termes [1]

[1] Faculty of Dentistry, Universitat Internacional de Catalunya (UIC), 08017 Barcelona, Spain; oriolcanto@uic.es (O.C.-N.); ruldoc@uic.es (R.M.-G.); ofigueras@uic.es (Ó.F.-Á.); cabratosa@uic.es (J.C.-T.)
[2] Bioengineering Institute of Technology, Universitat Internacional de Catalunya (UIC), 08190 Barcelona, Spain
[3] Automatic Control Department, Universitat Politècnica de Catalunya (UPC-BarcelonaTECH), 08034 Barcelona, Spain
[4] Department of Strength of Materials and Structural Engineering, Universitat Politècnica de Catalunya (UPC-BarcelonaTECH), 08034 Barcelona, Spain; miquel.ferrer@upc.edu
* Correspondence: xmarimon@uic.es

Citation: Cantó-Navés, O.; Medina-Galvez, R.; Marimon, X.; Ferrer, M.; Figueras-Álvarez, Ó.; Cabratosa-Termes, J. A 3D Finite Element Analysis Model of Single Implant-Supported Prosthesis under Dynamic Impact Loading for Evaluation of Stress in the Crown, Abutment and Cortical Bone Using Different Rehabilitation Materials. *Materials* **2021**, *14*, 3519. https://doi.org/10.3390/ma14133519

Academic Editor: Ivana Miletić

Received: 16 May 2021
Accepted: 18 June 2021
Published: 24 June 2021

Abstract: In the literature, many researchers investigated static loading effects on an implant. However, dynamic loading under impact loading has not been investigated formally using numerical methods. This study aims to evaluate, with 3D finite element analysis (3D FEA), the stress transferred (maximum peak and variation in time) from a dynamic impact force applied to a single implant-supported prosthesis made from different materials. A 3D implant-supported prosthesis model was created on a digital model of a mandible section using CAD and reverse engineering. By setting different mechanical properties, six implant-supported prostheses made from different materials were simulated: metal (MET), metal-ceramic (MCER), metal-composite (MCOM), carbon fiber-composite (FCOM), PEEK-composite (PKCOM), and carbon fiber-ceramic (FCCER). Three-dimensional FEA was conducted to simulate the collision of 8.62 g implant-supported prosthesis models with a rigid plate at a speed of 1 m/s after a displacement of 0.01 mm. The stress peak transferred to the crown, titanium abutment, and cortical bone, and the stress variation in time, were assessed.

Keywords: FEA; FEM; impact test; transient analysis; dynamical forces; biomechanical behavior; implant rehabilitation; rehabilitation materials; crown materials

1. Introduction

Currently, implant-supported prostheses are widely used for the rehabilitation of partially and fully edentulous patients. This type of treatment has undergone significant changes in the choice of materials since the first treatments carried out by Brånemark. The use of gold or gold alloys, with and without resin veneering [1,2], has been discarded for economic, esthetic, and functional reasons [3–5]. The increase in the price of gold led to the use of much cheaper non-noble metals, although with different mechanical and biological characteristics [3–6]. The composites and resins used at the end of the last century showed significant deficiencies in esthetics and wear; they were replaced by ceramics and, currently, by zirconia, [6–9] with different mechanical characteristics. The choice of the material used for implant-supported prosthesis manufacturing is a crucial issue due to the dynamic characteristics of the stomatognathic system.

Static forces are applied from the mandible to the maxilla, without mandibular movements, and the intensity remains constant over time. In contrast, dynamic forces are related to mandibular movements, and the intensity varies with time. The dynamic force magnitude is calculated by multiplying the mass of the moving object and its acceleration in

that direction. Static (clenching) and dynamic forces (chewing, swallowing, and eccentric bruxism) occur in the masticatory system [10–15]. The literature shows that forces are transferred to a lesser or greater extent to the peri-implant area [16] depending on whether the applied force is static or dynamic [17–24]. Moreover, the results in recent publications showed that static loading, compared with dynamic loading, caused increased stress, which proves the need of transient analysis of dental implants [25,26].

The chosen material for single implant-supported prostheses manufacturing has little relevance in the transmission of static forces, as explained in the Saint-Venant principle, which states that the difference between the effects of two different but statically equivalent loads becomes minimal at sufficiently large distances from the load [27–29]. Dynamic forces and the impact of the moving mandible against the maxilla are transferred very differently in single and multiple implant-supported prostheses, depending on the material that the prostheses are made from. Rigid materials, such as zirconia, ceramics, and metals, generate higher dynamic forces [17,19–21] than other materials used in veneering prosthetic frameworks (composites, hybrid composites, or resins) or in prosthetic framework manufacturing (carbon fiber, fiberglass, or polyether-ether-ketone (PEEK)), which absorb and dissipate the impact energy with lower dynamic forces [28–40].

There are different in vitro methods for studying the transmission of static and dynamic forces to the peri-implant area from single and partial implant-supported prostheses made from different materials, such as the use of photoelastic resins [18,29,41–43], digital image correlation (DIC) [29,44,45], strain gauges [19,46], loss coefficient (LC) [21], and finite element analysis (FEA) in two (2D FEA) and three dimensions (3D FEA) [22,24,31,47–51]. All of them provide very similar results [29,52–54] in terms of stress.

Photoelastic resins allow visualizing the stress generated in the peri-implant area after the application of a static or dynamic force with isochromatic fringes. The color and number of the shown isochromatic fringes indicates the magnitude of the generated stress. Digital image correlation (DIC) is an optical-numerical system using resins with randomly colored microdots, where the displacement of these microdots is calculated after the application of a force, both vertically and horizontally. The magnitude of transferred forces is determined according to the magnitude of the displacements.

Magne et al. [21] used the Periometer (University of Southern California, Los Angeles, CA, USA) to calculate the energy absorbed by prostheses made with different frameworks and veneer materials, such as composite, ceramic, and zirconia. The Periometer is a handheld percussion probe that records the rebound suffered by the object of study, so the energy absorbed by the material can be calculated by subtracting the applied force and the rebound force.

Another system is the use of strain gauges, which are sensors that measure the material strain when loads are applied. Gracis [19] recorded the impact force transmitted by a steel ball rolled along a slope to discs made from different materials. Menini [17,20], used strain gauges to design a device that applied oscillating movements to monolithic prostheses of different materials (gold, zirconia, ceramics, composites, and resins) against an upper dental arch made of a Co-Cr alloy. The force transferred to the crowns (made from different materials) by the simulation of the mandibular movements was recorded.

Dental biomechanics based on finite element analysis (FEA) is attracting huge interest in many areas: biomedical sciences, anthropology and, odontology. However, several shortcomings in FEA modeling exist, mainly due to unrealistic (static) loading imposition [55]. FEA analysis is the most widely used numerical procedure today, since it allows reproducing mechanical behavior under a mechanical load based on the known properties of the material. Density, the Poisson coefficient, and Young's modulus values can be set in 2D or 3D FEA software, which also includes the depth dimension. Three-dimensional FEA permits the visualization of the stresses on the entire body of the implants. In the consulted dental literature, dynamic FEA studies are still scarce [25,26,55–58] compared to the large number of existing FEA studies with static loads. Moreover, very few studies that simulate dynamic forces under impact loading using 2D or 3D FEA have been found. Thus,

this article is devoted exclusively to the study of the impacts on dental implants, which is minimally covered in the literature.

Knowledge about stress distribution in the peri-implant area may be essential for predicting the survival of dental implants, especially in patients with risk factors such as smoking, poor hygiene habits, previous periodontitis, or predisposing genetic factors [59–63]. These patients present, to a greater or lesser extent, gingival inflammation that may cause peri-implant bone loss [64–72]. This peri-implant bone loss may be directly affected by the stress generated in the implant-bone-prosthesis area; the higher the transferred force, the higher the risk of peri-implantitis [21,73–79]. The amount of cortical bone could also be a factor to be considered when choosing the material for manufacturing the prosthesis, as this cortical bone is poorly vascularized, fragile, rigid, and regenerates slowly [80–84].

Numerous studies have shown, using 2D or 3D FEA, the behavior of implants rehabilitated with single crowns made with different materials. In these studies, all of them used a static force to simulate the oral environment. Our study has aimed to show, using dynamic 3D FEA, the dynamic impact forces related to oral function.

This in vitro study aims to evaluate, with three-dimensional finite element analysis (3D FEA), the stress transferred (time to peak, maximum peak, and variation in time) from an impact, a dynamic force, on a single implant-supported prosthesis made from different restorative materials (metal, metal-ceramic, metal-composite, carbon fiber-composite, PEEK-composite, and carbon fiber-ceramic), applied to the crown, titanium abutment, and cortical mandibular bone.

2. Materials and Methods

2.1. The Whole Implant Model

The 3D digital model simulated dental rehabilitation on the implants used in this study to evaluate the stress (von Mises stress) on the inner part of the crown, the external part of the neck of the titanium abutment, and the top of the cortical bone, using different implant crowns in a dynamic situation (chewing, swallowing, or eccentric bruxing). This was obtained from the integration of six independently developed models from real elements: (1) the crown, (2) an anti-rotatory abutment, (3) a fixation screw, (4) a single implant-supported prosthesis, (5) a section of the mandibular bone (cortical and cancellous bone), and (6) the plate. Total osseointegration of the implant was considered, assuming a perfect relation between the nodes at the interface of the implants and the bone.

2.1.1. The Crown

In order to obtain a solid model of the crown, a high-resolution 3D Exocad model was imported to SolidWorks. Then, two parts were created within the crown geometry (the core and the esthetic veneering), separated by an inner boundary. The framework and the veneering material were delimited from the single implant-supported prosthesis. The total volume of the crown was 411.5 mm^3. The framework core accounted for 51.3% of the total crown volume, and the remaining 39.7% was esthetic veneering.

2.1.2. The Abutment and Fixation Screw

The abutment's function is to join the crown and the implant with a thread mechanism. Also, an anti-rotation system must be available to prevent the relative movement between the implant and the abutment (in this case, a hexagonal anti-rotational system). The abutment and the fixation screw were fully modeled using the CAD software SolidWorks v.2021 (Dassault Systèmes, SolidWorks Corp., Waltham, MA, USA) [85] in order to reduce the typical surfaces of a 3D scanning process to triangular forms, thus maintaining simpler geometries. The abutment used in this study was the MIS implant with an internal hexagonal connection.

2.1.3. The Implant

Accurate measurements of implant geometry were obtained by 3D digital scan (Visual Computing Lab, Pisa, Italy) of a 4.2 × 11.5 mm implant with an internal hexagon (MIS Implants Technology, Bar-Lev, Tel Aviv-Yafo, Israel), which was converted into an STL (Standard Tessellation Language) mesh. Then, it was converted into a solid with the SolidWorks Software (Dassault Systèmes, Vélizy-Villacoublay, France) in order to obtain the measurements of the implant. Finally, it was modeled with the CAD SolidWorks software in order to guarantee more precise geometry and to avoid too many surfaces being shown.

2.1.4. The Mandible

The section of the mandible bone was designed from a sectional image of cone-beam computed tomography (CBCT) (NewTom Giano, Newtom, Imola, Italy). Keypoints were drawn at a fixed distance over the section image of the CT scan in order to transfer it to the computer. The geometry of the mandible could be obtained with SolidWorks software by measuring the distances of the points and calculating the real value through the scanning scale. Two different bounded solids were created over the mandible geometry to apply the mechanical properties of both trabecular and cortical bone.

2.1.5. The Plate

A fixed rigid body with a flat surface was required to simulate impact loads on the tooth during chewing. To this end, a rectangular-shaped plate (w = 10, h = 12, e = 2 mm) was set up to apply the impact load on the three parts of the whole model: the crown, the implant, and the mandible. The initial distance between the plate and the crown was only 0.01 mm. The collision with the plate was frictionless. This means that a zero coefficient of friction was assumed and allowed free sliding. In addition, normal pressure equaled zero if separation occurred.

2.2. Material Properties

All materials were modeled as linear elastic isotropic and homogeneous. Young's modulus and Poisson ratio of each material are shown in Table 1. The mechanical properties of the different materials of the crowns have been provided by the manufacturers.

Table 1. Properties of materials used in the prothesis and the bone (trabecular and cortical).

Kerrypnx	Material Name	Manufacturer	*E* Young Modulus (MPa)	*v* Poisson Ratio	*ρ* Density (g/cm^3)
Crown	**FCOM**				
	Carbon fiber-composite	[86]			
	BioCarbon Bridge fibers	Micro Medica	300,000	0.3	1.40
	Composite BioXfill	Micro Medica	22,000	0.3	8.30
	MCER				
	Metal-ceramic	[87,88]			
	Co-Cr alloy	Renishaw	208,000	0.31	8.90
	Ceramic VMK 95	Vita	69,000	0.28	2.50
	MCOM				
	Metal-composite	[86,87]			
	Co-Cr alloy	Renishaw	208,000	0.31	8.90
	Composite BioXfill	Micro-Medica	22,000	0.3	8.30

Table 1. *Cont.*

Kerrypnx	Material Name	Manufacturer	*E* Young Modulus (MPa)	*v* Poisson Ratio	*ρ* Density (g/cm^3)
	MET	[89]			
	Full metal				
	Co-Cr Alloy, Mo, W	Heraeus Kulzer	208,000	0.31	8.90
	FCCER	[86,90]			
	Carbon fiber-ceramic				
	Carbon Fiber Bridge	Micro-Medica	66,000	0.3	1.4
	Ceramic IPS e.max	Ivoclar Vivadent	95,000	0.2	2.5
	PKCOM	[86,91]			
	PEEK-composite				
	PEEK Optima	Invibio	4100	0.36	1.3
	Composite BioXfill	Micro-Medica	22,000	0.3	8.30
Implant	Ti-6-Al-4V ELI	MIS [92]	113,800	0.34	4.43
Bone	Cortical bone	[93,94]	15,000	0.3	1.79
	Trabecular bone	[93]	500	0.3	0.45

Abbreviated names of the crown materials are the following: FCOM is a carbon fiber-composite crown, MCER is a metal-ceramic crown, MET is a metal crown alloy (Cr-Co, Mo, and W).

2.3. Numerical Methods

All independent models were put together by assembly modeling, generating a unique prosthesis-implant-bone model (Figure 1). The geometry was converted to an IGES file, and Ansys Workbench Software (Ansys Inc., Canonsburg, PA, USA) was used to determine the stress transferred to the crown, titanium abutment, and cortical bone before the FEA simulation by the implant-supported prosthesis made from different materials.

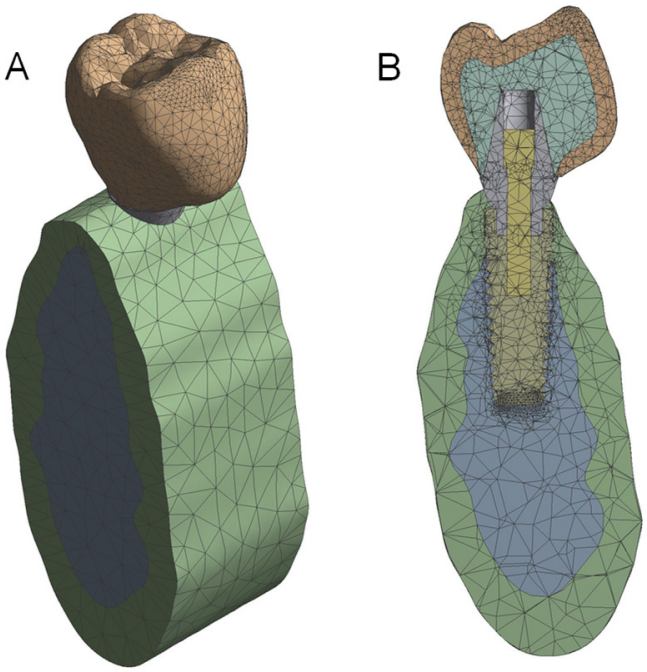

Figure 1. View of the whole 3D FEA model (**A**). Sectional model (**B**).

The prosthesis-implant-bone model was simulated to collide with a 10 × 12 × 2 mm fixed and rigid plate at a speed of 1 m/s after a displacement of 0.01 mm. For accurate results, the size of the elements is very important. The FEA model had 96,160 nodes and 62,606 elements to simulate the real models (prosthesis, implant, and bone) (see Figure 1). Young's modulus, Poisson's coefficient, and density were assigned to each material used in the manufacturing of the implant-supported prosthesis: CoCr (MET), CoCr-Ceramic (MCER), CoCr-Composite (MCOM), Carbon Fiber-Composite (FCOM), PEEK-Composite (PKCOM), Carbon Fiber-Ceramic (FCCER), the titanium abutment, and the cortical bone of the model (Table 1). For the FEA, all materials were considered isotropic and homogeneous, displacements were only in the vertical direction, perfect osseointegration was assumed, the impact was carried out on a rigid object (plate), and, finally, the collision was frictionless.

2.3.1. Mesh Definition

Before performing the simulation with the finite element method, the mesh size and the element type must be defined. The accuracy of the results depends directly on the size of the elements. The smaller the elements, the more accurate the solution. Therefore, small elements were used in order to improve precision. However, this affected the computational time. While CPU time is not that important in static analyses, it is crucial in transient dynamic analyses.

The solid 3D element SOLID187 (Ansys Inc., Canonsburg, PA, USA) [85] was used, with 10 nodes and quadratic interpolation functions that are more suitable for irregular geometries. The element had three degrees of freedom per node, i.e., the three translations in the global coordinate directions x, y, z. Surface-to-surface contact was defined with the element CONTA174.

In the process of creating the mesh, a refinement process was carried out in order to obtain a stable solution independent of the mesh size, especially around the impact zone, thereby ensuring high accuracy in this area. Therefore, as this refinement had been done, it was not necessary to use an area to obtain an average solution, since the nodal solution was especially accurate. Thus, the corresponding mesh was then considered to be optimal.

In addition, Ansys software performs control of the aspect ratio systematically. The accuracy of the results depends directly on the size of the finite element mesh. The smaller the mesh, the more accurate the solution obtained. Near the loading point and the threaded part, where higher accuracy was needed, the size was 0.2 mm, but in the other parts it was larger, from 0.5 to 2 mm. Even if the different parts of the implant are assembled together, the finite element results can be analyzed independently. Six solids were considered individually: the crown, the abutment, the implant, the fixation screw, the mandible, and the plate.

2.3.2. Simulation Time

Regarding simulation time, 0.4 ms were simulated. The number of substeps is the number of intervals into which the simulation time is divided. That is to say, the calculation time-step between one instant to the next. If they are too small, the computing time increases considerably and, if they are set too high, the accuracy of the time-history response decreases. A value of 53 substeps, i.e., a time-step of 7.55 µs, was found to be reasonable.

3. Results

3.1. Stress Results

The von Mises stress value (obtained from a Cauchy stress tensor) was calculated over time in the dynamic FEA simulation and compared for each node (Figure 2) in a time interval of 0.4 ms. The stress peak values in the crown, titanium abutment, and cortical bone are summarized in Table 2.

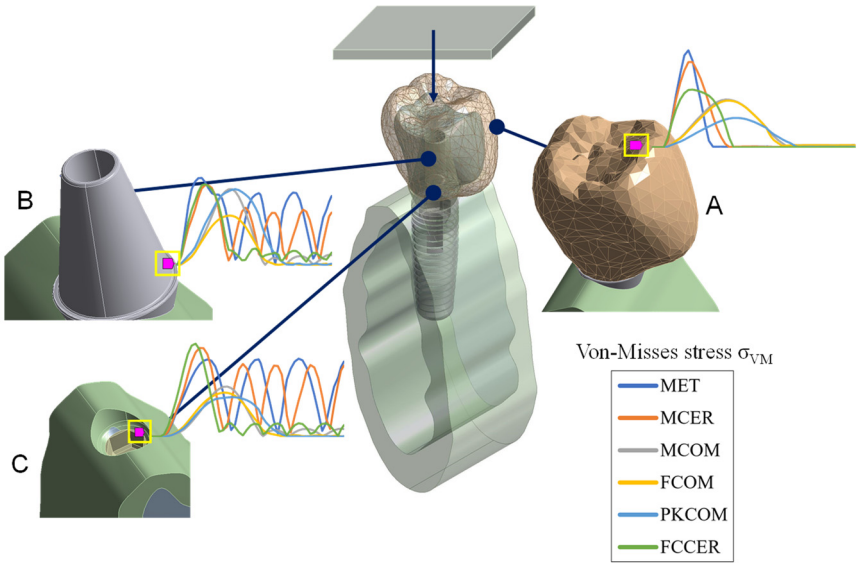

Figure 2. The nodes selected for numerical simulation. (**A**) Sectional view of the 3D FEA model at the crown node. (**B**) The abutment node. (**C**) The node on top of the cortical bone.

Table 2. Maximum equivalent von Mises stress transferred to the crown, the titanium abutment, and the cortical bone by the different prosthesis materials.

Node/Material	Maximum von Mises Stress σ_{VMmax} (MPa)					
	MET	**MCER**	**MCOM**	**FCOM**	**PKCOM**	**FCCER**
Crown	103.81	91.18	51.05	49.98	31.51	61.82
Abutment	89.27	81.91	77.82	50.80	77.78	82.80
Cortical	63.35	72.06	40.71	35.70	32.05	75.46

At the crown node (Figure 3) the maximum peaks were found at the MET and MCER crown, followed by that at FCCER. The lower values were found at MCOM and FCOM, and the lowest at the PKCOM crown.

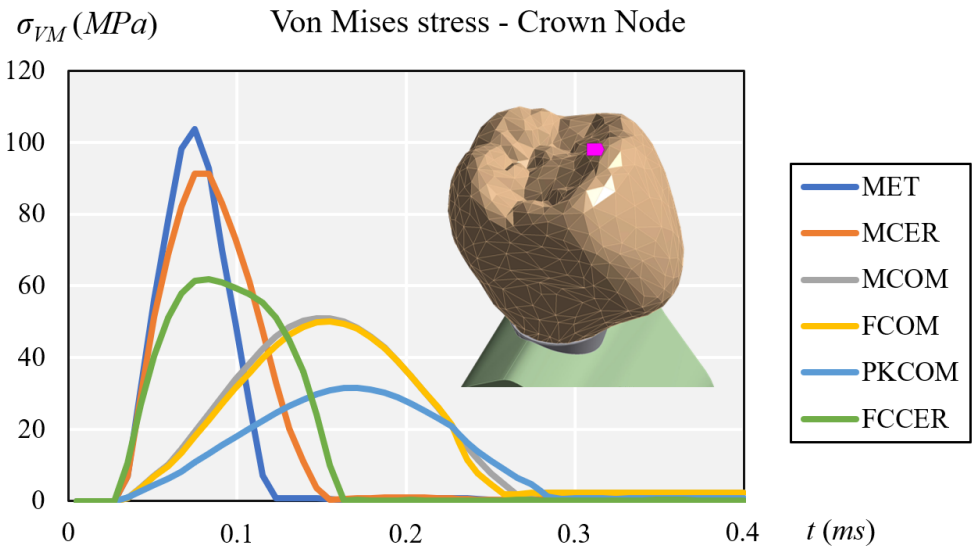

Figure 3. Comparison of equivalent von Mises stress at the crown node.

At the same time, Figure 4 compares the displacement of each crown during impact.

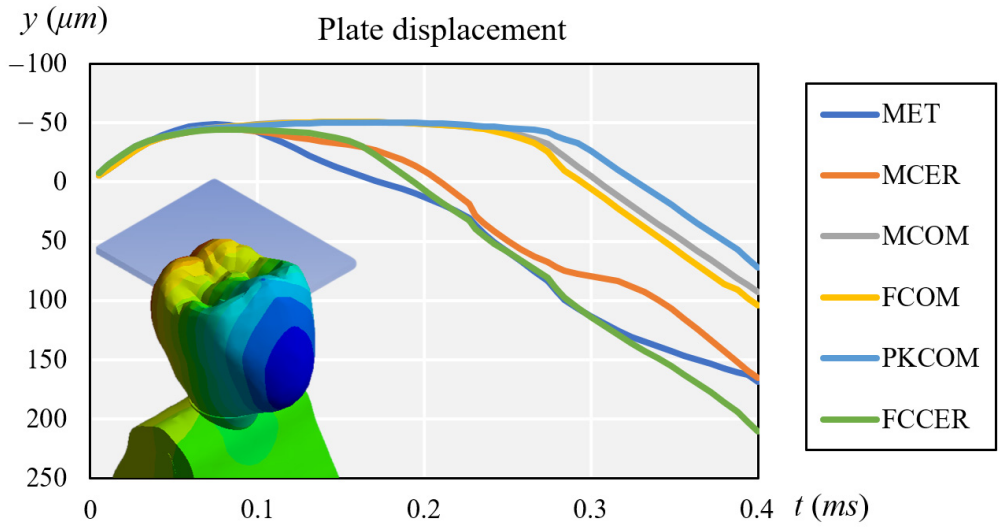

Figure 4. Comparison of plate displacement for each crown after impact.

All the crowns except FCOM showed high peak intensity values at the titanium abutment node (Figure 5). MET and MCER showed higher stress rebound over time, while MCOM, FCOM, PKCOM, and FCCER showed no rebound peaks after the impact (See Figure 5).

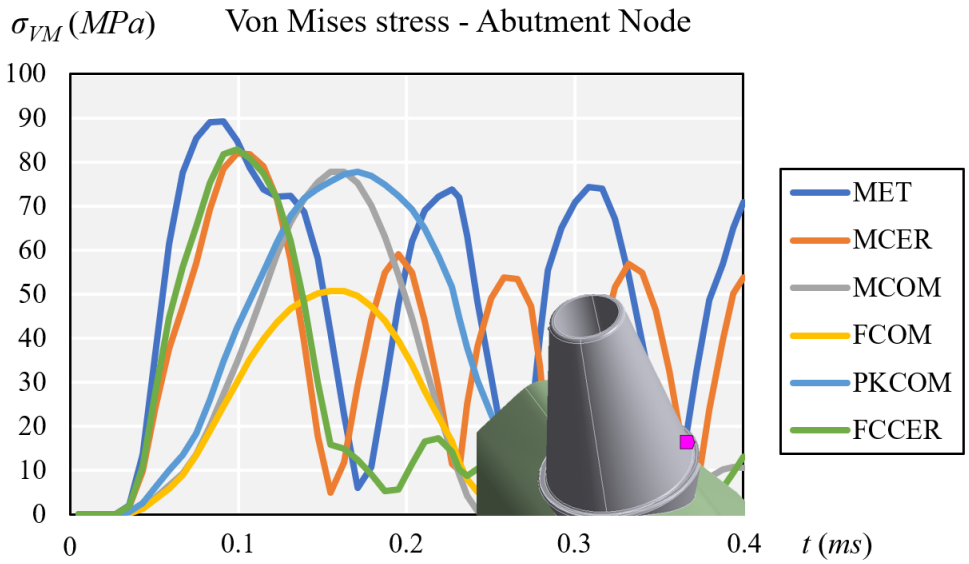

Figure 5. Comparison of equivalent von Mises stress at the titanium abutment node.

Composite-veneered implant-supported prostheses (MCOM, FCOM, and PKCOM) generated lower stress peaks at the cortical bone than ceramic-veneered (MCER and FCCER) or all-metal (MET) implant-supported prostheses. The implant-supported ceramic-veneered (MCER and FCCER) or all-metallic (MET) prostheses exhibited a more significant and earlier stress peak on the cortical bone than those veneered with composite (MCOM, PKCOM, and FCOM) (Figure 6). The highest stress rebound peaks happened in MET and MCER implant-supported prostheses. Implant-supported prostheses made of carbon fiber-ceramic (FCCER) showed the highest maximum peak of stress, but it dissipated quickly with rebound peaks of lower intensity. A rapid reduction in stress was observed in implant-supported prostheses veneered with composite (MCOM, PKCOM, and FCOM) and in those made with carbon fiber-ceramic (FCCER) (Figure 6).

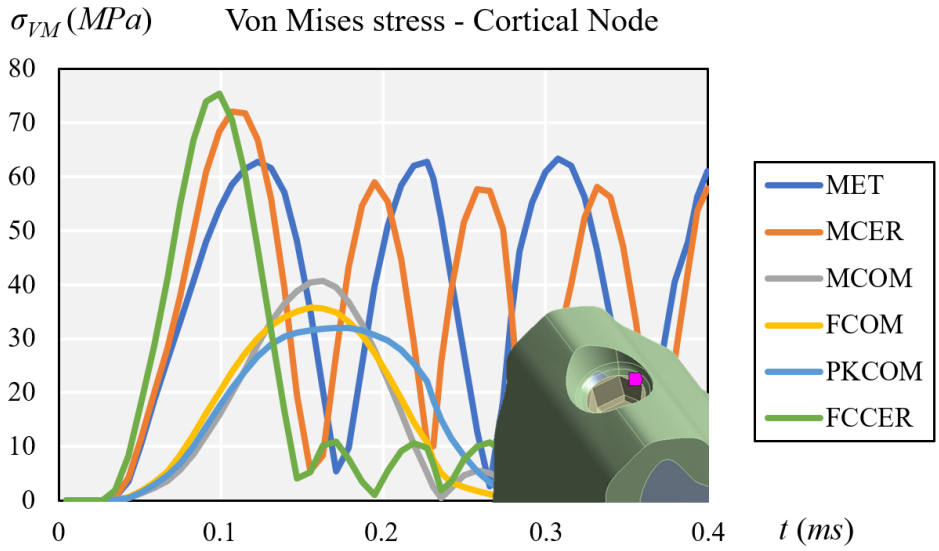

Figure 6. Comparison of equivalent von Mises stress at the cortical node.

3.2. Elastic Failure Test

A failure test was carried out to see if the dental implants could withstand the mechanical conditions to which they were subjected. Elastic failure criteria establish different approaches for different materials. In this case, the von Mises or maximum elastic distortion energy criterion was used. This criterion says that a structural element fails when at some point the distortion energy per unit volume exceeds a certain threshold. In stress terms, this means that the equivalent stress at a point, which is the von Mises stress, cannot exceed the elastic limit or the yield strength of the material, σ_y:

$$\sigma_{VM} \leq \sigma_y \tag{1}$$

Consequently, research on the elastic limits of the different materials was needed. After obtaining the values, a comparison was made for each model of the dental implant with each of the studied nodes used before. In Table 3, the yield stress, σ_y, and the maximum value of stress, $\sigma_{VM\max}$, are compared for each material and node. In this table, we can observe how the largest stresses occurred in the most rigid models.

In order to prevent uncertainties that may occur when real loads act on the implant, a safety factor is used. The safety factor is defined as the ratio between the yield strength of the material and the maximum value of von Mises equivalent stress. A usually applied Safety Factor is 1.5.

$$\gamma_{SF} = \frac{\sigma_y}{\sigma_{VM}} = 1.5. \tag{2}$$

Taking yield strength as the 100% value and rearranging Equation (2):

$$\sigma_{VM} \leq \frac{100\% \cdot \sigma_y}{1.5} = 66.67\% \cdot \sigma_y \tag{3}$$

Figure 7 shows the yield strength ratio for each material and node. The red line indicates the 66.67% value of yield stress.

Table 3. Comparison of the yield stress, σ_y, and the maximum value of stress, $\sigma_{VM\max}$, for each material and node.

Material	Node	Yield Strength σ_y (MPa)	Maximum von Mises $\sigma_{VM\max}$ (MPa)
MET	Crown	145–270	103.81
	Abutment	880–920	89.27
	Cortical	100–150	63.35
MCER	Crown	150	91.18
	Abutment	880–920	81.91
	Cortical	100–150	72.06
MCOM	Crown	280	51.05
	Abutment	880–920	77.82
	Cortical	100–150	40.71
FCOM	Crown	280	49.99
	Abutment	880–920	50.80
	Cortical	100–150	35.70
PKCOM	Crown	280	31.51
	Abutment	880–920	77.78
	Cortical	100–150	32.05
FCER	Crown	380	61.82
	Abutment	880–920	82.80
	Cortical	100–150	75.46

There was no elastic failure in any model, since all von Mises stresses were below the elastic limit, taking an arbitrary safety factor of 1.5. In the bar plots, we can observe how the von Mises stresses did not surpass 66.67% of the yield stress (red line). The most rigid models with the highest von Mises stresses were the ones closest to the 66.67% of the yield stress of each material.

In summary, the assumption of linearity of the behavior of materials was fulfilled in the studied model, and the calculated stresses were below the yielding limits of the materials, so we can consider that there was no plasticization.

The spider plots of Figure 8 show a comparison between the yield strength, σ_y, of the materials and the maximum values of von Mises stress, $\sigma_{VM\max}$, obtained in the numerical simulations for each node.

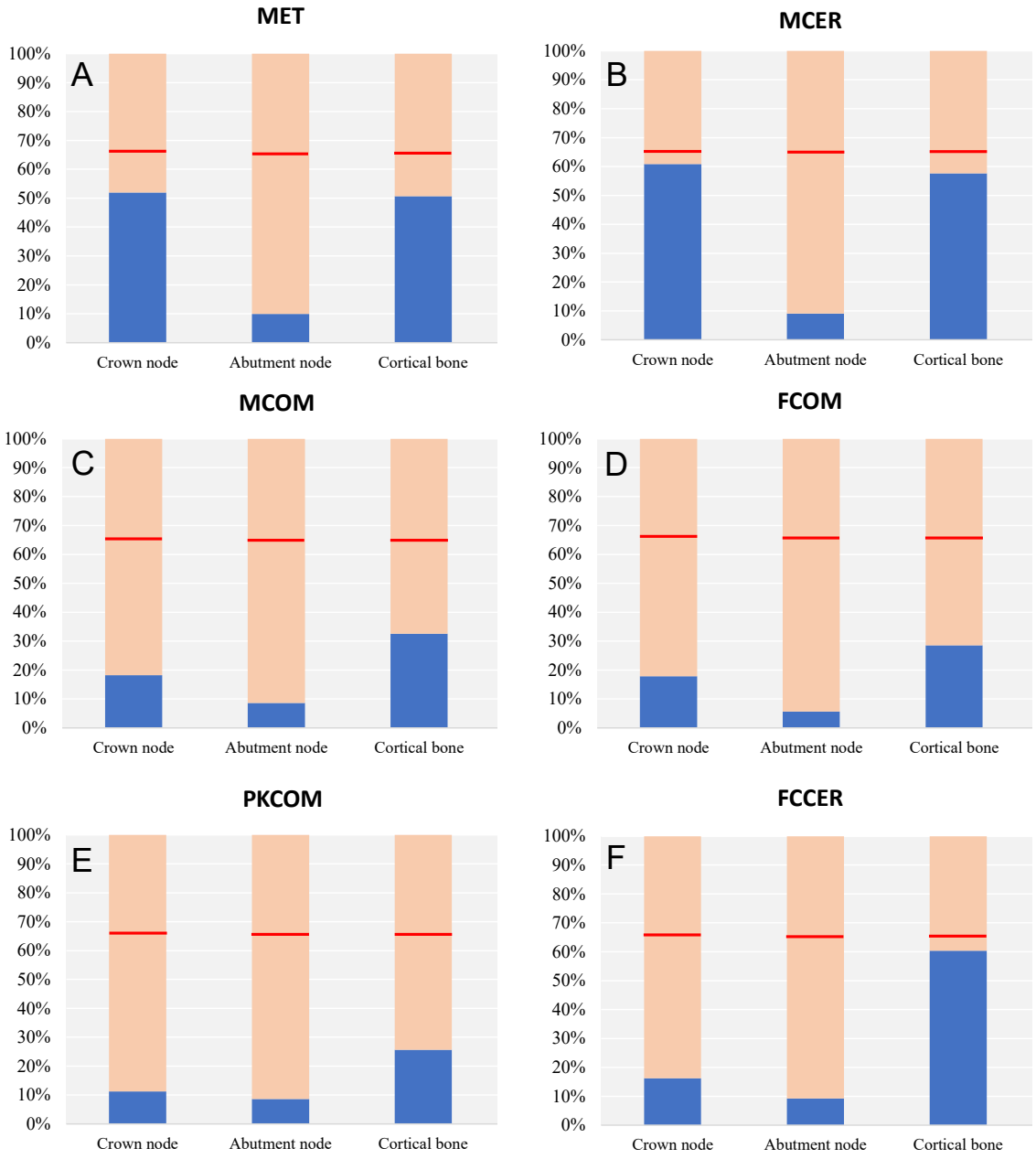

Figure 7. Comparison of the yield strength ratio depending on the node and crown material.

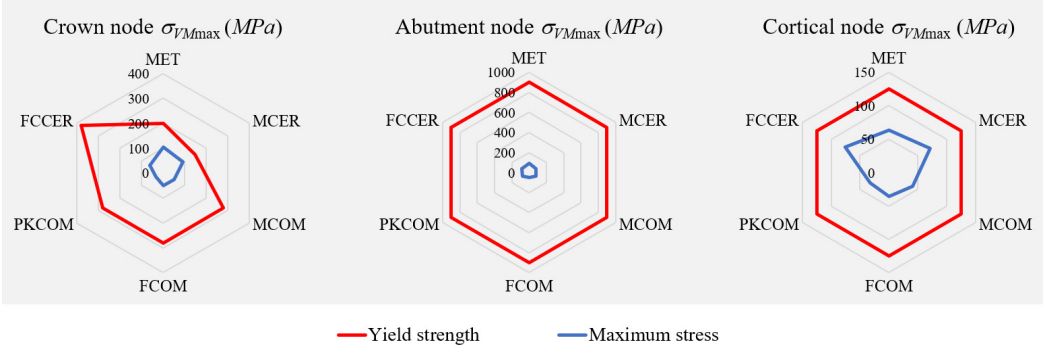

Figure 8. Spider plots comparing the yield strength of the materials and the maximum von Mises stress obtained for each node.

4. Conclusions

Denture forces, such as those from chewing, are transferred to implants and cause stress in the bone and the implant. That is why it is important to study the stresses (or strains) transferred to the implant and the bone in situations of maximum stress, modeled by dynamic forces under impact loading.

It can be concluded from the results of this study that the stress transferred to the crown, the abutment, and the peri-implant bone by an impact load on an implant-supported prosthesis varies according to the rigidity of the material and whether it is used as a framework or veneering material. It can also be stated that the more elastic material used for the crown, the lower the stresses generated in the bone. Too much stress induces bone resorption, which ultimately causes loosening of the implant, and overstrain can instigate bone failure. It turns out that the use of PEEK or carbon fibers as framework materials made stress dissipate faster than when using metal at the bone. By using these materials that can absorb and/or dissipate the stress transferred to the implant, we can reduce the risk of having bone resorption around the implant.

Therefore, with the use of more elastic materials that can better dissipate the impact energy and reduce the stress transferred to the implant, the risk of having bone resorption around the implant can also be reduced, especially in patients at risk of gingival inflammation that may cause peri-implant bone loss.

Author Contributions: Conceptualization, O.C.-N., R.M.-G. and J.C.-T.; data curation, X.M.; formal analysis, X.M., M.F. and J.C.-T.; funding acquisition, Ó.F.-Á. and J.C.-T.; investigation, O.C.-N. and X.M.; methodology, M.F.; project administration, J.C.-T.; resources, O.C.-N. and Ó.F.-Á.; software, X.M. and M.F.; supervision, Ó.F.-Á. and J.C.-T.; validation, O.C.-N., R.M.-G., X.M. and Ó.F.-Á.; visualization, X.M.; writing—original draft, O.C.-N. and X.M.; writing—review and editing, O.C.-N., R.M.-G., X.M., M.F. and J.C.-T. All authors have read and agreed to the published version of the manuscript.

Funding: This research received no external funding.

Institutional Review Board Statement: Not applicable.

Informed Consent Statement: Not applicable.

Data Availability Statement: Not applicable.

Acknowledgments: We gratefully acknowledge the support of the NVIDIA Corporation with the donation of the Titan X Pascal GPU used for this numerical analysis.

Conflicts of Interest: The authors declare no conflict of interests.

Abbreviations

MET	CoCr Metal
MCOM	CoCr Metal-Composite
MCER	CoCr Metal-Ceramic
FCOM	Carbon Fiber-Composite
PKCOM	PEEK-Composite
FCCER	Carbon Fiber-Ceramic

References

1. Jemt, T.; Lekholm, U.; Adell, R. Osseointegrated implants in the treatment of partially edentulous patients: A preliminary study on 876 consecutively placed fixtures. *Int. J. Oral Maxillofac. Implant* **1989**, *4*, 211–217.
2. Adell, R.; Eriksson, B.; Lekholm, U.; Branemark, P.I.; Jemt, T. Long-term follow-up study of osseointegrated implants in the treatment of totally edentulous jaws. *Int. J. Oral Maxillofac. Implant* **1990**, *5*, 347–359.
3. Roberts, H.W.; Berzins, D.W.; Moore, B.K.; Charlton, D.G. Metal-ceramic alloys in dentistry: A review. *J Prosthodont* **2009**, *18*, 188–194. [CrossRef] [PubMed]
4. Wataha, J.C. Biocompatibility of dental casting alloys: A review. *J. Prosthet. Dent.* **2000**, *83*, 223–234. [CrossRef]

5. Tuna, S.H.; Pekmez, N.O.; Keyf, F.; Canli, F. The electrochemical propierties of four dental casting suprastructure alloys coupled with titanium implants. *J. Appl. Oral Sci.* **2009**, *17*, 467–475. [CrossRef]
6. Bagegni, A.; Abou-Ayash, S.; Rucker, G.; Algarny, A.; Att, W. The influence of prosthetic material on implant and prosthetic survival of implant-supported fixed complete dentures: A systematic review and meta-analysis. *J. Prosthodont. Res.* **2019**, *63*, 251–265. [CrossRef]
7. Hu, M.L.; Lin, H.; Zhang, Y.D.; Han, J.M. Comparison of technical, biological, and esthetic parameters of ceramic and met-al-ceramic implant-supported fixed dental prostheses: A systematic review and meta-analysis. *J. Prosthet. Dent.* **2019**, *124*, 26–35. [CrossRef] [PubMed]
8. Le, M.; Papia, E.; Larsson, C. The clinical success of tooth- and implant-supported zirconia-based fixed dental prostheses. A systematic review. *J. Oral Rehabil.* **2015**, *42*, 467–480. [CrossRef] [PubMed]
9. Deany, I.L. Recent advances in ceramics for dentistry. *Crit Rev. Oral Biol. Med.* **1996**, *7*, 134–143.
10. Yamaguchi, S.; Okada, C.; Watanabe, Y.; Watanabe, M.; Hattori, Y. Analysis of masticatory muscle coordination during unilateral single-tooth clenching using muscle functional magnetic resonance imaging. *J. Oral Rehabil.* **2018**, *45*, 9–16. [CrossRef] [PubMed]
11. Moss, R.A.; Villarosa, G.A.; Cooley, J.E.; Lombardo, T.W. Masticatory muscle activity as a function of parafunctional, active and passive oral behavioural patterns. *J. Oral Rehabil.* **1987**, *14*, 361–370. [CrossRef]
12. Takeda, H.; Saitoh, K. Impact of proprioception during the oral phase on initiating the swallowing reflex. *Laryngoscope* **2016**, *126*, 1595–1599. [CrossRef]
13. Safari, A.; Jowkar, Z.; Farzin, M. Evaluation of the relationship between bruxism and premature occlusal contacts. *J. Contemp. Dent. Pract.* **2013**, *14*, 616–621. [CrossRef] [PubMed]
14. Van der Bilt, A.; Engelen, L.; Pereira, L.J.; van der Glas, H.W.; Abbink, J.H. Oral physiology and mastication. *Physiol. Behav.* **2006**, *89*, 22–27. [CrossRef] [PubMed]
15. Trulsson, M. Force encoding by human periodontal mechanoreceptors during mastication. *Arch. Oral Biol.* **2007**, *52*, 357–360. [CrossRef] [PubMed]
16. Cicciu, M.; Cervino, G.; Milone, D.; Risitano, G. FEM Investigation of the Stress Distribution over Mandibular Bone Due to Screwed Overdenture Positioned on Dental Implants. *Materials* **2018**, *11*, 1512. [CrossRef] [PubMed]
17. Menini, M.; Conserva, E.; Tealdo, T.; Bevilacqua, M.; Pera, F.; Signori, A.; Pera, P. Shock Absorption Capacity of Restorative Materials for Dental Implant Prostheses: An In Vitro Study. *Int. J. Prosthodont.* **2013**, *26*, 549–556. [CrossRef] [PubMed]
18. Cehreli, M.; Duyck, J.; De Cooman, M.; Puers, R.; Naert, I. Implant design and interface force transfer. *Clin. Oral Implant. Res.* **2004**, *15*, 249–257. [CrossRef]
19. Gracis, S.E.; Nicholls, J.I.; Chalupnik, J.D.; Yuodelis, R.A. Shock-absorbing behavior of five restorative materials used on im-plants. *Int. J. Prosthodont.* **1991**, *4*, 282–291. [PubMed]
20. Menini, M.; Conserva, E.; Tealdo, T.; Bevilacqua, M.; Pera, F.; Ravera, G.; Pera, P. The use of a masticatory robot to analyze the shock absorption capacity of different restorative materials for implant prosthesis. *J. Biol. Res. Boll. Della Soc. Ital. Biol. Sper.* **2011**, *84*, 118–119. [CrossRef]
21. Magne, P.; Silva, M.; Oderich, E.; Boff, L.L.; Enciso, R. Damping behavior of implant-supported restorations. *Clin. Oral Implant. Res.* **2011**, *24*, 143–148. [CrossRef]
22. Sevimay, M.; Turhan, F.; Kilicarslan, M.A.; Eskitascioglu, G. Three-dimensional finite element analysis of the effect of differ-ent bone quality on stress distribution in an implant-supported crown. *J. Prosthet. Dent.* **2005**, *93*, 227–234. [CrossRef] [PubMed]
23. Mizusawa, K.; Shin, C.; Okada, D.; Ogura, R.; Komada, W.; Saleh, O.; Huang, L.; Miura, H. The investigation of the stress distribution in abutment teeth for connected crowns. *J. Dent. Sci.* **2021**, *16*, 929–936. [CrossRef] [PubMed]
24. Kaleli, N.; Sarac, D.; Külünk, S.; Öztürk, Ö. Effect of different restorative crown and customized abutment materials on stress distribution in single implants and peripheral bone: A three-dimensional finite element analysis study. *J. Prosthet. Dent.* **2018**, *119*, 437–445. [CrossRef]
25. Geramizadeh, M.; Katoozian, H.; Amid, R.; Kadkhodazadeh, M. Static, Dynamic, and Fatigue Finite Element Analysis of Dental Implants with Different Thread Designs. *J. Autom. Inf. Sci.* **2016**, *26*, 347–355. [CrossRef]
26. Geramizadeh, M.; Katoozian, H.; Amid, R.; Kadkhodazadeh, M. Finite Element Analysis of Dental Implants with and without Microthreads under Static and Dynamic Loading. *J. Autom. Inf. Sci.* **2017**, *27*, 25–35. [CrossRef]
27. Karpov, E.G.; Danso, L.A.; Klein, J.T. Anomalous strain energy transformation pathways in mechanical metamaterials. *Proc. Math. Phys. Eng. Sci.* **2019**, *475*, 20190041. [CrossRef] [PubMed]
28. King, H. *Basic Finite Element Method Apllied to Injury Biomechanics*; Academic Press: Cambridge, MA, USA, 2018; ISBN 9780128098318.
29. Cantó-Navés, O.; Marimon, X.; Ferrer, M.; Cabratosa-Termes, J. Comparison between experimental digital image processing and numerical methods for stress analysis in dental implants with different restorative materials. *J. Mech. Behav. Biomed. Mater.* **2021**, *113*, 104092. [CrossRef] [PubMed]
30. Menini, M.; Pesce, P.; Pera, F.; Barberis, F.; Lagazzo, A.; Bertola, L.; Pera, P. Biological and mechanical characterization of carbon fiber frameworks for dental implant applications. *Mater. Sci. Eng. C* **2017**, *70*, 646–655. [CrossRef]
31. Erkmen, E.; Meriç, G.; Kurt, A.; Tunç, Y.; Eser, A. Biomechanical comparison of implant retained fixed partial dentures with fiber reinforced composite versus conventional metal frameworks: A 3D FEA study. *J. Mech. Behav. Biomed. Mater.* **2011**, *4*, 107–116. [CrossRef]

32. Passaretti, A.; Petroni, G.; Miracolo, G.; Savoia, V.; Perpetuini, A.; Cicconetti, A. Metal free, full arch, fixed prosthesis for edentulous mandible rehabilitation on four implants. *J. Prosthodont. Res.* **2018**, *62*, 264–267. [CrossRef]
33. Zaparolli, D.; Peixoto, R.F.; Pupim, D.; Macedo, A.P.; Toniollo, M.B.; Mattos, M.D.G.C.D. Photoelastic analysis of mandibular full-arch implant-supported fixed dentures made with different bar materials and manufacturing techniques. *Mater. Sci. Eng. C* **2017**, *81*, 144–147. [CrossRef]
34. Pera, F.; Pesce, P.; Solimano, F.; Tealdo, T.; Pera, P.; Menini, M. Carbon fibre versus metal framework in full-arch immediate loading rehabilitations of the maxilla-a cohort clinical study. *J. Oral Rehabil.* **2017**, *44*, 392–397. [CrossRef]
35. Segerstrom, S.; Ruyter, I.E. Effect of thermal cycling on flexural properties of carbon-graphite fiber-reinforced polymers. *Dent. Mater.* **2009**, *25*, 845–851. [CrossRef] [PubMed]
36. Segerstrom, S.; Ruyter, I.E. Adhesion properties in systems of laminated pigmented polymers, carbon-graphite fiber composite framework and titanium surfaces in implant suprastructures. *Dent. Mater.* **2009**, *25*, 1169–1177. [CrossRef] [PubMed]
37. Segerstrom, S.; Sandborgh-Englund, G.; Ruyter, E.I. Biological and physicochemical properties of carbon-graphite fi-bre-reinforced polymers intended for implant suprastructures. *Eur. J. Oral Sci.* **2011**, *119*, 246–252. [CrossRef] [PubMed]
38. Muhsin, S.A.; Hatton, P.; Johnson, A.; Sereno, N.; Wood, D.J. Determination of Polyetheretherketone (PEEK) mechanical properties as a denture material. *Saudi Dent. J.* **2019**, *31*, 382–391. [CrossRef]
39. Schwitalla, A.D.; Spintig, T.; Kallage, I.; Müller, W.-D. Pressure behavior of different PEEK materials for dental implants. *J. Mech. Behav. Biomed. Mater.* **2016**, *54*, 295–304. [CrossRef]
40. Schwitalla, A.D.; Spintig, T.; Kallage, I.; Müller, W.-D. Flexural behavior of PEEK materials for dental application. *Dent. Mater.* **2015**, *31*, 1377–1384. [CrossRef]
41. Gallucci, G.O.; Bernard, J.-P.; Bertosa, M.; Belser, U.C. Immediate loading with fixed screw-retained provisional restorations in edentulous jaws: The pickup technique. *Int. J. Oral Maxillofac. Implant.* **2004**, *19*, 524–533.
42. Norton, M.R. An in vitro evaluation of the strength of an internal conical interface compared to a butt joint interface in implant design. *Clin. Oral Implant. Res.* **1997**, *8*, 290–298. [CrossRef]
43. Tonella, B.P.; Pellizzer, E.P.; Ferraço, R.; Falcón-Antenucci, R.M.; Carvalho, P.S.P.D.; Goiato, M.C. Photoelastic analysis of cemented or screwed implant-supported prostheses with different prosthetic connections. *J. Oral Implantol.* **2011**, *37*, 401–410. [CrossRef] [PubMed]
44. Peixoto, R.F.; Tonin, B.S.H.; Martinelli, J.; Macedo, A.P.; Mattos, M.D.G.C.D. In vitro digital image correlation analysis of the strain transferred by screw-retained fixed partial dentures supported by short and conventional implants. *J. Mech. Behav. Biomed. Mater.* **2020**, *103*, 103556. [CrossRef] [PubMed]
45. Hoult, N.A.; Take, W.A.; Lee, C.; Dutton, M. Experimental accuracy of two dimensional strain measurements using Digital Image Correlation. *Eng. Struct.* **2013**, *46*, 718–726. [CrossRef]
46. Bassit, R.; Lindström, H.; Rangert, B. In Vivo registration of force development with ceramic and acrylic resin occlusal materials on implant-supported prostheses. *Int. J. Oral Maxillofac. Implants.* **2002**, *17*, 17–23.
47. Bijjargi, S.; Chowdhary, R. Stress dissipation in the bone through various crown materials of dental implant restoration: A 2-D finite element analysis. *J. Investig. Clin. Dent.* **2012**, *4*, 172–177. [CrossRef] [PubMed]
48. Sevimay, M.; Usumez, A.; Eskitascioglu, G. The influence of various occlusal materials on stresses transferred to im-plant-supported prostheses and supporting bone: A three-dimensional finite-element study. *J. Biomed. Mater. Res. B Appl. Biomater.* **2005**, *73*, 140–147. [CrossRef] [PubMed]
49. Bacchi, A.; Consani, R.L.; Mesquita, M.F.; dos Santos, M.B. Stress distribution in fixed-partial prosthesis and peri-implant bone tissue with different framework materials and vertical misfit levels: A three-dimensional finite element analysis. *J. Oral Sci.* **2013**, *55*, 239–244. Available online: http://www.ncbi.nlm.nih.gov/pubmed/24042591 (accessed on 15 May 2019). [CrossRef] [PubMed]
50. Merz, B.R.; Hunenbart, S.; Belser, U.C. Mechanics of the implant-abutment connection: An 8-degree taper compared to a butt joint connection. *Int. J. Oral Maxillofac. Implant.* **2000**, *15*, 519–526.
51. Valera-Jiménez, J.; Burgueño-Barris, G.; Gómez-González, S.; López-López, J.; Valmaseda-Castellón, E.; Fernández-Aguado, E. Finite element analysis of narrow dental implants. *Dent. Mater.* **2020**, *36*, 927–935. [CrossRef] [PubMed]
52. Anami, L.C.; Lima, J.M.D.C.; Takahashi, F.E.; Neisser, M.P.; Noritomi, P.Y.; Bottino, M.A. Stress Distribution Around Osseointegrated Implants With Different Internal-Cone Connections: Photoelastic and Finite Element Analysis. *J. Oral Implant.* **2015**, *41*, 155–162. [CrossRef]
53. Carvalho, L.; Roriz, P.; Simões, J.; Frazão, O. New Trends in Dental Biomechanics with Photonics Technologies. *Appl. Sci.* **2015**, *5*, 1350–1378. [CrossRef]
54. Karl, M.; Dickinson, A.; Holst, S.; Holst, A. Biomechanical methods applied in dentistry: A comparative overview of photoelastic examinations, strain gauge measurements, finite element analysis and three-dimensional deformation analysis. *Eur. J. Prosthodont. Restor. Dent.* **2009**, *17*, 50–57.
55. Benazzi, S.; Nguyen, H.N.; Kullmer, O.; Kupczik, K. Dynamic Modelling of Tooth Deformation Using Occlusal Kinematics and Finite Element Analysis. *PLoS ONE* **2016**, *11*, e0152663. [CrossRef]
56. Razaghi, R.; Haghpanahi, M. Dynamic simulation and finite element analysis of the maxillary bone injury around dental implant during chewing different food. *Biomed. Eng. Appl. Basis. Commun.* **2016**, *28*, 1–10. [CrossRef]

57. Kayabaşı, O.; Yüzbasıoğlu, E.; Erzincanlı, F. Static, dynamic and fatigue behaviors of dental implant using finite element method. *Adv. Eng. Softw.* **2006**, *37*, 649–658. [CrossRef]
58. Chang, Y.; Tambe, A.A.; Maeda, Y.; Wada, M.; Gonda, T. Finite element analysis of dental implants with validation: To what extent can we expect the model to predict biological phenomena? A literature review and proposal for classification of a validation process. *Int. J. Implant Dent.* **2018**, *4*, 1–14. [CrossRef]
59. Lindhe, J.; Meyle, J.; Group D of the European Workshop on Periodontology. Peri-implant diseases: Consensus Report of the Sixth European Workshop on Periodontology. *J. Clin. Periodontol.* **2008**, *35*, 282–285. [CrossRef]
60. Sanz, M.; Lang, N.P.; Kinane, D.F.; Berglundh, T.; Chapple, I.; Tonetti, M.S. Seventh European Workshop on Periodontol-ogy of the European Academy of Periodontology at the Parador at la Granja, Segovia, Spain. *J. Clin. Periodontol.* **2011**, *38* (Suppl. 11), 1–2. [CrossRef]
61. Ramseier, C.A.; Needleman, I.G.; Gallagher, J.E.; Lahtinen, A.; Ainamo, A.; Alajbeg, I.; Albert, D.; Al-Hazmi, N.; Antohé, M.E.; Beck-Mannagetta, J.; et al. Consensus Report: 2nd European Workshop on Tobacco Use Prevention and Cessation for Oral Health Professionals. *Int. Dent. J.* **2010**, *60*, 3–6.
62. Mazel, A.; Belkacemi, S.; Tavitian, P.; Stéphan, G.; Tardivo, D.; Catherine, J.H.; Aboudharam, G. Peri-implantitis risk factors: A pro-spective evaluation. *J. Investig. Clin. Dent.* **2019**, *10*, e12398. [CrossRef]
63. Tsigarida, A.; Dabdoub, S.; Nagaraja, H.; Kumar, P. The Influence of Smoking on the Peri-Implant Microbiome. *J. Dent. Res.* **2015**, *94*, 1202–1217. [CrossRef]
64. Derks, J.; Tomasi, C. Peri-implant health and disease. A systematic review of current epidemiology. *J. Clin. Periodontol.* **2015**, *42*, S158–S171. [CrossRef] [PubMed]
65. Duyck, J.; Vandamme, K. The effect of loading on peri-implant bone: A critical review of the literature. *J. Oral Rehabil.* **2014**, *41*, 783–794. [CrossRef]
66. Naert, I.; Duyck, J.; Vandamme, K. Occlusal overload and bone/implant loss. *Clin. Oral Implant Res.* **2012**, *23*, 95–107. [CrossRef] [PubMed]
67. Klinge, B.; Meyle, J.; Working Group 2. Peri-implant tissue destruction. The Third EAO Consensus Conference 2012. *Clin. Oral Implants Res.* **2012**, *23*, 108–110. [CrossRef] [PubMed]
68. Mombelli, A.; van Oosten, M.A.; Schurch, E., Jr.; Land, N.P. The microbiota associated with successful or failing osseointe-grated titanium implants. *Oral Microbiol. Immunol.* **1987**, *2*, 145–151. [CrossRef]
69. Kozlovsky, A.; Tal, H.; Laufer, B.Z.; Leshem, R.; Rohrer, M.D.; Weinreb, M.; Artzi, Z. Impact of implant overloading on the pe-ri-implant bone in inflamed and non-inflamed peri-implant mucosa. *Clin. Oral Implants Res.* **2007**, *18*, 601–610. [CrossRef]
70. Afrashtehfar, K.I.; Afrashtehfar, C.D. Lack of association between overload and peri-implant tissue loss in healthy conditions. *Evid. Based Dent.* **2016**, *17*, 92–93. [CrossRef]
71. Esposito, M.; Hirsch, J.-M.; Lekholm, U.; Thomsen, P. Biological factors contributing to failures of osseointegrated oral implants, (I). Success criteria and epidemiology. *Eur. J. Oral Sci.* **1998**, *106*, 527–551. [CrossRef] [PubMed]
72. Mattheos, N.; Collier, S.; Walmsley, A.D. Specialists' management decisions and attitudes towards mucositis and peri-implantitis. *Br. Dent. J.* **2012**, *212*, E1. [CrossRef]
73. Hermann Schoolfield, J.D.; Schenk, R.K.; Buser, D.; Cochran, D.L.J.S. Influence of the size of the microgap on crestal bone changes around titanium implants. A histometric evaluation of unloaded non-submerged implants in the canine mandible. *J. Periodontol.* **2001**, *72*, 1372–1383. [CrossRef] [PubMed]
74. VanSchoiack Wu, J.C.; Sheets, C.G.; Earthma, J.C.L.R. Effect of bonedensity on thedampingbehavior of dental implants: An in vitro method. *Mater. Sci. Eng.* **2006**, *26*, 1307–1311. [CrossRef]
75. Lima de Andrade, C.; Carvalho, M.A.; Bordin, D.; da Silva, W.J.; Del Bel Cury, A.A.; Sotto-Maior, B.S. Biomechanical Behavior of the Dental Implant Macrodesign. *Int. J. Oral Maxillofac. Implants* **2017**, *32*, 264–270. [CrossRef] [PubMed]
76. Coltro, M.P.L.; Ozkomur, A.; Villarinho, E.A.; Teixeira, E.R.; Vigo, A.; Shinkai, R.S.A. Risk factor model of mechanical complica-tions in implant-supported fixed complete dentures: A prospective cohort study. *Clin. Oral Implants Res.* **2018**, *29*, 915–921. [CrossRef]
77. Karakis, D.; Dogan, A. The craniofacial morphology and maximum bite force in sleep bruxism patients with signs and symptoms of temporomandibular disorders. *CRANIO®* **2014**, *33*, 32–37. [CrossRef]
78. Mengatto, C.M.; Coelho-de-Souza, F.H.; de Souza Junior, O.B. Sleep bruxism: Challenges and restorative solutions. *Clin. Cosmet. Investig. Dent.* **2016**, *8*, 71–77. [CrossRef]
79. Mikeli, A.; Walter, M.H. Impact of Bruxism on Ceramic Defects in Implant-Borne Fixed Dental Prostheses: A Retrospective Study. *Int. J. Prosthodont.* **2016**, *29*, 296–298. [CrossRef]
80. Insua, A.; Monje, A.; Wang, H.-L.; Miron, R.J. Basis of bone metabolism around dental implants during osseointegration and peri-implant bone loss. *J. Biomed. Mater. Res. Part A* **2017**, *105*, 2075–2089. [CrossRef]
81. Sathapana, S.; Monsour, P.; Naser-ud-Din, S.F.A. Age-related changes in maxillary and mandibular cortical bone thickness in relation to temporary anchorage device placement. *Aust. Dent. J.* **2013**, *8*, 67–74. [CrossRef]
82. Tomar, V. Modeling of Dynamic Fracture and Damage in Two-Dimensional Trabecular Bone Microstructures Using the Cohesive Finite Element Method. *J. Biomech. Eng.* **2008**, *130*, 021021. [CrossRef] [PubMed]
83. Li, J.; Yin, X.; Huang, L.; Mouraret, S.; Brunski, J.; Cordova, L.; Salmon, B.; Helms, J. Relationships among Bone Quality, Implant Osseointegration, and Wnt Signaling. *J. Dent. Res.* **2017**, *96*, 822–831. [CrossRef]

84. Asa'Ad, F.; Monje, A.; Larsson, L. Role of epigenetics in alveolar bone resorption and regeneration around periodontal and peri-implant tissues. *Eur. J. Oral Sci.* **2019**, *127*, 477–493. [CrossRef] [PubMed]
85. Solidworks Dassault Systemes. 2020. Available online: http://www.solidworks.com (accessed on 15 May 2019).
86. Micro Medica Srl. 2021. Available online: http://micromedicasrl.it (accessed on 15 May 2019).
87. Renishaw. 2021. Available online: https://www.renishaw.com (accessed on 15 May 2019).
88. VITA Zahnfabrik, H. Rauter GmbH & Co 2021. Germany. Available online: www.vita-zahnfabrik.com (accessed on 15 May 2019).
89. Heraeus Kulzer GmbH. 2021. Available online: https://www.kulzer.de (accessed on 15 May 2019).
90. Ivoclar Vivadent 2021. Available online: https://www.ivoclarvivadent.es (accessed on 15 May 2019).
91. Invibio 2021. Available online: https://invibio.com (accessed on 15 May 2019).
92. MIS Implants Technologies Ltd. 2021. Available online: https://www.mis-implants.com (accessed on 15 May 2019).
93. Lakatos, É.; Magyar, L.; Bojtár, I. Material Properties of the Mandibular Trabecular Bone. *J. Med. Eng.* **2014**, *2014*, 470539. [CrossRef] [PubMed]
94. Geng, J.P.; Tan, K.B.; Liu, G.R. Application of finite element analysis in implant dentistry: A review of the literature. *J. Pros-thet. Dent.* **2001**, *85*, 585–598. [CrossRef]

materials

MDPI

Article

Bone Stress Evaluation with and without Cortical Bone Using Several Dental Restorative Materials Subjected to Impact Load: A Fully 3D Transient Finite-Element Study

Raul Medina-Galvez [1], Oriol Cantó-Navés [1], Xavier Marimon [2,3,*], Miguel Cerrolaza [2,4], Miquel Ferrer [5] and Josep Cabratosa-Termes [1]

1 Faculty of Dentistry, Universitat Internacional de Catalunya (UIC), 08017 Barcelona, Spain; ruldoc@uic.es (R.M.-G.); oriolcanto@uic.es (O.C.-N.); cabratosa@uic.es (J.C.-T.)
2 Bioengineering Institute of Technology, Universitat Internacional de Catalunya (UIC), 08190 Barcelona, Spain; mcerrolaza@uic.es
3 Automatic Control Department, Universitat Politècnica de Catalunya (UPC-BarcelonaTECH), 08034 Barcelona, Spain
4 School of Engineering, Science & Technology, Valencian International University, 46002 Valencia, Spain
5 Department of Strength of Materials and Structural Engineering, Universitat Politècnica de Catalunya (UPC-BarcelonaTECH), 08034 Barcelona, Spain; miquel.ferrer@upc.edu
* Correspondence: xmarimon@uic.es

Citation: Medina-Galvez, R.; Cantó-Navés, O.; Marimon, X.; Cerrolaza, M.; Ferrer, M.; Cabratosa-Termes, J. Bone Stress Evaluation with and without Cortical Bone Using Several Dental Restorative Materials Subjected to Impact Load: A Fully 3D Transient Finite-Element Study. *Materials* **2021**, *14*, 5801. https://doi.org/10.3390/ma14195801

Academic Editors: Michele Bacciocchi and Mutlu Özcan

Received: 21 August 2021
Accepted: 1 October 2021
Published: 4 October 2021

Abstract: Statement of problem. Previous peri-implantitis, peri-implant bone regeneration, or immediate implant placement postextraction may be responsible for the absence of cortical bone. Single crown materials are then relevant when dynamic forces are transferred into bone tissue and, therefore, the presence (or absence) of cortical bone can affect the long-term survival of the implant. **Purpose**: the purpose of this study is to assess the biomechanical response of dental rehabilitation when selecting different crown materials in models with and without cortical bone. **Methods**: several crown materials were considered for modeling six types of crown rehabilitation: full metal (MET), metal-ceramic (MCER), metal-composite (MCOM), peek-composite (PKCOM), carbon fiber-composite (FCOM), and carbon fiber-ceramic (FCCER). An impact-load dynamic finite-element analysis was carried out on all the 3D models of crowns mentioned above to assess their mechanical behavior against dynamic excitation. Implant-crown rehabilitation models with and without cortical bone were analyzed to compare how the load-impact actions affect both type of models. **Results**: numerical simulation results showed important differences in bone tissue stresses. The results show that flexible restorative materials reduce the stress on the bone and would be especially recommendable in the absence of cortical bone. **Conclusions**: this study demonstrated that more stress is transferred to the bone when stiffer materials (metal and/or ceramic) are used in implant supported rehabilitations; conversely, more flexible materials transfer less stress to the implant connection. Also, in implant-supported rehabilitations, more stress is transferred to the bone by dynamic forces when cortical bone is absent.

Keywords: FEA; FEM; impact test; transient analysis; dynamical forces; biomechanical behavior; implant rehabilitation; rehabilitation materials; crown materials; bone loss

1. Introduction

The quantity and quality of bone tissue around a rehabilitated implant play a key role in its long-term survival [1]. After peri-implantitis, immediate implant placement, or regenerated bone, cortical bone is missing for a variable period [2]. Moreover, the absence of cortical bone can affect the biomechanical behavior of both the bone tissue and its ability to withstand impact loads [3].

Different models and techniques are used to analyze the behavior of dental implants [4] including two-dimensional (2D) or three-dimensional (3D) finite element analyses (FEA),

photo-elastic studies, or digital image-correlations (DIC). Also, ultrasonic wave analysis [5,6] can be used successfully in dental implant analysis [7].

FEA, whether in 2D or 3D, is a numerical and approximate technique that yields results depending on both the geometry and mechanical properties of the materials. Regarding photo-elastic techniques, when either static or dynamic forces are applied, isochromatic fringes appear in photo-elastic studies [8], thereby allowing the stress distribution at implants to be calculated. The DIC is an image-based analysis that shows how points inside resin blocks move when static or dynamic forces are applied [9]. On the other hand, the analysis of implant behavior requires that the difference between static forces (due to clenching) and dynamic forces (due to mastication or eccentric bruxism) be very clear, particularly when selecting the rehabilitation materials [10,11].

Other works reported similar results for implant behavior [4,8]. These authors showed that the main differences are due to variables such as the type of implant connection, the diameter/length of the implant, the type of rehabilitation material or whether the load was applied statically or dynamically [8,12]. However, the presence or absence of cortical bone is an issue that, to date, was not studied or quantified sufficiently. The absence of cortical bone can lead to the implant loosening and eventually to implant failure [13–17].

From a mechanical perspective, and according to some previous works [18–22], static analysis is not completely enough to get precise and reliable results. Several authors agreed that it is needed to perform dynamic analysis. Dynamic analysis can be found in literature [18,22] but addressing fatigue analysis and not impact dynamic loading.

In previous works [23] the authors analyzed the mechanical behavior of implants with different restorative materials subjected to static loads by three different methods: finite element method (FEM), digital photoelasticity (DP), and digital image correlation (DIC). They concluded that (1) all 3 methods provide very close solutions; (2) FEM is enough reliable and robust for predicting the tooth-implant mechanical behavior, and (3) dynamic impact analysis is mandatory for getting more accurate and closer results to the problem's physical reality.

Therefore, in this work a fully 3D dynamic FEA study of the influence of different crown materials on the implant behavior with and without cortical bone when subjected to impact dynamic loads is performed. Moreover, we also discuss two clinical cases: (a) both trabecular and cortical bone, and (b) only trabecular bone.

Significant differences in the mechanical response when the peri-implantitis generated a loss of cortical bone were encountered. The study concludes with a comparative dynamic analysis of crowns made with different restorative materials.

2. Materials and Methods

2.1. The Model

A 3D dynamic finite-element model comprising a crown, an abutment screw, an abutment, an implant, and the surrounding bone was set up to evaluate the von Mises stresses at both the cortical and trabecular bone (See Figure 1). Ethics approval was not required for this in-vitro study. All the parts of the model are described hereafter.

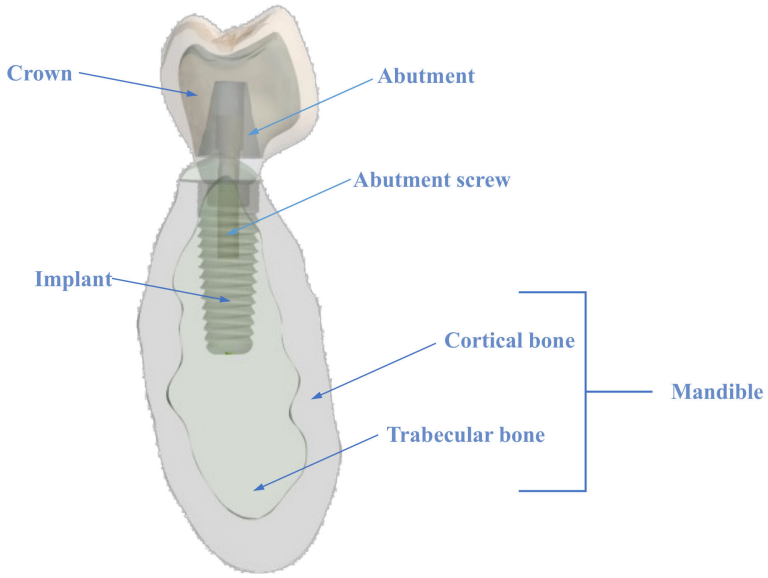

Figure 1. Cross-sectional view of 3D model.

2.1.1. The Crown

The crown model was processed using Solidworks (version 2021, Dassault Systèmes, Waltham, MA, USA) [24] by importing a CAD model generated by Exocad-3D (v3.0, Exocad GmbH, Darmstadt, Germany). The model was built by assembling two components: the core (51% of the total volume) and the aesthetic veneering (40% of the total volume), as displayed in Figure 2. The volume of the resulting crown model is 411.5 mm^3.

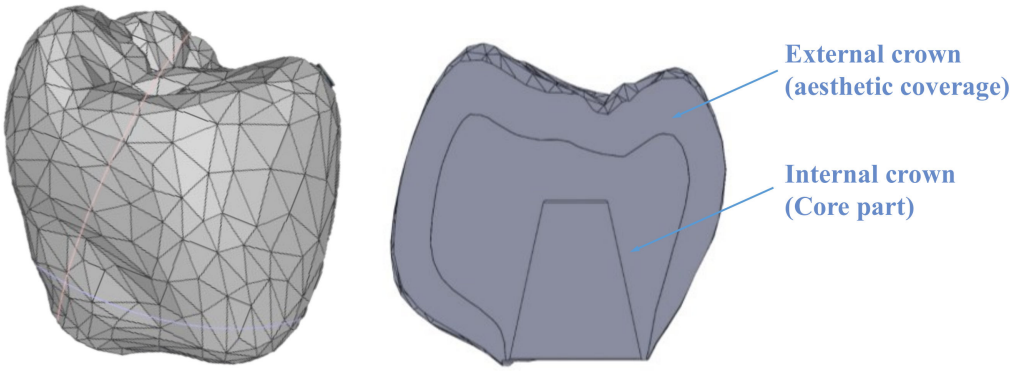

Figure 2. Crown model. Left: cross section showing both internal and external crown.

2.1.2. The Abutment and Screw

The abutment is a metal component whose function is to attach the crown and the implant. Also, a hexagonal antirotation system prevents the relative movement between the abutment and the implant. The screw allows the connection between the abutment and the implant.

Solidworks was also used to model the abutment and the screw, thus reducing the classical surfaces to a simpler triangular shapes (see Figure 3). The model corresponds to the hexagonal-connection abutment of the MIS implant [25].

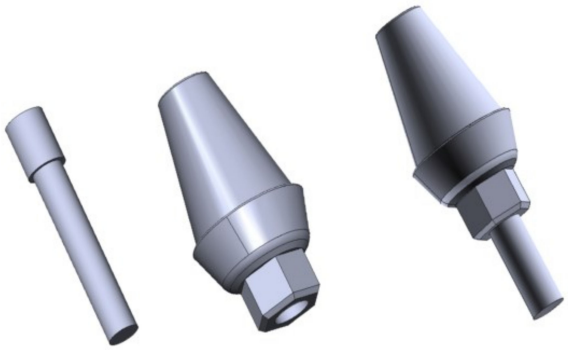

Figure 3. Left: abutment screw; center: abutment with hexagonal antirotational system; right: screw-abutment assembly.

2.1.3. The Implant

Figure 4 displays the implant created with Solidworks to obtain more accurate geometric shapes. The implant used in this study was a 4.2 × 11.5 mm^2 MIS implant [25], because it is a well-known and reliable implant used in the area of restorative dentistry and world-wide commercialized.

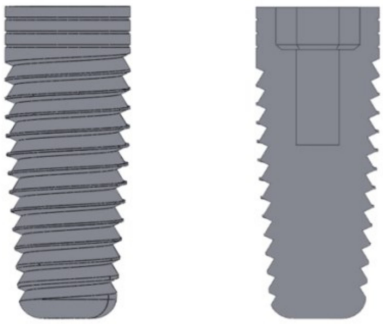

Figure 4. Implant. Left: lateral view; right: cross section.

2.1.4. The Mandible

The mandible section was made from a CT scan section [26]. The mandible's geometry was generated by following two steps: (a) some key points were defined at a known distance at the CT-scan section, and (b) the scan scale was then used to compute the actual distances at the real mandible. The 3D geometry of the mandible was split into an external region of cortical bone and an internal one of trabecular bone, each one with its specific mechanical properties (see Figure 5).

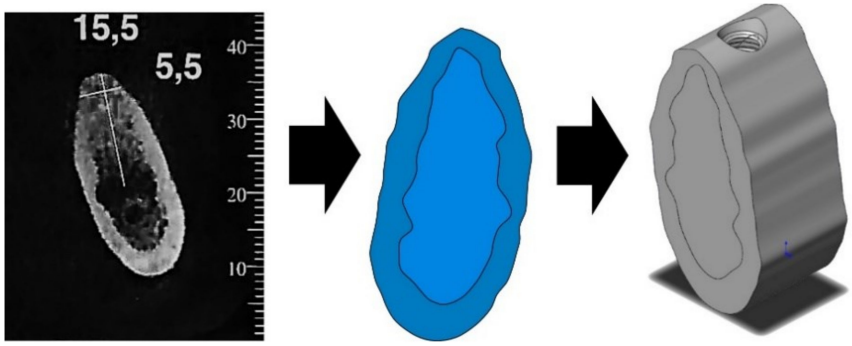

Figure 5. Left: CT scan. Center: mandible section obtained from CT scan. Right: isometric view of mandible's model.

2.1.5. The Loading Plate

The impact loads produced by chewing were applied to the model (crown, implant, and mandible) by using a rectangular rigid plate dimensioned as shown in Figure 6. Some boundary conditions were considered: (a) the initial separation between the plate and the crown was set to 0.01 mm; (b) free sliding is assumed, i.e., the impact of the plate on the model is frictionless; (c) normal stresses were considered null if the plate loses contact with the model.

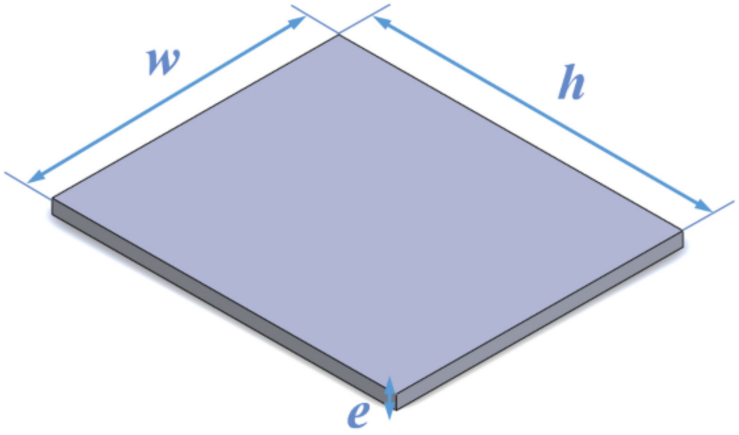

Figure 6. Dimensions of rigid plate (w = 10 mm, h = 12 mm, e = 2 mm).

2.2. Geometry of the Assembled Model

After all the individual parts were independently built, they were assembled together as shown in Figure 7.

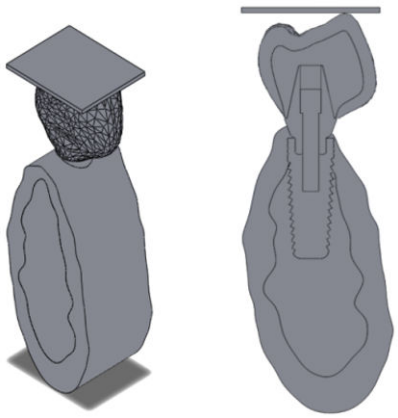

Figure 7. Assembled geometry. **Left**: isometric view; **right**: cross section.

Before conducting the FEA simulation, the assembled geometry was converted to IGES format, which was imported into Ansys Workbench Design Modeler (version 2021, ANSYS, Inc, Canonsburg, PA, USA). Perfect osseointegration between the implant and the bone was assumed. This means that the bone is integrated into all slots of the placed implant, although this does not always happen in clinical cases

2.3. Materials of the Model

The mechanical properties of the materials have a direct influence on the calculation of the stress response and its deformations. All materials were considered elastic, homogeneous, and isotropic. Mandible bone mechanical properties can be found elsewhere [27]. Different materials were used in the crown, to discover if the crown material has a direct effect on the implant stress distribution and mechanical performance (see Table 1 below):

Table 1. Crown materials and manufactures. Acronyms used in this study.

	Material Name	Manufacturer	Young Modulus [MPa]	Poisson Ratio	Density [g/cm^3]
Crown	**FCOM**				
	Carbon fiber-composite	Micro Medica	300,000	0.3	1.40
	BioCarbon Bridge fibers	Micro Medica	22,000	0.3	8.30
	Composite BioXfill				
	MCER				
	Metal-ceramic	Renishaw	208,000	0.31	8.90
	Co-Cr alloy	Vita	69,000	0.28	2.50
	Ceramic VMK 95				
	MCOM				
	Metal-composite	Renishaw	208,000	0.31	8.90
	Co-Cr alloy	Micro-Medica	22,000	0.3	8.30
	Composite BioXfill				
	MET				
	Full metal	Heraeus Kulzer	208,000	0.31	8.90
	Co-Cr Alloy, Mo, W				
	FCCER				
	Carbon fiber-ceramic	Micro-Medica	66,000	0.3	1.4
	Carbon Fiber Bridge	Ivoclar Vivadent	95,000	0.2	2.5
	Ceramic IPS e.max				
	PKCOM				
	PEEK-composite	Invibio	4,100	0.36	1.3
	PEEK Optima	Micro-Medica	22,000	0.3	8.30
	Composite BioXfill				
Implant	Ti-6-Al-4V ELI	MIS	113,800	0.34	4.43
Bone	Cortical bone	[27,28]	15,000	0.3	1.79
	Trabecular bone	[28]	500	0.3	0.45

A total of six crown rehabilitation materials were analyzed: the carbon fiber-composite crown (FCOM) had an aesthetic layer of a BioXfill composite [29] and carbon fiber framework of BioCarbon Bridge; the metal-ceramic crown (MCER) had a framework of LaserPFM Co-Cr metal alloy and aesthetic veneering of VITA VMK 95 ceramic material [30,31]; the metal-composite crown (MCOM) had a framework of LaserPFM Co-Cr metal alloy [30] and BioXfill composite [29]; the metal crown (MET) is made entirely of melted Co-Cr alloy [32]; the carbon fiber-ceramic crown (FCCER) had a framework of BioCarbon Bridge carbon fibers [29] and lithium disilicate ceramic aesthetic covering [33]; finally, the PEEK-composite crown (PKCOM) is made in the inner part of polymer polyetheretherketone (PEEK) and the aesthetic veneering with BioXfill composite [34].

All the mechanical properties of each crown, the implant, and both bone tissues (cortical and trabecular) used in the numerical simulation are listed in Table 1. The mechanical properties of the materials were obtained from the manufacturer datasheets indicated in the table.

2.4. Numerical Simulation

Although there are numerous studies centered on static forces, there are few studies of the dynamic forces applied during physiological functions. Some biomechanical estimated values can be obtained in the literature [35,36]. Therefore, a simulated impact between the rigid plate and the whole implant geometry was carried out. **Results were analyzed over time due to the dynamic response of the model**. The simulation was performed with ANSYS (version 2021, ANSYS, Inc, Canonsburg, PA, USA) [37] using the mechanical APDL solver and the Transient Structural analysis system.

2.4.1. Simulation Setup

A first simulation was performed to check that all the materials, hypotheses, and boundary conditions of the model were correctly defined. All the results were coherent, but the computational time was very high for two main reasons: there was a very large number of nodes and elements and the time set for analysis was more than was needed. Therefore, the time and number of elements and nodes were reduced. The distance between the plate and the crown was also shortened. Furthermore, to carry out reasonable comparisons, the dynamic characteristics of the impact, i.e., initial kinetic energy and linear momentum, should be the same in all the simulations.

Initially, all the mass particles of the dental implant have the same velocity as well as the kinetic energy due to the movement of the whole structure (mandible, implant, crown, and abutment), as shown below:

$$E_k = \sum \frac{1}{2} \cdot m_i \cdot v^2 \quad (1)$$

where E_k is the kinetic energy, m_i is the particle mass, v_i is the particle velocity.

When the dental implant collides with the plate the kinetic energy is transformed into strain energy. The strain energy for a deformable solid can be determined through the stress and strain tensors time-history.

If the deformation occurs within the linear-elastic range, the potential elastic deformation energy can be obtained from Equation (2):

$$E_{def} = \int_V \sigma_i \cdot \varepsilon_i \cdot dV \quad (2)$$

where E_{def} is the potential elastic deformation energy, σ_i is the stress state, ε_i is the strain state, dV is the volume differential.

The dynamic characteristics of an impact are determined by the system's initial energy ($0.5 \cdot m \cdot v^2$) and linear momentum ($m \cdot v$). Both features must have the same value in any case, which is guaranteed by introducing the same speed (v) and the same mass (m). On the other hand, the effect of the mandible's mass is not so significant because it is externally fixed.

Since each crown material has a different density, the initial mass of the system and, consequently, its initial kinetic energy would be different for every combination case. Then, the base mass (implant + mandible) was leveled in all models to balance the crown's mass changes. Note that the base mass represents the whole mass of the mandible, which should be assumed to be the same in all cases. Therefore, a uniformly distributed mass was added to the models to make the impacts equivalent energetically. Table 2 shows the additional mass added to each model.

Table 2. Initial and added masses to each model.

Model	Initial Mass (g)	Added Mass (g)
ET	8.62	0
MCER	6.73	1.89
MCOM	6.63	1.99
FCOM	5.23	3.39
PKCOM	7.20	1.42
FCCER	5.07	3.55

Two changes were made to the whole model to simulate the absence of cortical bone, as in peri-implantitis, peri-implant bone regeneration, or immediate implant placement. Firstly, the cortical part of the assembly was suppressed, and the rest of the mesh is kept intact. Therefore, the nodes chosen (see section 'Node selection') are the same and can be compared. Secondly, some mass was added to equal the impact energy. This added mass

corresponds to the suppressed cortical bone and is obtained by multiplying the volume by its density. It is constant for all models, and the value is 2.27 g. Table 3 lists the added mass in the lateral surface for each crown material:

Table 3. Added mass for both analyses: with and without cortical bone.

Model	Added Mass with Cortical (g)	Added Mass without Cortical (g)
MET	0	2.27
MCER	1.89	4.16
MCOM	1.99	4.26
FCOM	3.39	5.66
PKCOM	1.42	3.69
FCCER	3.55	5.82

2.4.2. Finite Element Mesh

Now, the next step is to generate a suitable finite element mesh, which must be done carefully since the precision of the results depends largely on how refined the mesh is. Then, if greater precision is needed, smaller elements should be used. The more refined the mesh, the more computer time is required. This does not have a large impact in finite element (FE) static analysis but, nevertheless, it is a key aspect in FE transient dynamic analysis.

A mesh sensitivity analysis was done to ensure a reliable model mesh. The refining process started from an initial mesh of 57,330 nodes until reaching a final mesh of 96,160 nodes, where the difference between stress values at some selected nodes did not exceed 5%. Figure 8 shows the finite elements mesh.

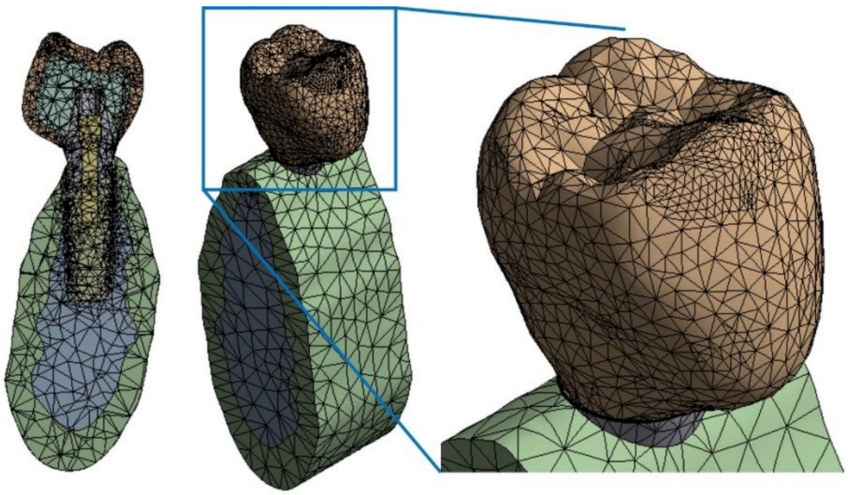

Figure 8. Model mesh (96,160 nodes and 62,606 elements). **Left**: cross section; **center**: isometric view; **right**: details on top of crown.

The Ansys 3D solid element type SOLID187 was used, with 10 nodes and quadratic interpolation functions, which fits better to irregular geometries. The element has three degrees of freedom per node, i.e., the three translations in the global coordinate directions x, y, z. The surface-to-surface contact was defined with the element CONTA174.

Also, a refinement was set for the impact zone, thereby ensuring better accuracy in this area. Therefore, as this refinement was done, it is not necessary to use an area to obtain an average solution, since the nodal solution is especially accurate. In addition, Ansys software performs a control of the aspect ratio systematically.

The size of the finite element mesh, related to its accuracy, is smaller at the loading point and the threaded part (0.2 mm), where higher accuracy is needed, but larger in the other parts (from 0.5 to 2 mm). To find the optimal mesh and an acceptable computational

time, a sensitivity analysis of the mesh was also carried out. First of all, a coarse mesh was used, and subsequently, finer meshes were tested. The refining process was stopped when results became stabilized.

2.4.3. Initial and Boundary Conditions

In dynamic analysis, the boundary conditions (BC) are displacements, velocities, and accelerations instead of static forces and displacements as in static analysis. There are many publications and studies offering strategies on how to configure the loads to obtain a realistic simulation in static analysis. But in dynamic analysis the loads are the result of the calculation, i.e., the input for an impact simulation is the model's initial energy, not an applied load.

Energy concepts allow us to relate the model mass (bone-implant-abutment-crown) and the velocity applied as an initial boundary condition. The mass was calculated according to a density and volume of 411.5 mm^3 for each crown (see Table 1). The model was also subjected to an initial velocity of 1 m/s as the initial kinematic condition.

Some studies focus on the mandibular kinematics by using small accelerometers [33]. The peak peripheral acceleration when opening the mouth can reach an average of 2.5 m/s^2. Considering this and keeping in mind that we are dealing with a brain-controlled occlusally system, the same acceleration (a) during occlusion can be assumed. An estimated velocity (v) can now be obtained using this value and the formula of the constant acceleration movement:

$$1v = a \cdot \Delta t \quad (3)$$

where, v is the velocity, a is the acceleration, Δt is the time increment.

Considering that the mastication occlusion lasts less than 0.5 s, according to Equation (3) we can write: $v = a \cdot \Delta t = 2.5 \cdot 0.5 = 1.25$ m/s. Therefore, a reasonable value for the velocity condition would be 1.25 m/s.

Note that the bottom surface of the plate was fixed. This means that it cannot move or rotate in any direction. During the impact, certain forces appear to counteract the vertical displacement of the rest of the bodies. The distance between the plate and the external crown is 0.01 mm. The lateral surfaces of the cortical and trabecular bones were fixed in the normal (z-axis) and tangential (x-axis) directions, thereby having a degree of freedom in the direction of the displacement (y-axis). As a result, the bones only move in the direction of the vertical axis and do not rotate in any direction.

2.4.4. Simulation Time

The simulation time-limit also has to be set. The impacts happen in a very short period. Some previous works in other scientific fields found that the impact lasts less than one millisecond [38,39], but there is very little (or almost no) published work on dynamic impact loads in dental applications. On the one hand, the duration of the simulations should be as short as possible to reduce the CPU computation time; but on the other, it should be longer than the impact duration and its further effects. Finally, the simulation time was set at 0.4 ms.

Now, the time interval between two analysis steps (known as time-step or Δt) needs to be defined. Similar to what was discussed about mesh's size, the shorter the time-step, the more accurate the results and the more computer time is required. After some sensibility numerical analyses, a time-step of $\Delta t = 7.55$ μs was found to lead to sufficiently accurate results.

2.4.5. Node Selection

To conduct this study, the energy of the object was computed over two benchmark nodes: one at the top of the cortical bone, and the other at the top of the trabecular bone (see Figure 9). The dynamic simulation was run on the six types of crown, with and without cortical bone. As the mesh is the same for all the models, the selected nodes are also the same.

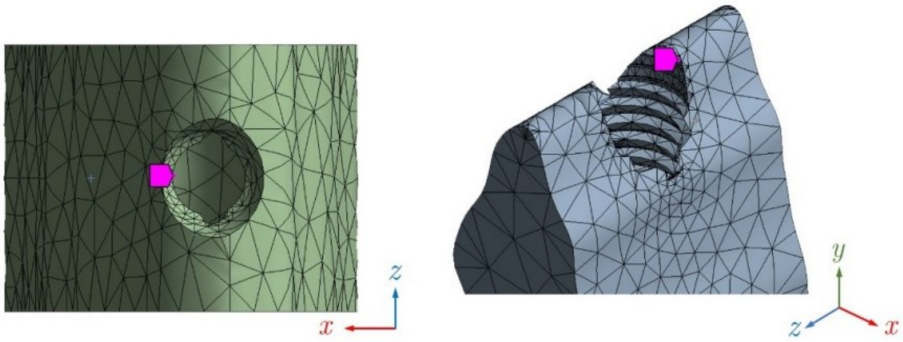

Figure 9. Benchmark nodes shown with a purple marker. **Left**: node at top of cortical bone; **right**: node at top of trabecular bone.

Two simulations were performed. In the first simulation, a healthy bone was considered, with a cortical and trabecular part, where the stresses at the cortical node and the trabecular node were measured. In the second simulation, a cortical bone absence was considered; this is only containing trabecular part, so stresses were measured only at the trabecular node (See Table 4).

Table 4. Bone part considered in each simulation.

	Node	Cortical Bone	Trabecular Bone
Simulation 1	Trabecular	X	X
	Cortical	X	X
Simulation 2	Trabecular		X

3. Results

The von Mises stress value was calculated and compared for each node. Table 5 shows the values of maximum von Mises stress obtained over time in the dynamic FEA simulation, with cortical bone at both nodes (cortical and trabecular) and the trabecular node without cortical bone.

Table 5. Maximum von Mises stresses obtained in cortical bone node (cortical and trabecular) and trabecular node without cortical bone.

		Maximum Von Mises Stress (MPa)					
Node	**Bone**	**MET**	**MCER**	**MCOM**	**FCOM**	**PKCOM**	**FCCER**
Cortical	trab + cort	63.35	72.06	40.71	35.70	32.05	75.46
Trabecular	trab + cort	12.09	15.23	10.30	10.01	9.15	16.69
Trabecular	Trab	30.80	33.87	29.30	31.14	22.80	43.33
trab vs. trab + cort $\Delta\sigma_{vM}$ (%)		60.75%	55.03%	64.85%	67.85%	59.87%	61.48%

The von Mises stresses increase of trabecular bone without cortical with respect to the trabecular bone with cortical were calculated as follows:

$$\Delta\sigma_{\mathrm{vM}}(\%) = \frac{\sigma_{\mathrm{vM\ trab+cort}} - \sigma_{\mathrm{vM\ trab}}}{\sigma_{\mathrm{vM\ trab+cort}}} \cdot 100 \quad (4)$$

where σ_{vM} is the von Mises stress. The distribution of stress varies according to the time, reaching the maximum values of stress during the impact (see Figure 10).

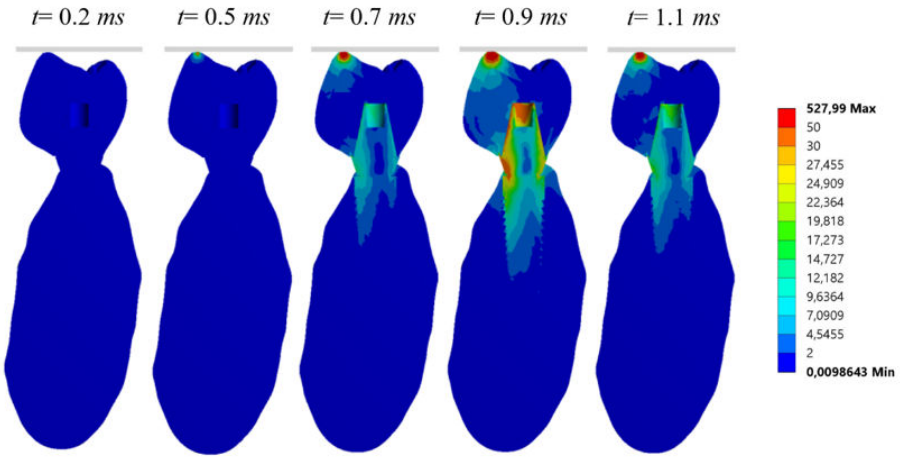

Figure 10. Von Mises stress distribution over time at a cross section using the Carbon Fiber-Ceramic crown (FCCER), considering both trabecular and cortical bone.

3.1. Cortical Node (with Cortical and Trabecular Bone)

Figure 11 shows the evolution of the von Mises stress of the dynamic simulation over time for the different models at the cortical node. The results obtained at the cortical node were (units in MPa): 32.05 (PKCOM), 35.70 (FCOM), 40.71 (MCOM), 63.35 (MET), 72.06 (MCER), and 75.46 (FCCER).

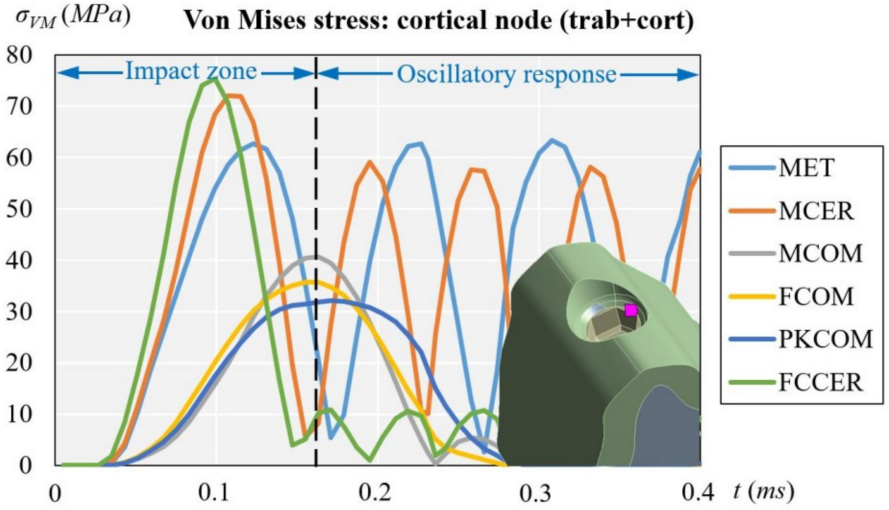

Figure 11. Comparison of equivalent von Misses stress over time on all crown materials at cortical node, considering both trabecular and cortical bone.

3.2. Trabecular Node (with Cortical and Trabecular Bone)

Figure 12 displays the evolution of the von Mises stress of the dynamic simulation over time for the different models at the trabecular node. The results obtained at the trabecular node (units in MPa) were: 9.15 (PKCOM), 10.01 (FCOM), 10.30 (MCOM), 12.09 (MET), 15.23 (MCER), and 16.69 (FCCER).

The evolution of the stress in the trabecular node displays the same pattern as in the cortical node but the stress values are considerably lower, since the trabecular bone is not very dense and is less rigid than cortical bone. Moreover, the trabecular bone receives the effects of the impact-load later. The shape of the function is almost equal to that of the cortical node, with more irregular oscillations at the end. Similar as the case of cortical node the maximum stress is in FCCER.

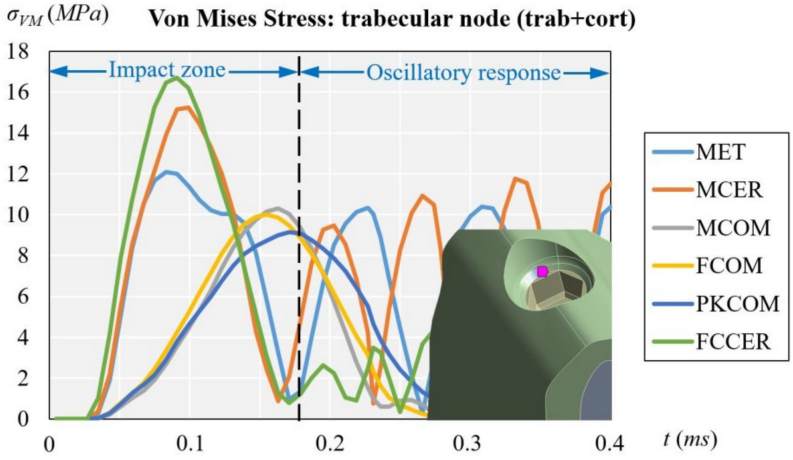

Figure 12. Comparison of equivalent von Mises stress over time depending on all crown materials at trabecular node, considering both trabecular and cortical bone.

Figure 11 (cortical node) and Figure 12 (trabecular node) show the high peak of stress and the duration over time for FCCER and MCER, which were much longer than for the composite-coated crowns, MCOM, FCOM, and PKCOM. The stress fluctuations due to the eccentricity of the impact load with respect to the implant longitudinal axis can also be observed. The maximum stress values in the ceramic models (MCER and FCCER) are notably higher than in the rest of the models.

3.3. Trabecular Node (with Trabecular Bone Only)

This section is devoted to analyzing the effects of the pathological bone without cortical bone (peri-implantitis, bone regeneration, or immediate implant placement). Figure 13 displays the evolution of the von Mises stress of the dynamic simulation over time for the different models at the trabecular node. The results obtained trabecular node (units in *MPa*) were: 22.80 (PKCOM), 31.14 (FCOM), 29.30 (MCOM), 30.80 (MET), 33.87 (MCER), and 43.33 (FCCER). Figure 12 shows, like Figure 11, a similar behavior of the oscillations after the first peak happens. In Figure 13 the frequency of the oscillations is lower as a result of a more damped impact. Results at the cortical node (see Figure 11) showed that the behavior of the stress in the trabecular node is the same as the cortical but the values are much lower. Since the trabecular bone is not very dense, it is more flexible and works as a stress reducer.

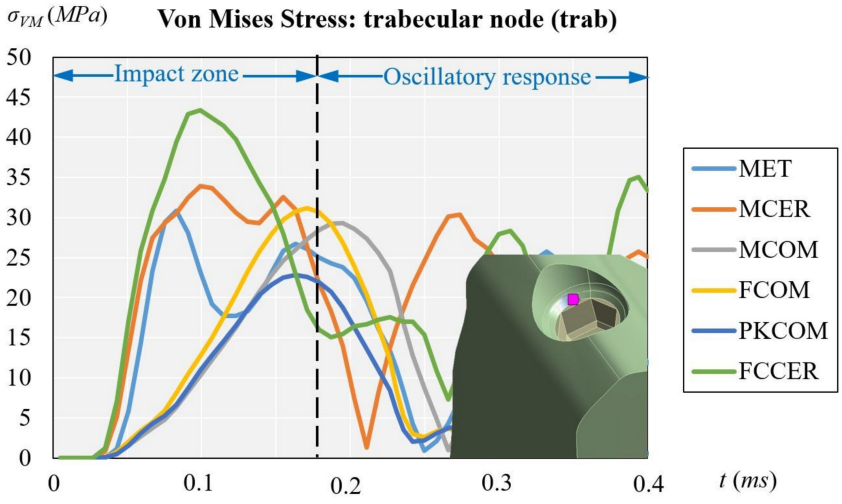

Figure 13. Comparison of equivalent von Mises stress over time at trabecular node, considering trabecular bone only.

Figure 14 shows a comparison between the maximum von Mises stress obtained in trabecular node with and without cortical bone.

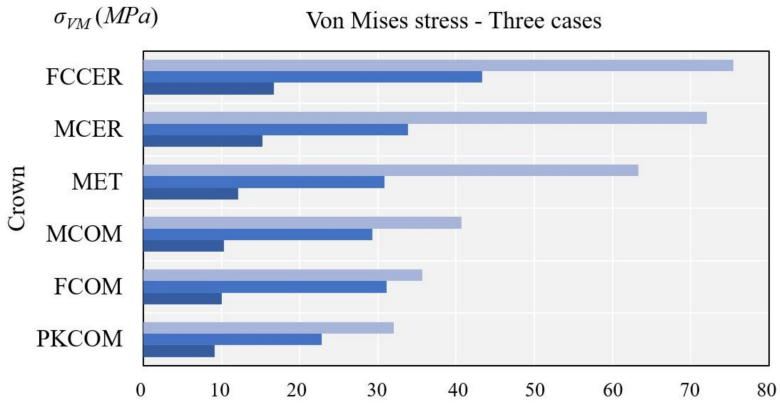

		PKCOM	FCOM	MCOM	MET	MCER	FCCER
Node cortical	trab+cort bone	32,05	35,70	40,71	63,35	72,06	75,46
Node trabecular	trab bone	22,80	31,14	29,30	30,81	33,87	43,33
	trab+cort bone	9,14	10,01	10,30	12,09	15,23	16,69

Figure 14. Comparison of maximum von Mises stress obtained at different nodes.

Figure 14 also shows a significant decrease of the von Mises equivalent stress at the trabecular bone with cortical compared to the case without cortical bone. The reason is that in the case with cortical bone, the impact was affecting the whole jawbone and cortical and trabecular bones, so the stress was divided into the two parts. The biggest increase in absolute value was observed in the MCER, with approximately 19 MPa difference.

4. Discussion

This study focused on comparing the stresses generated on cortical bone using six types of crown materials placed on a specific implant under impact-load conditions, so the same implant was maintained in all simulations. Therefore, the same methodology can be used to analyze the dynamic response of other implant models.

Since the forces applied in the masticatory process and eccentric bruxism are dynamic, it is important not only to study the mechanical behavior of the restorative materials in static forces, but also to know the mechanical behavior produced by dynamic forces. The rehabilitation materials used in the oral cavity could absorb impacts that may vary according to their mechanical properties [10,40–42]. Therefore, the evaluation of the mechanical behavior of the most widely-used materials in implant supported rehabilitations becomes a key issue. Moreover, the morphological, elemental, and biochemical structure without cortical bone is different to healthy bone structure [2].

Figures 11 and 12 (healthy bone) show that over time the reaction of the crown veneered with ceramic was different to that of the crown veneered with composite or with peek as a core. Many fluctuations in the MCER can be observed over time, and the results of the rebound produced by the material's stiffness, whereas in the crowns with less rigid materials (MCOM, PKCOM, or FCOM), only one fluctuation was observed.

Figure 13 (trabecular node: only trab.) does not have the damping effect of Figure 11 (cortical node: cort. and trab. bone) and Figure 12 (trabecular node: cort. and trab. bone). On the other hand, Figures 11 and 12 can be analyzed through the type of bone they represent, although the shape and location of the oscillations are similar, the Figure 12 has lower amplitudes.

The implant-crown rehabilitation materials made from a combination of metals and ceramics (FCCER, MET, MCER) are more rigid. In those materials, an initial stress peak of higher magnitude is observed, as compared to polymeric materials (PKCOM) that are less rigid. On the other hand, FCOM and PKCOM composites (less rigid) presented very low oscillations which were quickly damped.

It is important to transfer less stress to bone in cases of immediate implant placement, bone regeneration, or after peri-implantitis healing, given that there is no bone for some time in those cases. Hence, using materials that transfer less stress to the bone could avoid problems. In short, crowns made of rigid materials present a greater risk over time of bone loss around implants in the presence of gingival inflammation, since these materials transfer more stress to the bone, whether cortical or trabecular.

5. Conclusions

Our study demonstrated that more stress is transferred to the bone when stiffer materials (metal and/or ceramic) are used in implant supported rehabilitations and, conversely, more flexible materials transfer less stress to the implant connection. These relationships between materials' elastic properties and the dynamic force transmission are in accordance with the findings of different authors [10,40–43].

The presence (or absence) of cortical bone around the implant connection generates different behavior in rehabilitation implants when dynamic forces are applied, such as grinding, swallowing, or eccentric movements. Such transferred force, on the other hand, varies according to the rehabilitation material (more with ceramic than with composite), which is even more pronounced if cortical bone is present than if it is not.

The absence of cortical bone, in peri-implantitis, bone regeneration, or immediate implant placement cases, must be considered when choosing the crown material for the rehabilitation.

Author Contributions: Conceptualization, O.C.-N., R.M.-G. and J.C.-T.; data curation, X.M., M.C.; formal analysis, X.M., M.F., M.C. and J.C.-T.; funding acquisition, J.C.-T.; investigation, R.M.-G., X.M.; methodology, M.F.; project administration, J.C.-T.; resources, O.C.-N., J.C.-T.; software, X.M., M.F.; supervision, J.C.-T.; validation, O.C.-N., R.M.-G., X.M. and M.C.; visualization, X.M.; writing—original draft, R.M.-G., X.M., M.C.; writing—review and editing, O.C.-N., R.M.-G., X.M., M.F., M.C. and J.C.-T. All authors have read and agreed to the published version of the manuscript.

Funding: This research received no external funding.

Institutional Review Board Statement: Not applicable.

Informed Consent Statement: Not applicable.

Data Availability Statement: Not applicable.

Acknowledgments: We gratefully acknowledge the support of the NVIDIA Corporation with the donation of the Titan X Pascal GPU used for this numerical analysis.

Conflicts of Interest: The authors declare no conflict of interests.

Abbreviations

MET	Metal crown
MCER	Metal-Ceramic crown
MCOM	Metal-Composite crown
FCOM	Carbon fiber-Composite crown
PKCOM	Peek-Composite crown
FCCER	Carbon Fiber-Ceramic crown
FEA	Finite Element Analysis
DIC	Digital Image Correlation
CAD	Computer-Aided Design
CT Scan	Computer Tomography Scanner

References

1. Esposito, M.; Hirsch, J.M.; Lekholm, U.; Thomsen, P. Biological factors contributing to failures of osseointegrated oral implants. (I): Success criteria and epidemiology. *Eur. J. Oral Sci.* **1998**, *106*, 527–551. [CrossRef]
2. Maglione, M.; Vaccari, L.; Mancini, L.; Ciancio, R.; Bedolla, D.; Bevilacqua, L.; Tonellato, P. Micro-ATR FTIR, SEM-EDS, and X-ray Micro-CT: An Innovative Multitechnique Approach to Investigate Bone Affected by Peri-implantitis. *Int. J. Oral Maxillofac. Implants* **2019**, *34*, 631–641. [CrossRef]
3. Earthman, J.C.; Li, Y.; Van Schoiack, L.R.; Sheets, C.G.; Wu, J.C. Reconstructive Materials and Bone Tissue Engineering in Implant Dentistry. *Dent. Clin. N. Am.* **2006**, *50*, 229. [CrossRef]
4. Tribst, J.; Piva, A.D.; Borges, A. Biomechanical tools to study dental implants: A literature review. *Braz. Dent Sci.* **2016**, *19*, 5. [CrossRef]
5. Tang, Q.; Du, C.; Hu, J.; Wang, X.; Yu, T. Surface rust detection using ultrasonic waves in a cylindrical geometry by finite element simulation. *Infrastructures* **2018**, *3*, 29. [CrossRef]
6. Jerban, S.; Ma, Y.; Nazaran, A.; Dorthe, E.; Cory, E.; Carl, M.; D'Lima, D.; Sah, R.; Chang, E.; Du, J. Detecting stress injury (fatigue fracture) in fibular cortical bone using quantitative ultrashort echo time-magnetization transfer (UTE-MT): An ex vivo study. *NMR Biomed.* **2018**, *31*, e3994. [CrossRef] [PubMed]
7. Hériveaux, E.; Audoin, B.; Biateau, C.; Nguyen, V.H.; Haïat, G. Ultrasonic Propagation in a Dental Implant. *Ultrasound Med. Biol.* **2020**, *46*, 1464–1473. [CrossRef] [PubMed]
8. Pesqueira, A.; Goiato, M.; Filho, H.; Monteiro, D.; Dos Santos, D.; Haddad, M. Use of stress analysis methods to evaluate the biomechanics of oral rehabilitation with implants. *J. Oral Implantol.* **2014**, *40*, 217–228. [CrossRef]
9. McCormick, N.; Lord, J. Digital image correlation. *Materials Today* **2010**, *13*, 52–54. [CrossRef]
10. Magne, P.; Silva, M.; Oderich, E.; Boff, L.; Enciso, R. Damping behavior of implant-supported restorations. *Clin. Oral Implants Res.* **2013**, *24*, 143–148. [CrossRef] [PubMed]
11. Duyck, J.; Rønold, H.J.; Van Oosterwyck, H.; Naert, I.; Vander Sloten, J.; Ellingsen, J.E. The influence of static and dynamic loading on marginal bone reactions around osseointegrated implants: An animal experimental study. *Clin. Oral Implants Res.* **2001**, *12*, 207–218. [CrossRef]
12. Galindo-Moreno, P.; Fernández-Jiménez, A.; Avila-Ortiz, G.; Silvestre, F.J.; Hernández-Cortés, P.; Wang, H.L. Marginal bone loss around implants placed in maxillary native bone or grafted sinuses: A retrospective cohort study. *Clin. Oral Implants Res.* **2014**, *25*, 378–384. [CrossRef]
13. Lin, D.; Li, Q.; Li, W.; Swain, M. Dental implant induced bone remodeling and associated algorithms. *J. Mech. Behav. Biomed. Mater.* **2009**, *2*, 410–432. [CrossRef] [PubMed]
14. Cicciu, M.; Cervino, G.; Milone, D.; Risitano, G. FEM Investigation of the Stress Distribution over Mandibular Bone Due to Screwed Overdenture Positioned on Dental Implants. *Materials* **2018**, *11*, 1512. [CrossRef] [PubMed]
15. Li, J.; Jansen, J.; Walboomers, F.; van den Beucken, J. Mechanical aspects of dental implants and osseointegration: A narrative review. *J. Mech. Behav. Biomed. Mater.* **2020**, *103*, 103574. [CrossRef]
16. Kitagawa, T.; Tanimoto, Y.; Nemoto, K.; Aida, M. Influence of cortical bone quality on stress distribution in bone around dental implant. *Dent. Materials J.* **2005**, *24*, 219–224. [CrossRef] [PubMed]
17. Wachter, N.J.; Krischak, G.D.; Mentzel, M.; Sarkar, M.R.; Ebinger, T.; Kinzl, L.; Claes, L.; Augat, P. Correlation of bone mineral density with strength and microstructural parameters of cortical bone in vitro. *Bone* **2002**, *31*, 90–95. [CrossRef]
18. Kayabasi, O.; Yuzbasıoglu, E.; Erzincanli, F. Static, dynamic and fatigue behaviors of dental implant using finite element method. *J. Adv. Eng. Softw.* **2006**, *37*, 649–658. [CrossRef]
19. Benazzi, S.; Nguyen, H.N.; Kullmer, O.; Kupczik, K. Dynamic Modelling of Tooth Deformation Using Occlusal Kinematics and Finite Element Analysis. *PLoS ONE* **2016**, *11*, e0152663. [CrossRef]
20. Razaghi, R.; Mallakzadeh, M.; Haghpanahi, M. Dynamic simulation and finite Element analysis of the maxillary bone injury around dental implant during chewing different food. *Biomed. Eng. Appl. BasisCommun.* **2016**, *28*, 1650014. [CrossRef]
21. Chang, Y.; Tambe, A.; Maeda, Y.; Wada, M.; Gonda, T. Finite element analysis of dental implants with validation: To what extent can we expect the model to predict biological phenomena? A literature review and proposal for classification of a validation process. *Implant Dent.* **2018**, *4*, 7–12. [CrossRef]
22. Geramizadeh, M.; Katoozian, H.; Amid, R.; Kadkhodazadeh, M. Finite Element Analysis of Dental Implants with and without Microthreads under Static and Dynamic Loading. *J. Long-Term Eff. Med. Implants* **2017**, *27*, 25–35. [CrossRef]
23. Canto-Naves, O.; Marimon, X.; Ferrer, M.; Cabratosa-Termes, J. Comparison between experimental digital image processing and numerical methods for stress analysis in dental implants with different restorative materials. *J. Mech. Behav. Biomed. Mater.* **2021**, *113*, 104092. [CrossRef]
24. Solidworks Dassault Systemes. 2020. Available online: www.solidworks.com (accessed on 3 August 2021).
25. MIS Implants Tech. Ltd. 2021. Available online: https://www.mis-implants.com (accessed on 3 August 2021).
26. NewTom. 2021. Available online: https://www.newtom.it (accessed on 3 August 2021).
27. Lakatos, É.; Magyar, L.; Bojtár, I. Material Properties of the Mandibular Trabecular Bone. *J. Med. Eng.* **2014**, *2014*, 470539. [CrossRef]
28. Geng, J.P.; Tan, K.B.; Liu, G.R. Application of finite element analysis in implant dentistry: A review of the literature. *J. Prosthet. Dent.* **2001**, *85*, 585–598. [CrossRef]

29. Micro Medica Srl. 2021. Available online: http://micromedicasrl.it (accessed on 3 August 2021).
30. Renishaw. 2021. Available online: https://www.renishaw.com (accessed on 3 August 2021).
31. VITA Zahnfabrik, H. Rauter GmbH & Co. 2021. Available online: www.vita-zahnfabrik.com (accessed on 3 August 2021).
32. Heraeus Kulzer GmbH. 2021. Available online: https://www.kulzer.de (accessed on 3 August 2021).
33. Ivoclar Vivadent. 2021. Available online: https://www.ivoclarvivadent.es (accessed on 3 August 2021).
34. Invibio. 2021. Available online: https://invibio.com (accessed on 3 August 2021).
35. Van Eijden, T.M. Biomechanics of the Mandible. *Crit. Rev. Oral Biol. Med.* **2000**, *11*, 123–136. [CrossRef]
36. Peck, C.C. Biomechanics of occlusion—Implications for oral rehabilitation. *J. Oral Rehabil.* **2016**, *43*, 205–214. [CrossRef] [PubMed]
37. Ansys®Academic Research Mechanical, Release 18.1. 2020. Available online: www.ansys.com (accessed on 3 August 2021).
38. Minami, I.; Oogai, K.; Nemoto, T.; Nakamura, T.; Igarashi, Y.; Wakabayashi, N. Measurement of jerk-cost using a triaxial piezoelectric accelerometer for the evaluation of jaw movement smoothness. *J. Oral Rehabil.* **2010**, *37*, 590–595. [CrossRef] [PubMed]
39. Dattakumar, S.S.; Ganeshan, V. Converting Dynamic Impact Events to Equivalent Static Loads in Vehicle Chassis. Master Thesis, Chalmers University of Technology, Gothenburg, Sweden, 2017.
40. Conserva, E.; Menini, M.; Tealdo, T.; Bevilacqua, M.; Pera, F.; Ravera, G.; Pera, P. Robotic chewing simulator for dental materials testing on a sensor-equipped implant setup. *Int. J. Prosthodont.* **2008**, *21*, 501–508. [PubMed]
41. Menini, M.; Conserva, E.; Tealdo, T.; Bevilacqua, M.; Pera, F.; Ravera, G.; Pera, P. The use of a masticatory robot to analyze the shock absorption capacity of different restorative materials for implant prosthesis. *J. Biol. Res.* **2011**, *84*, 118–119. [CrossRef]
42. Menini, M.; Conserva, E.; Tealdo, T.; Bevilacqua, M.; Pera, F.; Signori, A. Shock Absorption Capacity of Restorative Materials for Dental Implant Prostheses: An In Vitro Study. *Int. J. Prosthodont.* **2013**, *26*, 549–556. [CrossRef] [PubMed]
43. Vigolo, P.; Gracis, S.; Carboncini, F.; Mutinelli, S. Internal- vs External-Connection Single Implants: A Retrospective Study in an Italian Population Treated by Certified Prosthodontists. *Int. J. Oral Maxillofac. Implants* **2016**, *31*, 1385–1396. [CrossRef] [PubMed]